National Library of Canada
Bibliothèque nationale du Canada

Canadian Theses Service
Service des thèses canadiennes

Ottawa, Canada
K1A 0N4

NOTICE

The quality of this microform is heavily dependent upon the quality of the original thesis submitted for microfilming. Every effort has been made to ensure the highest quality of reproduction possible.

If pages are missing, contact the university which granted the degree.

Some pages may have indistinct print especially if the original pages were typed with a poor typewriter ribbon or if the university sent us an inferior photocopy.

Previously copyrighted materials (journal articles, published tests, etc.) are not filmed.

Reproduction in full or in part of this microform is governed by the Canadian Copyright Act, R.S.C. 1970, c. C-30.

AVIS

La qualité de cette microforme dépend grandement de la qualité de la thèse soumise au microfilmage. Nous avons tout fait pour assurer une qualité supérieure de reproduction.

S'il manque des pages, veuillez communiquer avec l'université qui a conféré le grade.

La qualité d'impression de certaines pages peut laisser à désirer, surtout si les pages originales ont été dactylographiées à l'aide d'un ruban usé ou si l'université nous a fait parvenir une photocopie de qualité inférieure.

Les documents qui font déjà l'objet d'un droit d'auteur (articles de revue, tests publiés, etc.) ne sont pas microfilmés.

La reproduction, même partielle, de cette microforme est soumise à la Loi canadienne sur le droit d'auteur, SRC 1970, c. C-30.

NL-339 (r. 88/04)

Canada

THE UNIVERSITY OF ALBERTA

PHYSICO-CHEMICAL ASPECTS OF FREEZING SOILS

by

Wim Van Gassen

(C)

A THESIS

SUBMITTED TO THE FACULTY OF GRADUATE STUDIES AND RESEARCH

IN PARTIAL FULFILMENT OF THE REQUIREMENTS FOR THE DEGREE

OF MASTER of SCIENCE

Department of Civil Engineering

EDMONTON, ALBERTA

Fall 1988

Permission has been granted to the National Library of Canada to microfilm this thesis and to lend or sell copies of the film.

The author (copyright owner) has reserved other publication rights, and neither the thesis nor extensive extracts from it may be printed or otherwise reproduced without his/her written permission.

L'autorisation a été accordée à la Bibliothèque nationale du Canada de microfilmer cette thèse et de prêter ou de vendre des exemplaires du film.

L'auteur (titulaire du droit d'auteur) se réserve les autres droits de publication; ni la thèse ni de longs extraits de celle-ci ne doivent être imprimés ou autrement reproduits sans son autorisation écrite.

ISBN 0-315-45494-6

THE UNIVERSITY OF ALBERTA

RELEASE FORM

NAME OF AUTHOR Wim Van Gassen

TITLE OF THESIS PHYSICO-CHEMICAL ASPECTS OF FREEZING SOILS

DEGREE FOR WHICH THESIS WAS PRESENTED MASTER of SCIENCE

YEAR THIS DEGREE GRANTED Fall 1988

Permission is hereby granted to THE UNIVERSITY OF ALBERTA LIBRARY to reproduce single copies of this thesis and to lend or sell such copies for private, scholarly or scientific research purposes only.

The author reserves other publication rights, and neither the thesis nor extensive extracts from it may be printed or otherwise reproduced without the author's written permission.

(SIGNED) Wim. M. Jan.....

PERMANENT ADDRESS:

..#3..10638...88 AVE.....

..EDMONTON... ALBERTA.....

.....

DATED ..October...7.....1988

THE UNIVERSITY OF ALBERTA

FACULTY OF GRADUATE STUDIES AND RESEARCH

The undersigned certify that they have read, and recommend to the Faculty of Graduate Studies and Research, for acceptance, a thesis entitled PHYSICO-CHEMICAL ASPECTS OF FREEZING SOILS submitted by Wim Van Gassen in partial fulfilment of the requirements for the degree of MASTER in SCIENCE.

.....

Supervisor

.....

.....

.....

Date..OCTOBER..5,..1988.....

Acknowledgements

The thesis topic was suggested by Dr. Dave Sego, I would like to thank him for this, to me, very confusing topic. Since I spent quite some time in the lab, I needed and got a lot of help from the technicians Steve and Christine, as well as from the machine shop.

School is no fun without coffee time and ice cream with Jim, Sam, Barb, Dwayne, Chris, Peter, Bill, Linda, Tai, John, Les, Elisabeth, et les autres.

The basics were taught by Drs. D. Cruden, P. Kaiser, N. Morgenstern, D. Sego, and S. Thomson.

And of considerable importance: my parents and Preet for emotional and financial support!

Abstract

The pore pressures generated when soils freeze are evaluated. It is shown that the Clausius-Clapeyron equation does not describe the consolidation behavior of freezing soils in a satisfactor manner. Electro-osmosis is postulated to explain this observed behavior. Electric freezing potentials may cause electro-osmotic flow towards an ice lens, inducing high consolidation stresses in the freezing and frozen soil.

In order to evaluate the feasibility of electro-osmosis as a transport mechanism in freezing soils, the electro-osmotic conductivity as a function of temperature of Athabasca Clay was determined in an experimental programme. It was found that the electro-osmotic conductivity was constant in the temperature range from +22 to -0.5 °C, after which it decreased rapidly to a value 100 times smaller at a temperature of -1.5 °C.

Electro-osmosis induced ice lens formation in a frozen soil, and whenever water was predicted by theoretical considerations to accumulate ice lenses formed.

If the electric freezing potentials in soils are analogous in nature to the freezing potentials in dilute solutions electro-osmosis is bound to occur, being in part responsible for the transport of water towards an ice lens and the consolidation of the freezing soil.

Table of Contents

Chapter — Page

1. Introduction 1
2. Literature review 3
   - 2.1 Frost heave and solute transport 3
   - 2.2 Electro-osmosis in frozen soils 5
   - 2.3 The Workman-Reynolds effect 6
   - 2.4 Freezing potentials in soils 8
   - 2.5 The nature of electric potentials in soils 11
3. An electric source in freezing soil. 18
   - 3.1 Introduction 18
   - 3.2 Identification of an electric source. 19
   - 3.3 Electrode spacing and electro-osmosis 21
   - 3.4 The Clausius-Clapeyron equation. 26
   - 3.5 Consolidation due to freezing and thawing. 27
     - 3.5.1 Laboratory examples 27
     - 3.5.2 A field case 29
   - 3.6 Clausius-Clapeyron and overconsolidation. 30
   - 3.7 Collapse of interlaminar spacing 33
   - 3.8 Effective stress in freezing soil 37
   - 3.9 Pressures in the electro-osmotic model. 39
   - 3.10 Conclusions 41
4. Experimental programme 53
   - 4.1 Introduction 53
   - 4.2 Apparatus and sample preparation 53
   - 4.3 Test procedure and experimental results 57
   - 4.4 Discussion of experiments 59
   - 4.5 Finite difference model 61

4.6 Exploration of electro-osmosis problem 64

4.7 Dimensional analysis 67

4.8 Summary and discussion of results 74

5. Concluding remarks 108

5.1 Conclusions 109

5.2 Recommendations for future research 110

References 112

APPENDIX A: Finite difference code 121

APPENDIX B: Mode of consolidation of Beaufort Sea deposits. 123

APPENDIX C: Finite difference code 128

APPENDIX D: Experimental results 130

APPENDIX E: The Segregation Potential theory 145

E.1 Correlation of index properties and frost susceptibility 145

E.2 Review of Segregation Potential theory. 148

E.3 Conclusion 153

APPENDIX F: Some comments on the results of the finite difference program 183

List of Tables

Table		Page
2.1	Electro-osmosis in frozen soil (modified from Hoekstra and Chamberlain, 1964)	15
4.1	Properties of unfrozen Athabasca Clay (modified from Smith, 1972)	86
4.2	Summary of electro-osmosis experiments, I	87
4.3	Summary of electro-osmosis experiments, II	88
4.4	Coefficient of consolidation of Athabasca Clay	89
E.1	Time versus Water Intake Velocity record for sample NS-4.	154

List of Figures

Figure		Page
2.1	Schematic experimental set up for measurement of freezing potentials.	16
2.2	Electric freezing potential at a phase boundary (modified from Yarkin, 1986)	17
3.1	Freezing of dilute solutions; measurement of freezing current	42
3.2	Boundary conditions in electro-osmotic problem; A: after Esrig (1968); B: conditions assumed here.	43
3.3	Boundary conditions assumed in analysis.	44
3.4	Electro-osmotic consolidation diagram for d/L=1	45
3.5	Electro-osmotic consolidation diagram for d/L=.5	46
3.6	Electro-osmotic consolidation diagram for d/L=.1	47
3.7	Amount of consolidation as a function of time, for d/L = .1, .5, and 1.	48
3.8	Total water flow as a function of time, for d/L = .1, .5, and 1.	49
3.9	Relationship between 'd = half distance' and 'd(001) spacing'.	50
3.10	Pore pressures in montmorillonite when it is assumed that the Clausius-Clapeyron equation alone is valid.	51
3.11	Pressure relationships in electro-osmotic model.	52
4.1	Sketch of sample holder	90
4.2	Sketch of experimental apparatus	91
4.3	Water content profile, experiment #6	92
4.4	Heave of soil sample, experiment #6	93
4.5	Electrical current through resistance in series with sample, experiment #6	94

Figure Page

4.6 Accumulation of water in soil sample according to numerical analysis, $k_B/k_S=5.$, $V_B/V_S=1.$ 95

4.7 Accumulation of water in soil sample according to numerical analysis, $k_B/k_S=10.$, $V_B/V_S=1.$ 96

4.8 Accumulation of water in soil sample according to numerical analysis, $k_B/k_S=100.$, $V_B/V_S=1.$ 97

4.9 Accumulation of water in soil sample according to numerical analysis, $k_B/k_S=10.$, $V_B/V_S=3.$ 98

4.10 Accumulation of water in soil sample according to numerical analysis, $k_B/k_S=10.$, $V_B/V_S=0.33$ 99

4.11 Water flow entering the soil sample as a function of time, $k_B/k_S=10$, $V_B/V_S=1.$ 100

4.12 Consolidation of samples with different geometry 101

4.13 Electro-osmotic conductivity k_e of Athabasca Clay as a function of temperature. 102

4.14 Unfrozen water content of Athabasca Clay as a function of temperature 103

4.15 Relationship between distance from pore wall and electro-osmotic transport. 104

4.16 Influence of formation of ice in pores on distribution of ions. 105

D.1 Initial and final water content profiles, Exp. #4 131

D.2 Voltage drop across 120 Ohm resistor in series with the soil sample vs. time, Exp. #4 132

D.3 Initial and final water content profiles, Exp. #5 133

D.4 Heave of top of soil sample vs. time, Exp. #5 134

Figure Page

D.5 Voltage drop across 120 Ohm resistor in series with the soil sample vs. time, Exp. #5 135

D.6 Voltage drop across 120 Ohm resistor in series with the soil sample vs. time, Exp. #7 136

D.7 Initial and final water content profiles, Exp. #8 137

D.8 Voltage drop across 120 Ohm resistor in series with the soil sample vs. time, Exp. #8 138

D.9 Initial and final water content profiles, Exp. #9 139

D.10 Voltage drop across 120 Ohm resistor in series with the soil sample vs. time, Exp. #9 140

D.11 Initial and final water content profiles, Exp. #10 141

D.12 Heave of top of soil sample vs. time, Exp. #11 142

D.13 Voltage drop across 120 Ohm resistor in series with the soil sample vs. time, Exp. #11 143

D.14 Voltage drop across 120 Ohm resistor in series with the soil sample vs. time, Exp. #12 144

E.1 Relationship between SP, suction at bottom of frost front and cooling rate for sample E-6. 155

E.2 Relationship between SP, suction and cooling rate for Devon Silt. 156

E.3 Relationship between SP, suction and cooling rate for Devon Silt, (modified from Konrad, 1980) 157

E.4 SP versus Cooling Rate for Devon Silt, the data points are plotted after correction for the changed suction. 158

E.5 Example of ACFEL data, MFS-28, (modfied from ACFEL ,1951) 159

Figure Page

E.6 Relationship between SP, cooling rate and suction for a typical test from ACFEL data, MFS-28. 160

E.7 Relationship between SP and Cooling Rate for typical test from ACFEL data, MFS-28,data points are corrected for suction. 161

E.8 Example of ACFEL data, SC-1, after ACFEL(1951). 162

E.9 Relationship between SP, cooling rate and suction for a typical test (modified from ACFEL ,1951)..... 163

E.10 Relationship between SP and Cooling Rate for typical test from ACFEL data, SC-1, data points are corrected for suction. 164

E.11 Correlation between Index Properties and Segregation Potential. 165

E.12 Correlation between Index Properties and Segregation Potential. 166

E.13 Correlation between Index Properties and Segregation Potential. 167

E.14 Water Intake Velocity versus Temperature Gradient (modified from Konrad and Morgenstern, 1981). 168

E.15 Graphical representation of the consequences of an uncertainty ΔT of the temperature measuring system. 169

E.16 Graphical representation of the consequences of an uncertainty ΔT of the estimate of the segregation temperature. 170

E.17 Graphical representation of the accumulated influence of the three sources of error on the estimate of the moment of the initiation of the final ice lens. 171

F.1 ξ-distribution for a soil-bentonite sample under conditions as described in the text. 186

List of Plates

Plate		Page
4.1	Athabasca Clay frozen confined in a sample holder, #4	106
4.2	Ice structure after electro-osmosis experiment, #5	107

1. Introduction

Freezing soils display a number of intriguing and sometimes annoying phenomena, probably the most important being frost heave. Because of the detrimental effects of frost heaving of soil on roads and structures as well as agriculture it has received considerable attention from the scientific community. Although the understanding of freezing and frozen soils is still incomplete, significant advances have been made. For instance, it is known that there is mobile unfrozen water in frozen soil and that soil consolidates when frozen.

The planning and construction of chilled pipelines in the north has triggered a wave of studies on frost heaving. In this situation frost heave is not a seasonal or short term problem, but rather long term behavior needs to be predicted. Numerous frost heave models and mechanisms have been put forward in the literature (e.g. Harlan, 1973; Konrad and Morgenstern, 1980)

There is still a lack of understanding of the actual physico-chemical processes involved during the long term freezing of soils. In this thesis one of these processes is investigated.

It is postulated here that the process which causes electrical freezing potentials in soils is analogous to the process in dilute solutions (freezing potentals are the potential differences measured between the frozen and unfrozen constituents of a soil or solution). Then, it is

argued that this process can induce electro-osmosis at the interface between frozen and unfrozen soil in freezing soil. The electro-osmosis process would be responsible for transporting water toward the freezing front and would be responsible for inducing consolidation stresses in the freezing soil which are higher than predicted from conventional theory. Some evidence is provided for this hypothesis. The electro-osmotic characteristics of frozen soil are investigated during the experimental programme. The physics governing the behavior are deduced from the experimental results.

2. Literature review

The present knowledge on frost heaving is summarized by the Ad Hoc Study Group on Ice Segregation and Frost Heaving (1984) of the National Research Council of the United States. Few dramatic changes have occurred in the understanding of frost heave mechanics research since this report was issued. The literature review is therefore confined to issues that are directly concerned with the scope of the thesis as described in the previous section.

2.1 Frost heave and solute transport

In the past investigations have been undertaken to study the redistribution of water and salts in freezing soils. Many of these studies have been related to the study of agriculture.

Cary and Mayland (1972) studied the redistribution of salt and water with time in frozen soil as a consequence of a constant temperature gradient being maintained across the sample. They concluded that the flow of dissolved salts in a liquid film of water was the principle transfer mechanism, while salt sieving was not an important phenomenon in frozen soil.

Field measurements of water and salt contents in freezing soils have been carried out by Campbell et al. (1970) and Gray and Granger (1986). Both investigations led to the conclusion that salt may be transported upward in the winter due to freezing. Dissolved salts are tranported

upward by the water which is attracted to the freezing front.

Kay and Groenevelt (1984) studied solute redistribution in both the field and the laboratory. They hypothesised that exclusion of solutes does occur on a local scale, but not on a macroscale. They described the process:

> "As ice is forming, the freezing front advances slowly because of the release of latent heat. However, with this advancing freezing front is associated an accumulation of solute excluded from the ice. As the rate of ice formation diminishes, the rate of advance of the 0 °C isotherm begins to rapidly increase until nucleation occurs at some point just beyond the zone of solute accumulation. The process is then repeated."

Hallet (1978), reasoning along the same lines, concluded that the rejection of solutes may cause the existence of a frozen fringe, a zone of frozen soil on the warm side of an ice lens forming within the soil. Hallet also reported the deposition of $CaCO_3$, FeO_2, and MnO as a consequence of freezing.

Mackay (1974) discussed the origin of reticulate ice, vertical ice veins dividing a a blocky soil matrix. According to the mechanism he proposed the reticulate ice forms behind the freezing front, in the frozen soil. As the ice veins grow in the already frozen soil, this soil attracts water from the frozen soil causing a decrease in

void ratio. This overconsolidates the soil. He states that as pore water moves from the clay to the ice veins, some ion rejection would be expected at the contact. This is suggested as the source of the oxidized coating frequently observed on thawed clay blocks after exposure to air.

Chamberlain (1984) compared closed system frost heave experiments on soils saturated with fresh water and saline water. The magnitude of frost heave in the soils saturated with saline water was markedly lower than in soils saturated with fresh water. Chamberlain presents a model similar to that of Kay and Groenevelt (1984) to explain the results. In the experiments with soil saturated with fresh water he noted that the water content in the soil on the warm side of the ice lens decreased to the plastic limit. In the experiments on saline soils the water content on the warm side actually increased. He concluded that in the saline soils the water that formed the segregated ice lenses had been provided by the soil in between the lenses, while in the fresh water soil this water had been drawn from the unfrozen soil on the side of the ice lens where the temperature was higher (warm side).

2.2 Electro-osmosis in frozen soils

As indirect proof for the mobility of unfrozen water in soils below freezing temperature Hoekstra and Chamberlain (1964) conducted electro-osmosis experiments. Considerable water flow was induced by applying a voltage gradient across

a frozen soil sample. Their data is presented in Table 2.1. However, the moisture migration was only one part of the observations made; the other part can best be described in the authors' own words:

> "Initially, the film of unfrozen water is in equilibrium with ice in the sample, but when the unfrozen water is transported from the anode region the film of unfrozen water is depleted. It is replenished by the melting of ice in that region. In the final state all ice is removed from the anode region and large bodies of ice are formed in the vicinity of the cathode."

The large bodies of ice are ice lenses. This observation is important because it shows that applied thermal gradients are not required for ice lens formation within a soil.

2.3 The Workman-Reynolds effect

Another set of noteworthy observations is that related to the Workman-Reynolds effect or freezing potentials in pure solutions (Workman and Reynolds, 1950). A comprehensive review of this work is given by Gross (1968). A typical experimental set up is shown in Fig. 2.1. A solution is placed in a beaker, the bottom of which is usually made of platinum. The bottom is connected to a reservoir at a temperature below the freezing point of the solution and it acts as both heat sink and electrode. Another electrode is lowered into the solution, enabling potential differences to

be measured between the frozen and unfrozen parts. Charge transfer can be measured using a resistor or shunt placed in parallel with the solution. Important observations from this research were:

1. High freezing potentials (up to 200 V) measured in dilute solutions, depends on the type of salt, its concentration, and rate of freezing.
2. Substantial charge transfers were measured when using an experimental set up including a shunt.

A description of the process is given by Gross (1968, p. 33-34) (GROUP 1 SOLUTES are alkali halides and ammonium fluoride.): For brevity reference to figures in the original article is replaced by "...".

> "GROUP 1 SOLUTES. The anion is preferentially incorporated into the solid. Charge balance is restored by hydrogen ions. The number of hydrogen ions transferred into the ice equals, within experimental error, the number of charges transferred according to the current record. The difference between solute anions and solute cations in the ice increases with decreasing freezing rate....The anion concentration in the ice, and therefore the over-all impurity content, is affected little or not at all by a low resistance shunt....but the solute cation concentration decreases appreciably in favor of the hydrogen ion.... This difference between samples grown with

and those without shunt decreases as the sample length (resistance) increases. It also decreases with freezing rate.... This suggests that the degree to which solute cations can be rejected by the solid phase depends on the rate at which hydrogen ions can be made available to restore electrical and chemical neutrality. For this neutralisation current, the shunt provides an alternate path which under certain conditions has a lower resistance than the path through the interface."

2.4 Freezing potentials in soils

Freezing potentials in soils are measured with a high impedance voltmeter between electrodes that are embedded in the soil. Shape and composition of electrodes, and type of voltmeter are important factors, but are often not reported in the literature.

Measurements of freezing potentials in frozen soils have been carried out by Jumikis (1958,1960), Yarkin (1978, 1986), Hanley and Rao (1982), Hanley (1985), and Parameswaran and Mackay (1983). Potentials developed during thawing of frozen ground have also been reported by Parameswaran et al. (1985).

Jumikis reported freezing potentials of 40-120 mV in a silty glacial outwash soil. Jumikis (1958) called this electrical potential a secondary or induced potential, in contrast with a primary potential, which is applied

externally to the system (e.g. the thermal potential applied to a freezing soil). He also stated that the induced potential may act, and contribute to the moisture flow, in the same direction as the flow which caused the primary potential, or it may act in the opposite direction. Whereas the above was a general statement, Jumikis (1960) discussed the problem in more detail. He compared the electrical freezing potentials with streaming potentials, which are electrical potentials generated as a consequence of water flowing through the soil system. They therefore impede water flow.

Yarkin (1986) studied freezing potentials in a variety of soils, such as sand, fine sand, and clayey soils. According to his study there is a strong dependence of the measured freezing potential on the water content of the soil, as well as on the freezing rate applied to the soil. He also noticed that the sign of the freezing potential was different for sand and clay. The electrical potentials were measured with electrodes at different spacings; the measured potential became smaller as the distance between the electrodes decreased. Yarkin concluded that the width of the region in which a sharp change in electrical potential occurred was about 20 mm, and delineated three regions of change of potential near the freezing boundary.

These regions are (Fig. 2.2):

1. a jump of potential, which may be associated with the phase boundary.

2. a region of linear change occuppying a width of about 10 mm in either the frozen or unfrozen portion of the soil sample.
3. a region of smooth, slower growth of the potential difference beyond the linear region.

He argued that depending on the soil type, type of freezing experiment and moisture content of the soil, the electrical potential of the unfrozen part becomes positive or negative compared to the frozen part. In the case of positive potentials moisture migration towards the freezing front is induced, in the latter it is hindered.

Hanley and Rao (1982) measured the freezing potentials of clay suspensions, and proposed a mechanism, which they verified experimentally. Their model includes charge transfer in the freezing soil. However, they assumed that the measured potential is directly proportional to the charge density, an assumption that contradicts the Nernst equation for pure electrolytes, and is incorrect in clay suspensions. As a consequence their model is invalid.

Parameswaran and Mackay (1983) conducted a field investigation, measuring electrical freezing potentials in the active layer at locations in the Northwest Territories. Potential differences of 1350 mV and 650 mV, in saturated sand and in silty clay respectively, were recorded. These maxima occurred close to an advancing freezing front.

Parameswaran et al.(1985) measured potentials in thawing soil in the field. The reported potentials were of

the same magnitude as the freezing potentials reported in Parameswaran and Mackay (1983). The maximum value measured in clay was 540 mV, and 180 mV in sandy gravel. The authors wondered whether the thawing potential is actually the reverse of the freezing potential, without reaching a conclusive answer.

2.5 The nature of electric potentials in soils

Work on unfrozen soils can shed light on the nature of electric freezing potentials in partially frozen soils. Electrical potentials in soils can be caused by several mechanisms; four are listed below.

1. Concentration differences in pure electrolytes cause potential differences according to Nernst law, as discussed in any basic chemistry textbook (Boikess and Edelson, 1978).
2. The charge of clay particles causes a Donnan potential or membrane potential between a clay suspension and the supernatant liquid (van Olphen, 1963).
3. Weathering or ageing of soil may cause oxidation-reduction potentials; these are described by Veder (1981) and Olsen (1985).
4. The flow of liquid through a clay system under hydraulic gradients causes streaming potentials to occur. Values of several 10's of mV may occur (Mitchell, 1976).

The Donnan potential warrants some additional information. It has been discussed by Peech et al. (1953),

but, the issue is still confused, as can be exemplified by a more recent article by Elrick et al. (1976) dealing with the same problem. Elrick et al. measured the potential drop over a clay plug placed between two baths with electrolytes of different concentration. They measured potential differences up to 110 mV, varying as flow through the clay was induced. The authors' discussion is quoted in the following:

> "The effects observed ... are complicated and will be interpreted from a physical point of view. There are three components to ΔV. The first arises from "asymmetry".... and can be neglected. The second is due to the concentration difference across the membrane. The third component is due to the difference in the transference number of cations and anions. Although the mobility of the Cl^- is slightly higher than that of the Na^+, the number of Na^+ ions outweighs that of Cl^-. This makes the transference number of Na^+ much larger than that of Cl^-. This component we refer to as "membrane potential". The second and third effects are additive when measured with an electrode pair reversible to the anion (Shainberg and Kemper, 1972). The observed maximum ΔV of about +110 mV we interpret to be composed of about 59 mV that arises because of the 10-fold concentration difference and a further contribution because of the ion-selective properties of the montmorillonite."

With "asymmetry" the authors describe the fact that the two electrodes may not have exactly the same composition.

Examples of oxidation-reduction potentials and their consequences can be found in Olsen (1969,1985) and Veder (1981). Olsen studied the transport of water and charges through saturated kaolinite. A problem is the occurrence of water flow when no external gradients are applied, and alternatively, the existence of gradients when no flow occurs. This has led to much speculation. Olsen (1985) suggested that electrochemical gradients generated by chemical reactions within the sample could be the cause of this discrepancy. When no flow of water occurred, and no hydraulic gradient was applied, Olsen (1969) measured electric potentials in the order of some mV for kaolinite. Note though, that these experiments were conducted with a relatively pure mineral. In natural soils one should expect considerably higher values, especially in a soil with a high organic content, in which oxidation-reduction reactions are common, as pointed out by Lessard and Mitchell (1985).

Veder (1981) suggested that oxidation-reduction reactions within a soil mass may cause water migration, which may induce landslides. Some reactions that occur commonly in soil are described in his book, as well as in Lessard and Mitchell (1985). An example of a very common reaction is the oxidation and reduction of iron within the soil.

When discussing electric potentials in soil, Veder attributed those entirely to oxidation-reduction reactions. Obviously this is not a correct interpretation as the Donnan potential was ignored. According to Veder, large jumps in the measured potentials took place especially between soil layers of different composition. It was between layers of different composition that the Donnan potential comes into play. For instance, the potential difference between a layer of chemically inert clay and chemically inert sand was completely accounted for by the Donnan potential, and may be of the order of some 100's of mV.

Concluding, oxidation-reduction reactions may cause potentials in soils. These potentials depend on the concentration of the pore water and its composition. Values of several 10's of mV may be expected.

After this short review, one can contend that an accurate quantitative analysis is not available at present. A combination of all four effects constitutes the measured electrical potential in a freezing soil. As the contribution of each component of a clay soil on the freezing potential is impossible to determine, the meaning and consequence of the freezing potential is hard to evaluate in soils with a significant clay content.

Table 2.1 Electro-osmosis in frozen soil (modified from Hoekstra and Chamberlain, 1964)

Initial and final water contents (weight of water per weight of clay x 100 per cent) after the frozen sample was exposed to an electrical gradient of 1 V/cm for 24 hours.

Soil	Temperature	Initial Water Content.	Final Water Content within 1 cm from Anode	Final Water Content within 1 cm from Cathode
Wyoming Bentonite	-2.0°C	341	275	456
	-1.5°C	265	134	310
New Hampshire Silt	-1.5°C	30	27	32
	-1.0°C	28	21	40

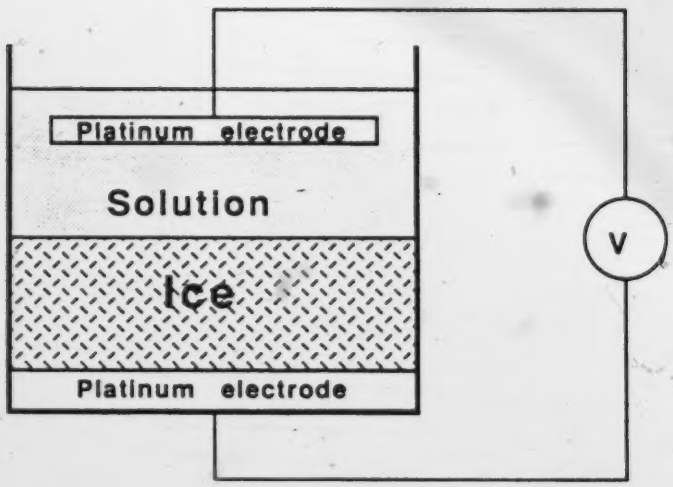

Figure 2.1 Schematic experimental set up for measurement of freezing potentials.

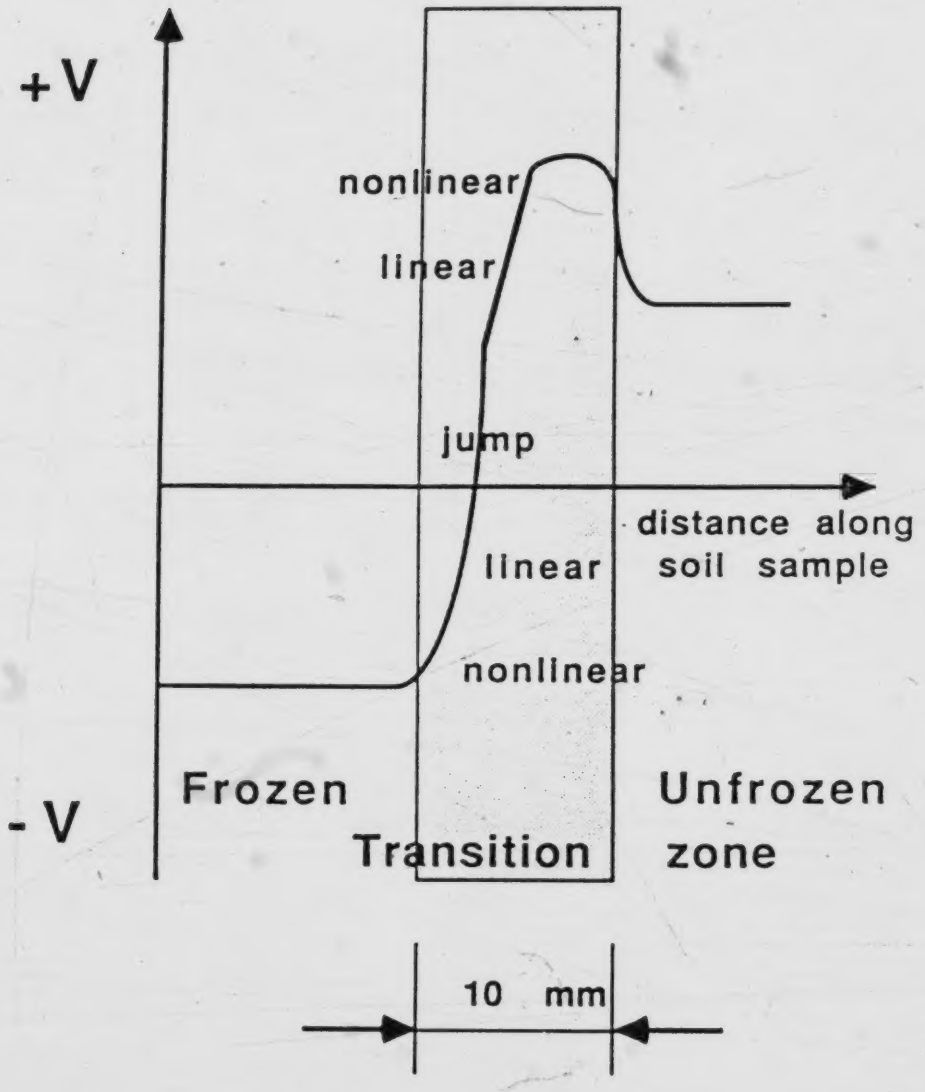

Figure 2.2 Electric freezing potential at a phase boundary (modified from Yarkin, 1984)

3. An electric source in freezing soil.

3.1 Introduction

In this section an electric source within a freezing soil is postulated, implying that electro-osmosis can take place in a freezing soil. Evidence for the existence of such an electric source is provided. As the size of this electrical source is unknown, and is expected to extend over rather limited distances, the influence of the size of the electric source on water transport within a soil is studied theoretically and solvedusing a finite difference program. It is concluded from this analysis that the efficiency of electro-osmosis is not adversely affected by close electrode spacing, which suggests that the dimension of the electric source has little influence on the process.

If electro-osmosis takes place to any extent in freezing soils it follows that the Clausius-Clapeyron equation should not explain all phenomena in freezing soils. It is demonstrated that the pressures developed in soils overconsolidated due to freeze-thaw effects can not be explained with the Clausius-Clapeyron equation. It is suggested that electro-osmosis may cause high consolidation stresses in freezing soils. Evidence of high consolidation stresses due to freezing is presented.

3.2 Identification of an electric source.

When an external electric current is applied to a frozen soil sample considerable water redistribution, and ice lensing, may occur as pointed out in Table 2.1. If an internal source of electric current exists in the freezing soil, part of the ice lensing process would have to be ascribed to electro-osmosis. Since no obvious electric power source is available in thermally induced frost heaving. Howevever, in this chapter a possible internal electric source will be identified. For this purpose the freezing potentials in dilute solutions, discussed in the previous chapter, will be returned to, with special interest directed to the charge transfer mechanism between the frozen and unfrozen solution.

Gross (1968) explains the development of freezing potentials and charge transfer in solutions. Electric potentials are generated because ions are selectively rejected as a solution freezes, and replaced by hydrogen ions in order to retain charge balance within the frozen solution. Charge transfer, as well as the number of ions replaced by hydrogen, is strongly dependent on the availability of hydrogen ions within the solution.

Charge transfer can be increased by a slow freezing rate or by the introduction of a shunt. The shunt may be external or internal; an internal shunt is a metal rod placed in the container in which the freezing experiment takes place. A shunt basically forms a short circuit between

the frozen and unfrozen solution. A slow freezing rate allows hydrogen ions to diffuse towards the freezing front (Gross, 1968). When an external shunt is used H_2 and O_2 development may be discerned at the anode and cathode respectively, according to the scheme in Fig 3.1.

The same mechanism probably takes place in freezing soil during ice lens formation; its influence on soil freezing will be discussed below.

The high potential differences in dilute solutions are sustained because the electrical conductivity of the system is extremely low; in particular the conductivity of the ice - solution interface is thought to be very low (Hobbs, 1974). In soils this is in general not true; the mineral skeleton, including the water of the double layer, forms a matrix of relatively high conductivity. Dilute solutions have a well defined freezing interface, while this is not the case for soils. The existence of a frozen fringe in soils is well established, e.g. Booth (1982) and Penner (1986). As a consequence it is hard to imagine an interface between the ice lens and the soil matrix that is abrupt and of high electrical resistance as one finds in dilute solutions. One can visualize the soil particles acting as small internal shunts. This would explain the smaller values of the electric freezing potentials in soils.

When water molecules break up to form hydrogen and oxygen ions, the hydrogen ions move across the phase boundary into the ice. When this process takes place in

soil, electro-osmosis, being the process when water is transported due to drag forces exerted by the movement of ions, is actually under way. It is not possible now to give an indication of the distance that the hydrogen ions have to travel through the unfrozen soil. The only data on the dimension of an electric source is given by Yarkin (1986); he found that the changes in electric potential in a freezing sand took place in a region with a thickness of 20 mm.

However, the distance over which the electric potential drop occurs does not necessarily influence the efficiency of the mechanism dramatically. In the following section this problem will be discussed in detail.

3.3 Electrode spacing and electro-osmosis

Analytical solutions for electro-osmotic consolidation problems are presented by Esrig (1968). However, only the consolidation of soil between two rows of electrodes is considered, as it is assumed that no water flows from beyond the anode (Fig. 3.2A)

Bjerrum et al. (1967) describe an application of electro-osmosis, and from their results it can be seen that the flow of water from the area beyond the anode is considerable. No solutions are available in the literature for a configuration where water flow is allowed beyond the anode (Fig. 3.2B).

A solution to this problem will be presented in this section. The assumptions made are those listed by Mitchell (1976):

1. Homogeneous and saturated soil.
2. The physical and physico-chemical properties of the soil are uniform and constant with time.
3. No soil particles are moved by electrophoresis.
4. The velocity of water flow by electro-osmosis is directly proportional to the voltage gradient.
5. All the applied voltage is effective in moving water.
6. The electric field remains constant with time.
7. The coupling of hydraulically- and electrically- induced flows can be described by equations of irreversible thermodynamics, (see Mitchell, 1976).
8. There are no electrochemical reactions.

Based on these assumptions Esrig (1968) developed the formulation using the following symbols.

v_e = velocity of water due to electric gradient;

v_h = velocity of water due to hydraulic gradient;

k = coefficient of hydraulic permeability;

k_e = coefficient of electro-osmotic permeability;

γ_w = unit weight of water;

V = voltage difference applied;

u = pore pressure;

c_v = coefficient of consolidation, $c_v = \frac{k}{m_v \gamma_w}$;

m_v = coefficient of compressibility;

ξ = variable defined below;

t = time;

x = distance;

d = distance between anode and cathode;

H = height of sample;

L = length of sample;

l = L - d;

$$v_e = k_e \frac{\partial V}{\partial x} \qquad [3.1]$$

$$v_h = \frac{k}{\gamma_w} \frac{\partial u}{\partial x} \qquad [3.2]$$

$$\frac{\partial v_e}{\partial x} + \frac{\partial v_h}{\partial x} = m_v \frac{\partial u}{\partial t} \qquad [3.3]$$

$$\frac{\partial^2 u}{\partial x^2} + \frac{k_e}{k} \gamma_w \frac{\partial^2 V}{\partial x^2} = \frac{1}{c_v} \frac{\partial u}{\partial t} \qquad [3.4]$$

$$\xi = \frac{k_e \gamma_w}{k} V + u \qquad [3.5]$$

$$c_v \frac{\partial^2 \xi}{\partial x^2} = \frac{\partial \xi}{\partial t} \qquad \left(\frac{\partial V}{\partial t} = 0.\right) \qquad [3.6]$$

The only deviations from Esrig's formulation are the boundary conditions. The boundary conditions considered in this study are (see Fig. 3.3):

<u>At t = 0,</u>

1. $0 < x < 1$, $V = 0.$, $u = 0.$, $\xi = 0.$
2. $1 < x < L$, $V = \frac{x-1}{L-1} V_{max}$, $u = 0.$,

   Choose V_{max} such that $\xi_{max} = \frac{k_e \gamma_v}{k} V_{max} = -100.$

   Thus $\xi = - \frac{x-1}{L-1} 100.$

<u>At t = t,</u>

1. $x = 0.$, no inflow of water, $\frac{\partial \xi}{\partial x} = 0.$
2. $x = 1.$, continuity of flow, $\left[\frac{\partial \xi}{\partial x}\right]_1 = \left[\frac{\partial \xi}{\partial x}\right]_2$
3. $x = L$, no pressure build up, ξ = constant = $-100.$

It is also assumed that the permeability of the electrodes is such that they do not influence the flow of water in any manner.

As the boundary conditions are rather complex, the method of finite differences which is simple and straight forward to carry out was employed to solve this boundary value problem. A computer code was written for this purpose and it is presented in Appendix A.

It may be useful to recall that this problem was studied to investigate the influence of electrode spacing on water redistribution within a sample, due to an internal electric source existing in freezing soil for which the physical extent is unknown. Three values for the proportion of the spacing between the electrodes (d) and the length of the sample (L) were studied: d/L : 1.0; 0.5; 0.1. The calculations for these values give an appreciation of the

influence of electrode spacing on the water transport within a sample. Results for each case are presented in Figs. 3.4-3.6. For a sample of a constant size, in which the distance (d) between the eletrodes is varied and the cathode is fixed at the end of the sample, the conclusions are summarized below. As a check of the computational procedure it is interesting to note that Fig. 3.4 should be the same as Fig 15.18 in Mitchell (1976) after some accommodation in the nomenclature.

A comparison of the percent consolidation, or average consolidation, is shown in Fig. 3.7. The "time constant" is defined as $T_c = \frac{c_v\ t}{H^2}$, the average consolidation is defined as in Lambe and Whitman (1969, p. 410). Note that the consolidation occurs faster as the distance between the electrodes decreases.

The volumetric strain, which can be interpreted as water flow, which for this study is of more importance, for the three cases is shown in Fig. 3.8. The total volumetric strain is defined as the consolidated volume compared to the total initial volume of the sample. It is remarkable that the volumetric strain for closely spaced electrodes is considerably higher than for widely spaced electrodes, and this effect is more pronounced at small time constants.

It is important to note that the velocity of water flow by electro-osmosis is assumed to be directly proportional to the voltage gradient. In the cases outlined, the voltage gradient is the reciprocal of the spacing between the

electrodes. From the figures, however, it is possible to calculate water flow for other configurations (for example: constant voltage gradient, but different spacing).

Before further discussion of electro-osmosis in freezing soil, the Clausius-Clapeyron equation and its application in freezing soils will be outlined.

3.4 The Clausius-Clapeyron equation.

The Clausius-Clapeyron equation describes the pressure and temperature differences between two phases for a system in equilibrium. A discussion of this equation can be found in Edlefson and Anderson (1943) and Miller (1980).

Although equilibrium is formally required, the equation has been used extensively for freezing soils, which is indeed not an equilibrium condition. With some reservation, however, the use of the Clausius-Clapeyron equation is accepted (Konrad, 1980). Usually it is used with $P_i = 0$ (P_i = pressure in ice), when no overburden pressure is applied, or P_i equal to the overburden stress (see for instance Low et al., 1968a; and Miller, 1980).

Here, the use of the Clausius-Clapeyron equation itself is not under discussion. However, it will be shown that the Clausius-Clapeyron equation is not capable of explaining some phenomena observed during soil freezing.

3.5 Consolidation due to freezing and thawing.

The consolidation of soil due to freezing and subsequent thawing is a well known fact, and although it has even been used for practical applications (e.g. Katz and Mason, 1970), the mechanism is not well understood. First some laboratory results will be discussed, then one remarkable field example.

3.5.1 Laboratory examples

Nixon and Morgenstern (1973) studied the residual stress in soils developed due to freezing and thawing. They presented a mechanism which explained the processes that occur in the freezing soil. Their mechanism included consolidation of the soil due to freezing.

Chamberlain and Gow (1978) and Chamberlain and Blouin (1978) studied the change of the macrostructure of a soil as a consequence of freezing. They suggested that overconsolidation occurred. This overconsolidation would be accompanied by macroscopic cracks (shown in their pictures) filled with ice lenses, and on a microscopic scale particle rearrangement would occur.

Chamberlain (1980) introduced Casagrande's empirical approach (Casagrande, 1936) to derive overconsolidation stresses from void ratio - effective stress measurements. This method allowed the overconsolidation stresses in the mechanism proposed by Nixon and Morgenstern (1973) to be quantified. He presented two examples in which this method

was used. Overconsolidation pressures of 240 and 660 kPa were attained after 3 and 4 freeze-thaw cycles in Ellsworth clay which had been initially consolidated to pressures of 16 and 228 kPa respectively.

Pusch (1977) investigated the change in microstructure of two clays as a consequence of freezing; one consisting mainly of carbonate minerals, illite and quartz; the other of feldspar, quartz and illite. The salt content of the clays was respectively lower than 0.5 %, and approximately 3.5 %. One sample of each clay type was frozen in liquid nitrogen (quickly) and another was frozen relatively slowly. The difference of the subsequent microstructure was apparent, with the slowly frozen samples showing prolific domain formation, which was related to consolidation, while the structure of the rapidly frozen samples was supposedly not altered significantly. Clay aggregates were mostly preserved, which, according to Pusch, indicates that intra-aggregate water did not freeze, and was not tranfered to the freezing zone to any great extent. Another observation that can be made from this data was that the rate of freezing influences the development of microstructure within the fine grained soils.

The formation of domains of soil particles as a consequence of freezing seems to be in agreement with observations by Yong et al. (1985), who observed a decrease of the liquid limit due to repeated freezing. The liquid limit decreases as domains are formed. They do not break

apart when water is added and the soil is remoulded.

Tsytovich (1975) stated that soil in between ice lenses may be consolidated up to the point when it reaches its plastic limit. This, indeed, implies the development of very high stresses.

3.5.2 A field case

A remarkable and well documented example from the field illustrating the very high consolidation stresses which can be reached by freezing is presented by Chamberlain et al. (1978). Clay found in the Prudhoe Bay region was overconsolidated up to 3800 kPa. Sellman and Chamberlain (1979) added some information to the study previously cited. They reported that the determination of the preconsolidation pressure was difficult as the void ratio - log effective stress curves did not have a sharp well defined break. The maximum preconsolidation pressure in this report was determined to be 1900 kPa for a silty clay, instead of 3800 kPa reported earlier. In the sandy silt the preconsolidation pressure was 1600 kPa. They also reported a high areal variability in the preconsolidation pressure. From geologic and climatic evidence the authors concluded that consolidation could only be ascribed to freeze-thaw phenomena, with minor contributions due to chemical and loading effects. A discussion of other processes leading to "apparent" overconsolidation is given in Appendix B.

3.6 Clausius-Clapeyron and overconsolidation.

The suctions in freezing soils are usually completely interpreted as occurring due to phase change, and predicted by the Clausius-Clapeyron equation. (e.g. Konrad and Morgenstern, 1980)

In this section it is assumed that when no load is applied the magnitude of the effective stress on the soil skeleton and the suction in the soil water are equal in a freezing soil. As a consequence the calculated overconsolidation pressures are upper bounds for those actually existing in a freezing soil. When the pores in a freezing soil contain both water and ice this is a conservative assumption in light of the argument presented here. A more correct approach is presented by Miller (1978) and is discussed in Section 3.8.

Explanation of the overconsolidation stresses in the Prudhoe Bay with the Clausius-Clapeyron equation is impossible, as illustrated below.

The Clausius-Clapeyron equation can be applied in two ways,

1. in the first approach the pressure in the ice, P_i, will be assumed to be known; the temperature at which consolidation took place can then be calculated. The ice pressure is assumed to be equal to the overburden stress in the analysis.
2. in the second approach the freezing temperature, T, is assumed to be known and the pressure in the ice can then

be calculated.

The first approach:

For the soil from Prudhoe Bay, the freezing point depression of the soil water is reported to be T = -1.8 °C based on its electric conductivity. Equation (11.4) in Miller (1980):

T = freezing temperature (°C);

P_i = pressure in ice (kPa);

P_d = pressure in soil water (kPa);

Π_d = osmotic pressure of the soil water (kPa);

$$T = 8.2 \times 10^{-4} (P_d - \Pi_d) - 8.9 \times 10^{-4} P_i \quad °C \qquad [3.7]$$

with $P_d = P_i = 0.$; $\Pi_d = 2195$ kPa.

For the conditions in which the overconsolidation occurred in the clayey silt,

$P_d = -1900$ kPa

$P_i \simeq 200$ kPa

$\Pi_d = 2195$ kPa

$$T = 8.2 \times 10^{-4} (-1900 - 2195) - 8.9 \times 10^{-4} \times 200. \quad °C.$$

$$T = -3.18 \ °C$$

Similarly for the conditions in which the overconsolidation

occurred in the silty sand,

P_d = -1600 kPa

$P_i \simeq$ 200 kPa

Π_d = 2195 kPa

$T = 8.2 \times 10^{-4} (-1600 - 2195) - 8.9 \times 10^{-4} \times 200.$ °C.

$T = -2.93$ °C

If the Clausius-Clapeyron equation is assumed to explain the behavior of the soil, consolidation would have taken place at a temperature of -3.18 °C in the silty clay, and at -2.93 °C in the silty sand. This is unlikely to be true; the unfrozen water content at this temperature would be extremely small, leading to an insignificant mobility of pore water. This argument is especially valid for the silty sand layer (Mageau and Morgenstern, 1980).

The second approach:

A temperature just below the freezing point depression of the soil water at which this water is still mobile should be chosen.

Assume T = -2.2 °C.

Equation (11.5) in Miller (1980):

$$P_i = 0.917 \times (P_d - \Pi_d) - 1.12\ 10^3 \times T \quad \text{kPa} \qquad [3.8]$$

P_d = -1900 kPa

Π_d = 2195 kPa;

P_i = -1199 kPa.

From the discussion in Section 3.8 it follows that this result is contradictory to the stress distribution in freezing soils.

This case study shows that the Clausius-Clapeyron equation does not suffice to explain all phenomena in freezing soils. Another example is discussed in the next section.

3.7 Collapse of interlaminar spacing

An interesting problem is the collapse of the spacing between layers in montmorillonite upon freezing.

Anderson and Hoekstra (1965) measured the d(001) spacing of various homoionic derivatives of montmorillonite using X-ray diffraction. Fig 3.9 shows the geometry of a montmorillonite crystal and clarifies the terms d(001) and d = half distance. Consistently water moved away from between the interlaminar spaces when freezing was induced, reducing the d(001) spacing considerably.

For sodium montmorillonite at a water content of 232 % a decrease of the d(001) spacing from 33 Å to 19 Å was observed. On thawing the process seemed reversible. In a cooling cycle spontaneous freezing occurred at

-5 °C accompanied by collapse of the d(001) spacing. On warming, however, ice persisted till a temperature of -1 °C was reached, while the spacing remained 19 Å. Another noteworthy observation was that the water migration associated with the collapse of the d(001) spacing occurred within 2 minutes. Other investigators arrived at the same conclusions (e.g. Ahlrichs and White, 1962).

Bolt and Miller (1956) and Warkentin et al. (1957) provided data on the swelling pressure, along with a calculation procedure, for sodium montmorillonite. For a soil water composition of 10^{-4} moles NaCl they found swelling pressures of

1. 1000 kPa for a half distance of 15 Å
2. 2000 kPa for a half distance of 10 Å
3. 5000 KPa for a half distance of 5 Å

d = half distance between clay layers;

w = water content;

M = mass of clay;

P = concentration of clay per cent by weight;

V = volume of free liquid;

S = specific surface area.

The half distance is defined as:

$$d = \frac{V}{M \times S} = \frac{100 - P}{P \times S} \qquad [3.9]$$

The basic finding of the studies quoted above was that the swelling pressure can be attributed to the difference in osmotic pressure between the internal and external soil solution. Double layer calculations allow the swelling pressures for montmorillonite to be estimated with quite high accuracy.

Yong et al.(1963) studied the relationship between swelling pressure and temperature in the temperature range from 1 to 23 °C. The swelling pressure decreases slightly with temperature, as predicted by the theory (Bolt and Miller, 1956).

Apparently there is no reason why the results of swelling pressure and collapse of interlaminar spacing can not be related.

The collapse of the interlaminar spacing can be caused by two phenomena:

1. very high positive ice pressures, pushing the clay layers together,
2. or very high negative pore water pressures, sucking the pore water from between the clay layers.

The first mechanism seems highly unlikely, as the sample was thin and not confined (Anderson and Hoekstra, 1965).

The swelling pressure can be interpreted as the pressure needed to separate the clay layers, because that is the basis of the theory as presented by Bolt and Miller (1956). See Fig 3.9 for a scheme explaining the logic behind this, as well as Mitchell (1976, p. 263). A d(001) spacing

of 19 Å corresponds with a half distance of just less than 5 Å, as the thickness of the montmorillonite layer is 9.6 Å. This means that negative pore pressures of more than 5000 kPa occur when montmorillonite is frozen. Similarly as for the clay from Prudhoe Bay two approaches can be used, calculating the ice pressure being the first, calculating the freezing temperature the second.

The first approach gives:

$P_i = 0$ kPa

$P_d = -5000$ kPa

$T = -4.1$ °C

which is contradictory to the temperature cited by Anderson and Hoekstra (-1 °C).

The second approach gives (Fig. 3.10):

$T = -1$ °C

$P_d = -5000$ kPa

$P_i = -3465$ kPa

Some effort was spent searching for reported negative pressures in ice, and none were found. The most common assumption is that ice is at atmospheric pressure or at the overburden stress.

From the discussion in the next section it follows that negative ice pressures cannot exist. Therefore the Clausius-Clapeyron equation cannot account for these high overconsolidation pressures. which have been obseved both in the laboratory and in the field. Electro osmosis may, however, explain the observed behavior.

3.8 Effective stress in freezing soil

Miller (1978) proposed a method to calculate the stress conditions for what he called a SS soil. An SS soil is a soil in which all the particles are in direct solid to solid contact, e.g. dune sand or a poorly graded silt. The method is based on the principle of stress partition in unsaturated soils introduced by Bishop and Blight (1963).

σ = total stress;

σ' = effective stress;

χ_a = stress partitioning factor in air-water system;

χ_i = stress partitioning factor in ice-water system;

P_a = pressure in air;

P_d = pressure in pore water.

$$\sigma = \sigma' + \chi_a P_d + (1 - \chi_a) P_a \qquad [3.10]$$

Miller proposed for a freezing saturated soil:

$$\sigma = \sigma' + \chi_i P_d + (1 - \chi_i) P_i \qquad [3.11]$$

A similar formula can readily be adopted for any soil if the contact between the particles is not solid to solid. In unfrozen soils the uniqueness of χ_a has been disputed. However, it has no importance whether χ_i is unique or not for any soil, as long as its value is between 0. and 1. the argument presented here is valid. The formula is based on the condition of equilibrium, and that the ice can be considered as a viscous liquid.

Returning to the Prudhoe Bay example, with $\sigma \simeq 200$ kPa $\sigma' \simeq 200$ kPa;

$$200 \text{ kPa} = 200 \text{ kPa} + \chi_i P_d + (1 - \chi_i) P_i$$
$$0 = \chi_i P_d + (1 - \chi_i) P_i$$

with χ_i between 0 and 1., and $P_d = -1800$ kPa; P_i should be positive, which is contradictory to the pressures deduced from the Clausius-Clapeyron equation.

Similarly for the stresses deduced for the montmorillonite from Anderson and Hoekstra (1965):

$$0 = \chi_i P_d + (1 - \chi_i) P_i$$

with χ_i between 0 and 1., and $P_d = -5000$ kPa; P_i should be positive, which is contradictory to the pressures deduced from the Clausius-Clapeyron equation.

It is remarkable that Low et al. (1968a and b) also linked the data of Anderson and Hoekstra (1965) and those of Bolt and Miller (1956) and Warkentin et al. (1957) in their thermodynamic model without noting any inconsistency. This despite the fact that they assumed the ice to be under atmospheric pressure, and having the same thermodynamic properties as pure bulk ice.

From the above discussion it may be concluded that the pressures in the ice in the cited examples had to be positive.

3.9 Pressures in the electro-osmotic model.

In this section a consequence of the electro-osmotic model described previously on the pressure distribution in freezing soil is explored.

The freezing soil can be represented by the model shown in Fig 3.11. As ice is formed cations are rejected instantaneously, to retain charge balance hydrogen ions migrate towards the freezing front causing electro-osmosis.

Between the external solution (see Figs 3.10 and 3.11, terminology from Gray and Mitchell, 1967) and the ice phase the Clausius-Clapeyron equation is valid (although the two phases are not in equilibrium). Between the external and the internal solution, and within the internal solution, however, the pressure difference is dictated by electro-osmosis. As the flow of hydrogen ions, and thus water, is directed towards the ice, the pressures of the

internal solution will be lower than those in the external solution. Consequently the pressure of the internal solution will be lower than predicted by the Clausius-Clapeyron equation.

That high suctions can be generated in the internal solution may be demonstrated by the following example. The maximum pore pressure developed due to electro-osmosis is determined by the no flow condition:

$$u_{max} = \frac{k_e}{k} \gamma_w V \qquad [3.12]$$

assuming, at a temperature of say - 0.5 °C:

$k_e = 0.2 \times 10^{-5}$ cm^2/s V, from experimental results reported later

$k = 10^{-10}$ cm/s, from Nixon (1987)

V = 1 Volt over the frozen - unfrozen interface.

u_{max} = 20 000 g/cm^2 = 2000 kPa.

c_v in frozen soil is very low, $c_v = 10^{-6}$ cm^2/s from experiments reported later. As a consequence consolidation will be slow.

3.10 Conclusions

The two examples, soil from Prudhoe Bay and freezing of bentonite, illustrate that the consolidation stresses in freezing soils can't always be predicted by the Clausius-Clapeyron equation. Postulation of a charge imbalance between the frozen and unfrozen soil due to freezing, analogous to freezing of solutes, leading to electro-osmosis, may explain the observed stresses. ,

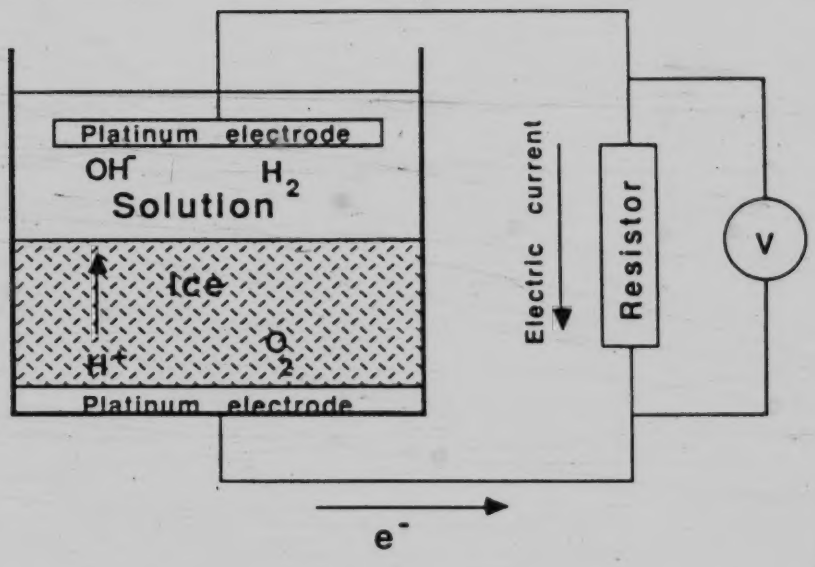

$$2\ H_2O + 2\ e^- \longrightarrow H_2 + 2\ OH^-$$

$$2\ H_2O \longrightarrow 4\ H^+ + O_2 + 4\ e^-$$

Figure 3.1 Freezing of dilute solutions; measurement of freezing current

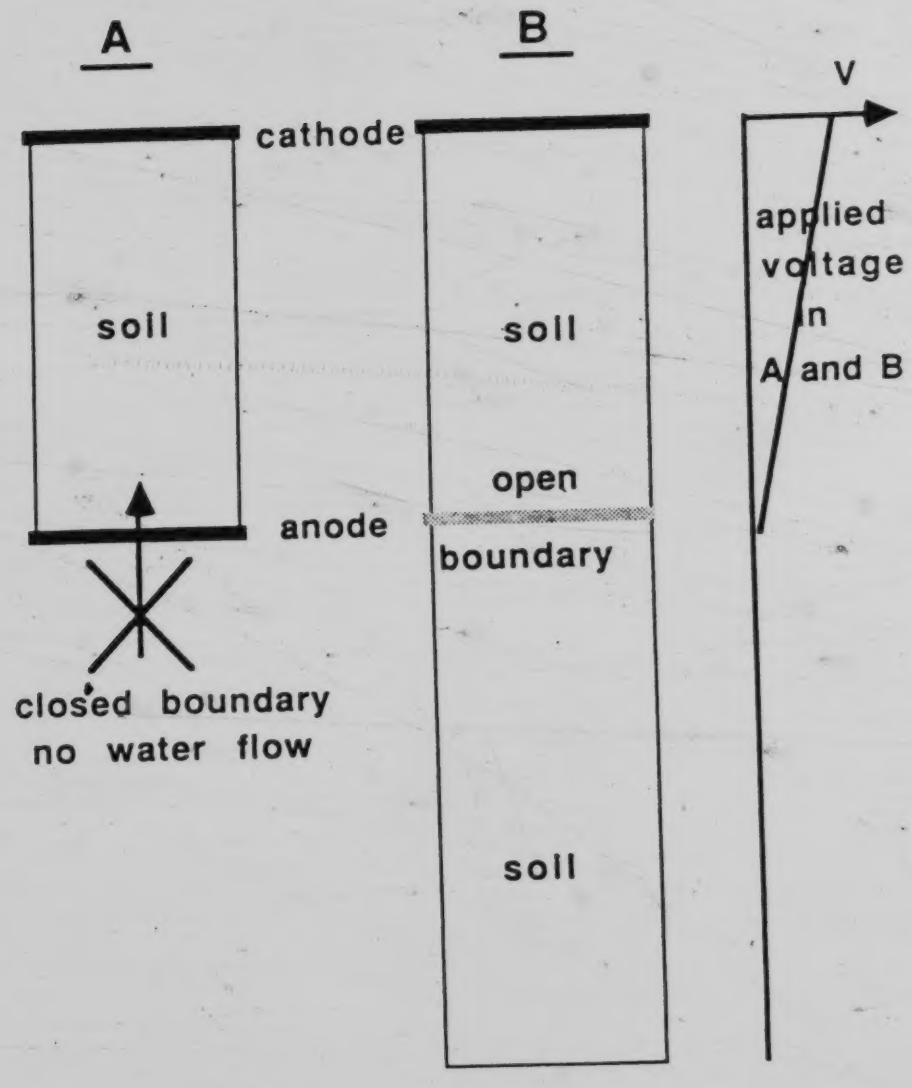

Figure 3.2 Boundary conditions in electro-osmotic problem;
A: after Esrig (1968); B: conditions assumed here.

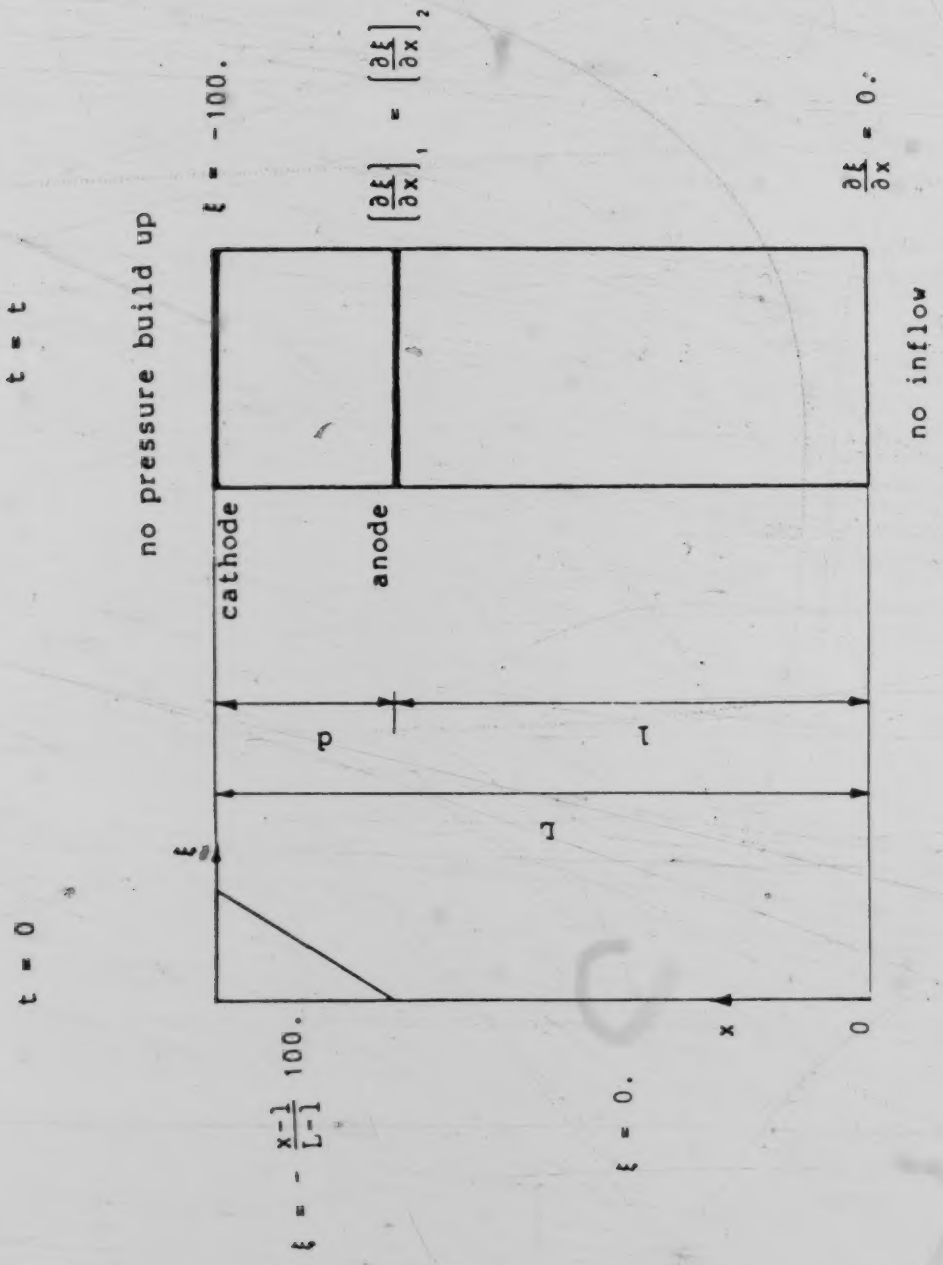

Figure 3.3 Boundary conditions assumed in analysis.

ELECTRO–OSMOTIC CONSOLIDATION

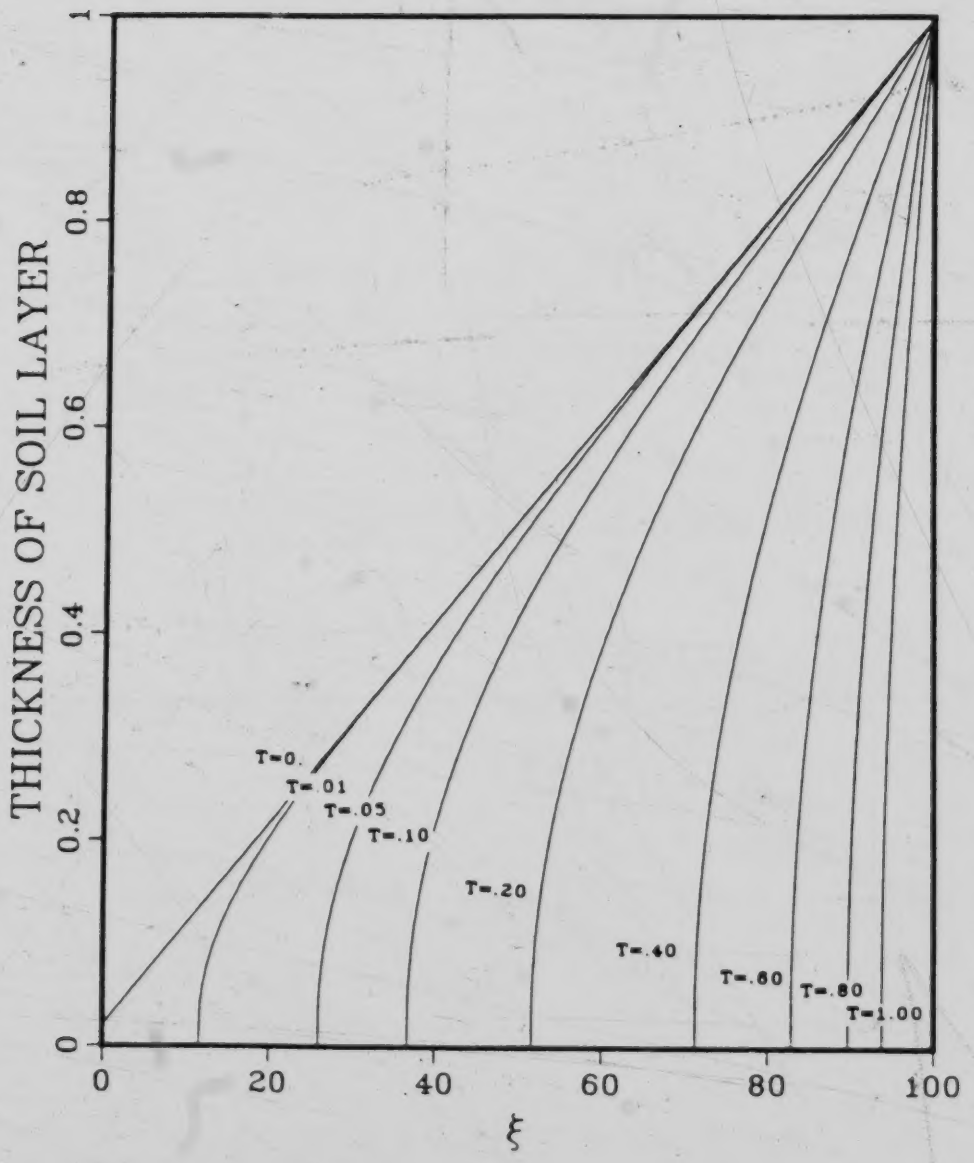

Figure 3.4 Electro-osmotic consolidation diagram for d/L=1

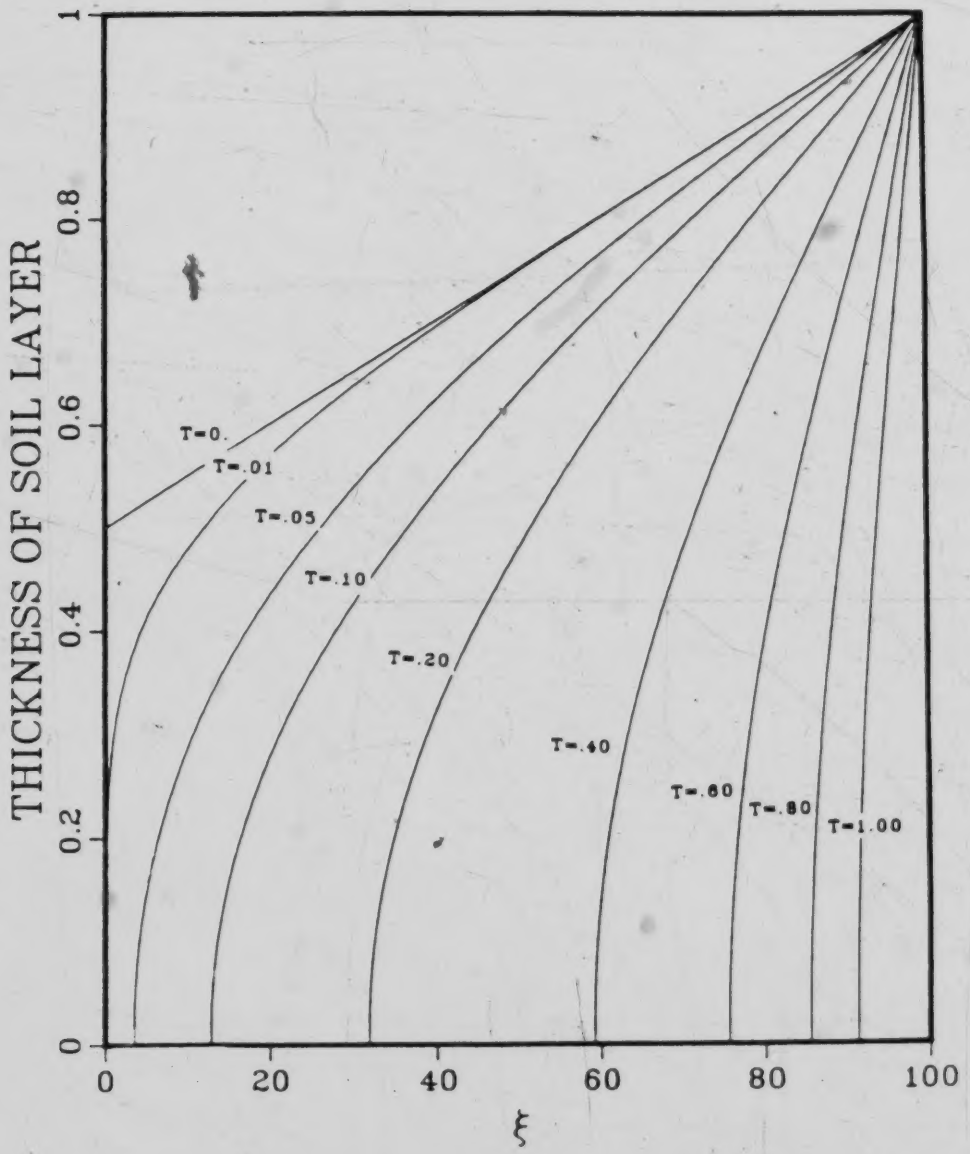

Figure 3.5 Electro-osmotic consolidation diagram for d/L=.5

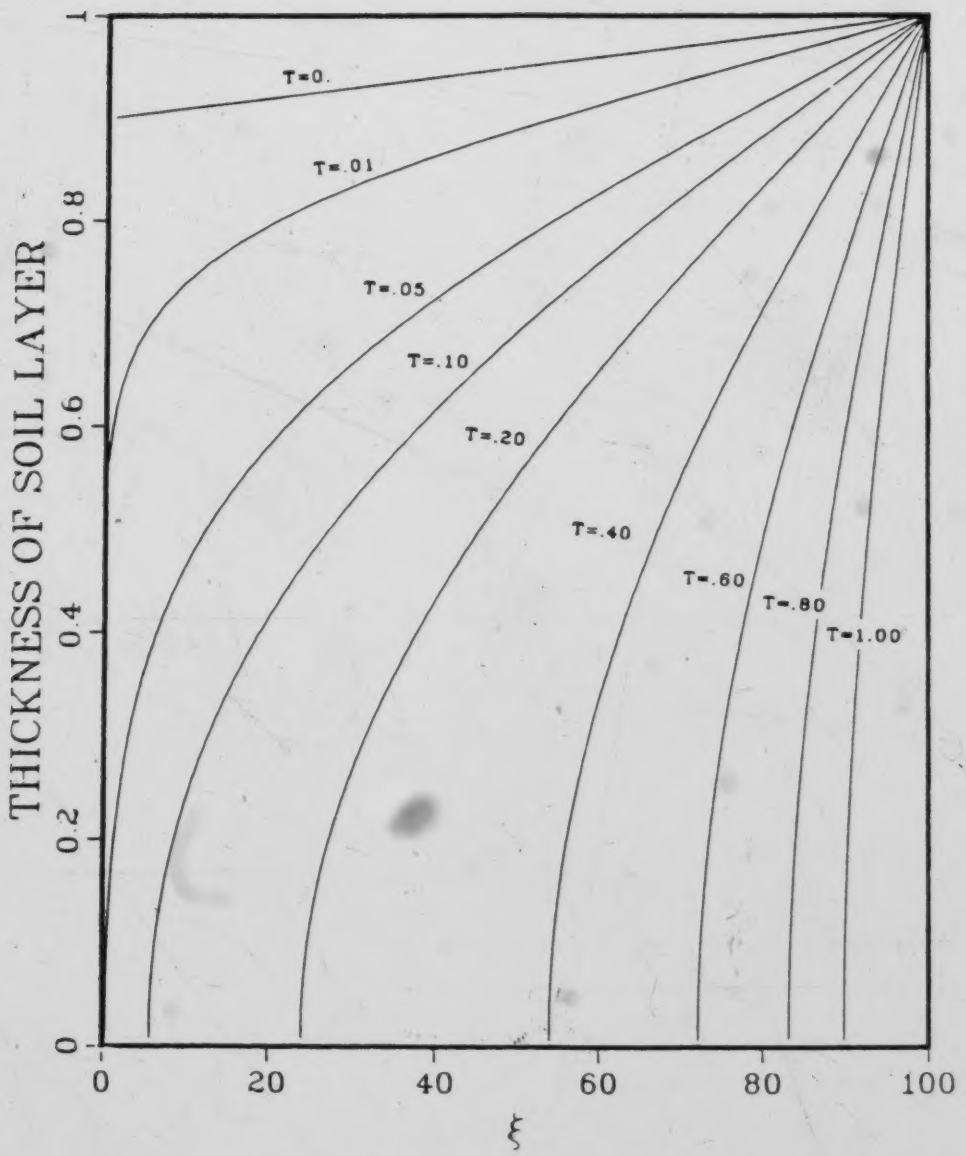

Figure 3.6 Electro-osmotic consolidation diagram for d/L=.1

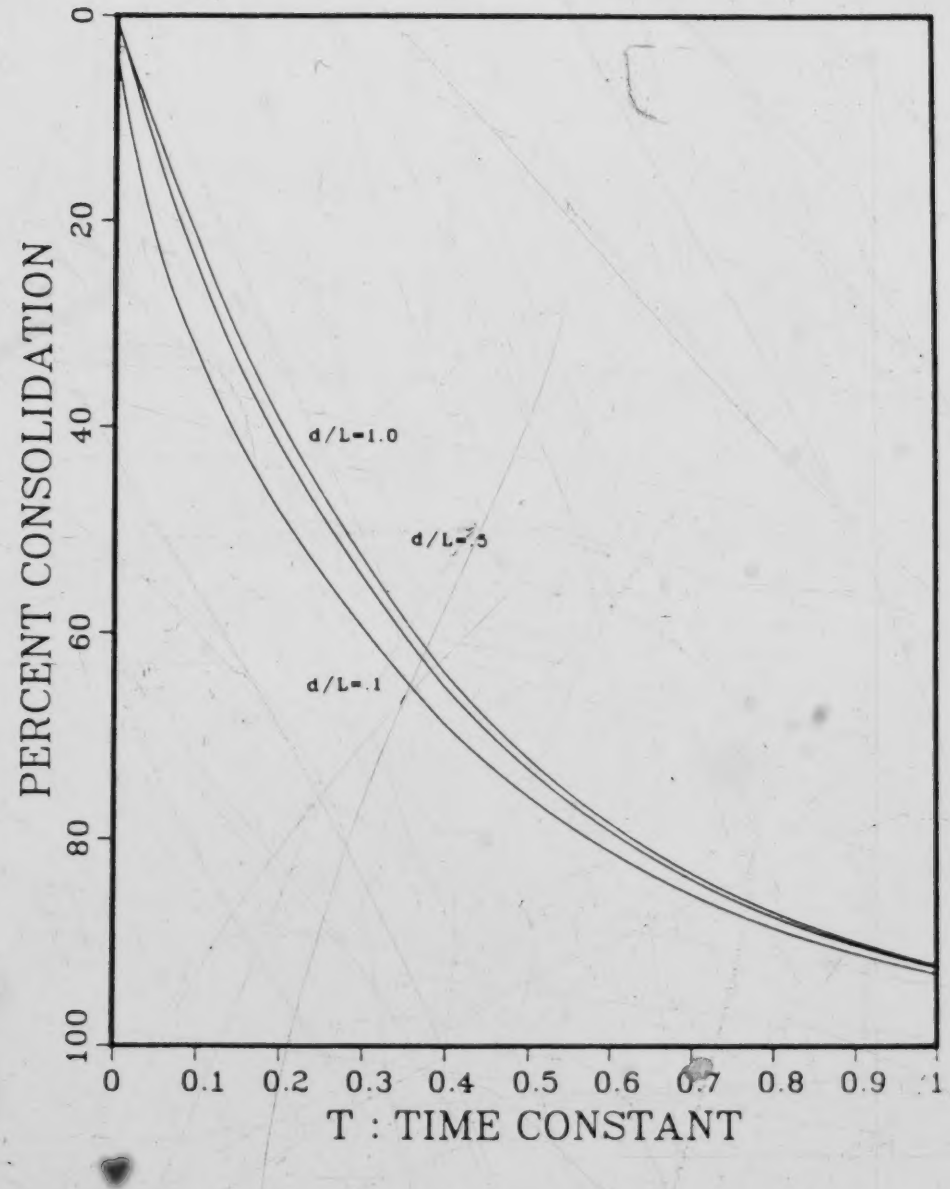

Figure 3.7 Amount of consolidation as a function of time, for d/L = .1, .5, and 1.

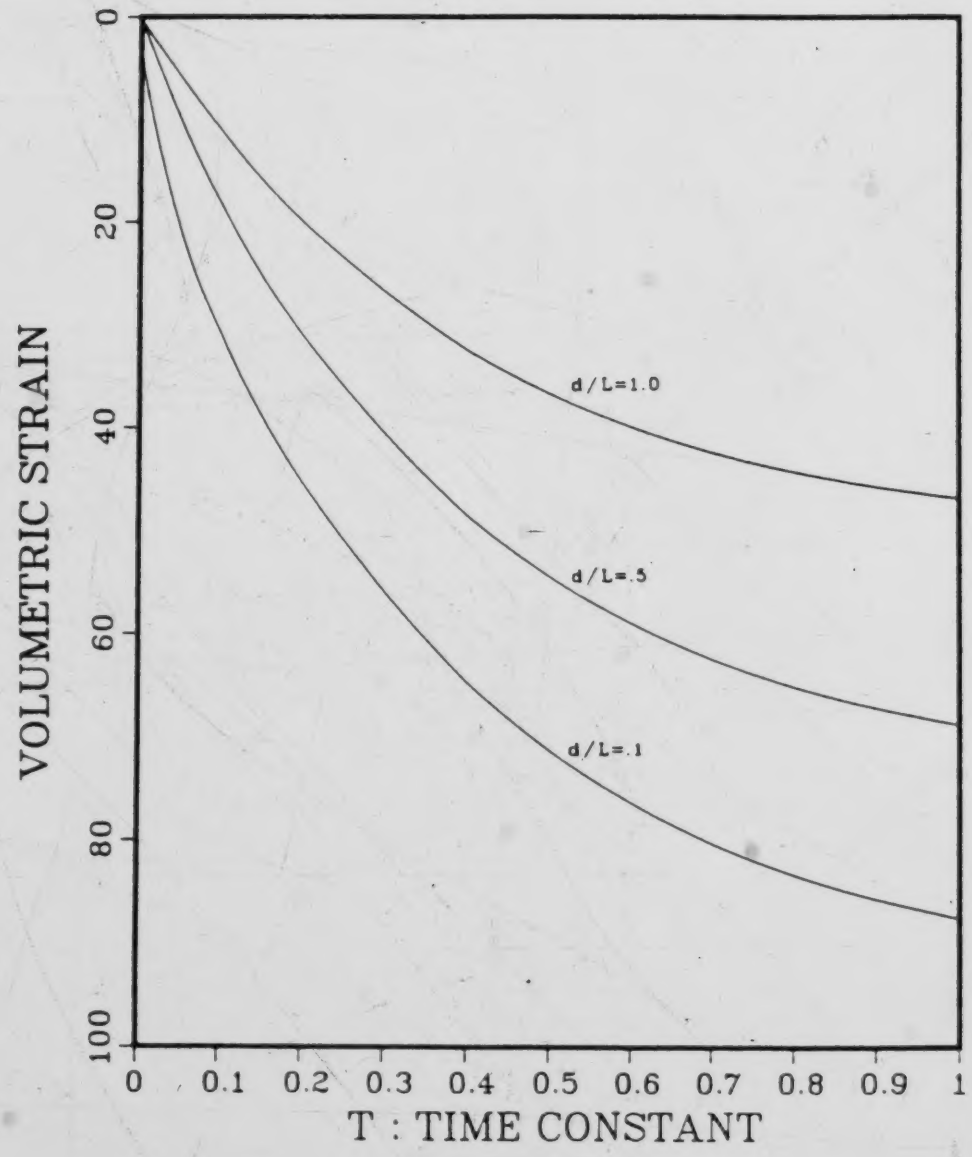

Figure 3.8 Total water flow as a function of time, for d/L = .1, .5, and 1.

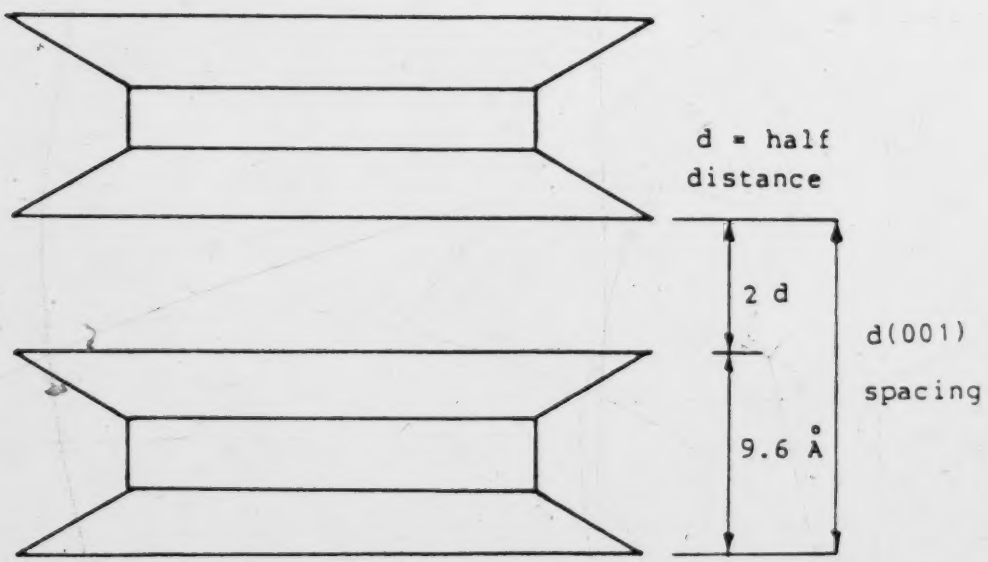

Figure 3.9 Relationship between 'd = half distance' and 'd(001) spacing'.

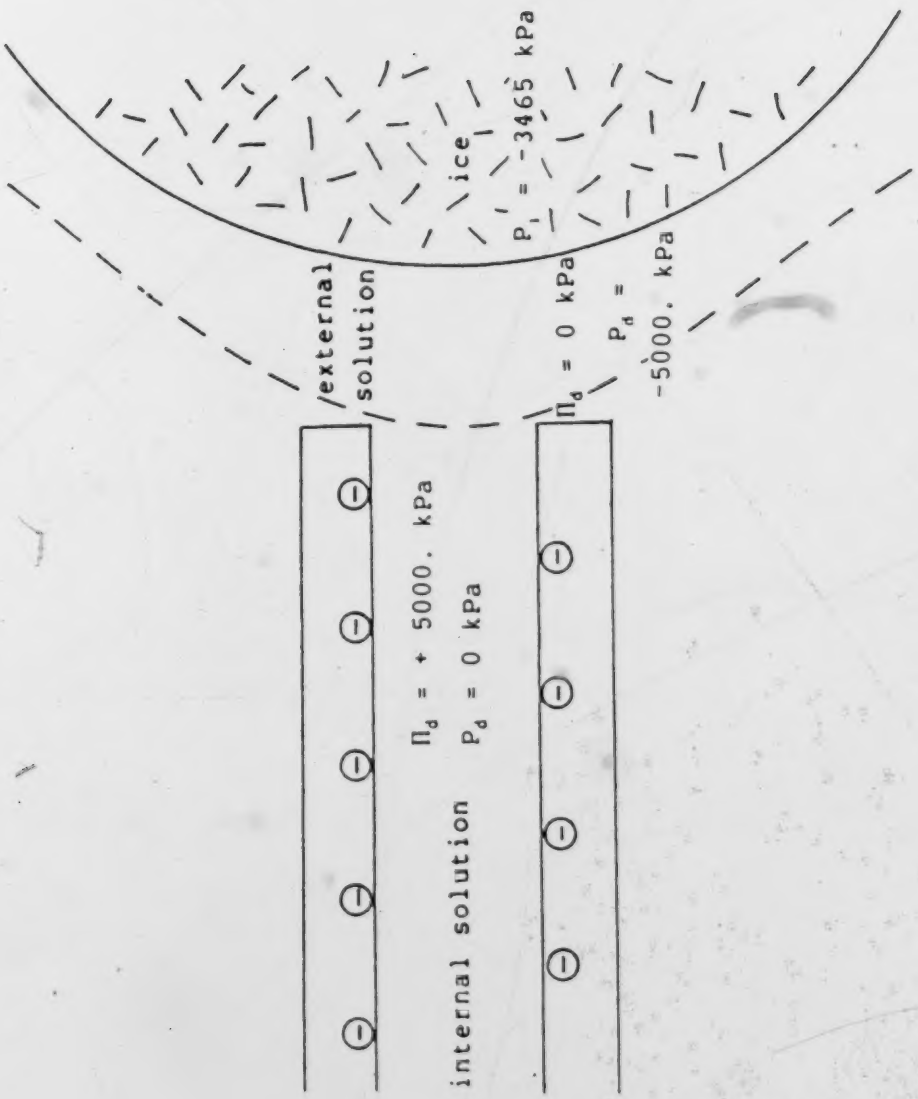

Figure 3.10 Pore pressures in montmorillonite when it is assumed that the Clausius-Clapeyron equation alone is valid.

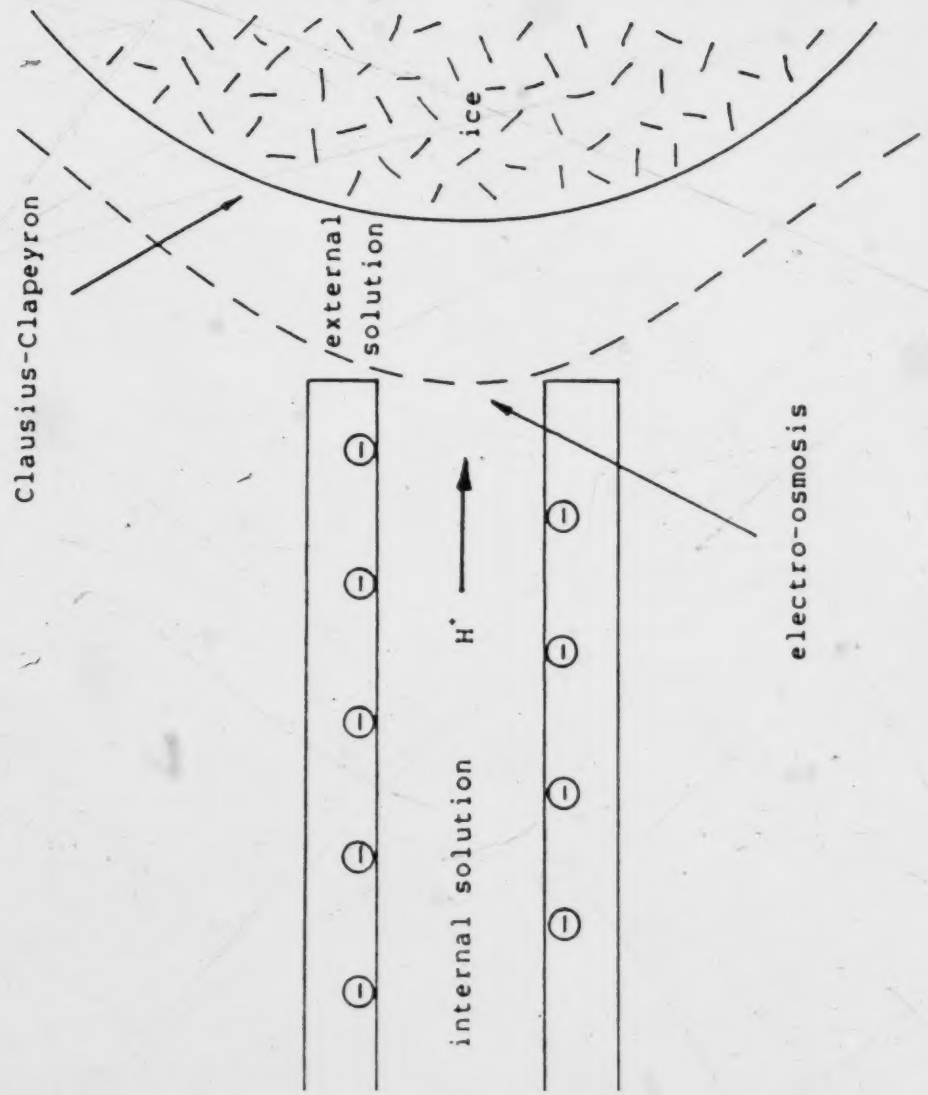

Figure 3.11 Pressure relationships in electro-osmotic model.

4. Experimental programme

4.1 Introduction

In the experimental programme electro-osmosis is studied under varying temperature conditions in the laboratory.

The purpose of this programme was to find the electro-osmotic conductivity (k_e) of frozen soils, and its variation with temperature. To study the implications of the measured freezing potentials a better knowledge of the physico-chemical properties of frozen soil is required. Electro-osmosis is also of interest for another reason. Like thermal gradients, electric gradients not only cause water to move through frozen soil, they also induce the formation of ice lenses. Besides the experiments by Hoekstra and Chamberlain (1964) no other experiments on electro-osmosis in frozen soil have been reported in the literature.

4.2 Apparatus and sample preparation

A Geonor triaxial cell was modified for electro-osmosis experiments at controlled temperature, Figs. 4.1 and 4.2. For this purpose a plastic tube with rubber seals embedded in the top and bottom were placed inside the cell, creating two separate spaces. A controlled temperature bath circulating fluid around the inner chamber to control the sample temperature. The temperature was maintained constant by pumping a mixture of glycol and water at constant

temperature at a rate of 1 to 2 litres per minute through this space. The mixture was kept at a constant temperature using a Hotpack refrigerated bath-circulator. Temperature control in the cold bath was accurate to within 0.05 °C, and was monitored with RTD's located in the cold bath, connected to a data aquisition system. The plastic lines between the cold bath and the electro-osmosis cell were insulated with foam of 10 mm thickness.

The inner chamber provided space for a sample holder. The sample holder consisted of a plastic sleeve, one half of which had a slightly greater inside diameter than the other, creating a little rim in the middle of the tube. The soil sample was placed in the half of the tube with the greater diameter such that it rested on the rim. A bentonite slurry filled the other half of the tube. Silver-silverchloride electrodes were placed at the top and bottom of the sample holder.

In order to ensure that no heat would flow from the metal top and bottom of the cell, the sample holder and electrodes were placed on a plastic pedestal and a plastic cap was placed on the top. The loading ram of the triaxial cell was left in place and was used to measure the deformation of the sample and to apply a small load to the sample. A Linear Voltage Displacement Transducer (LVDT) was fitted to the loading ram to measure the vertical deformation of the sample during the experiment.

In order to connect the electrodes to a power source holes were drilled in the bottom of the cell, the pedestal, the top cap, and the loading ram.

The whole assembly was placed inside an insulating box, which was placed in a cold room held at a temperature between -1 °C and +2 °C. The power source was a Hewlett and Packard 6216A, the applied voltage was measured using a Fluke 8050A, and the current through the sample was measured with a shunt: a resistor placed in series with the soil sample, over which the voltage drop was measured. Preparation of the electrodes was according to a modification of the procedure described by Elrick et al. (1976). Two silver plates were placed 30 mm apart in a 250 ml beaker filled with saturated KCl, silver cables connected them with a power source. Approximately 1.2 V was applied which coloured one electrode (grey-purple, $Ag + Cl^- \rightarrow AgCl + e^-$) and created gas bubbles (H^2) at the other. When the polarity was switched no gas bubbles were seen on the coated electrode.

Athabasca Clay was used throughout the experimental programme. A slurry of Athabasca Clay was consolidated to 210 kPa in five steps in a large consolidometer. Samples with a diameter of 25 mm were cut from the resulting block with a Shelby tube.

The Athabasca Clay had LL = 44.8 % and PL = 20. %. Additional information can be gained from Smith (1972), who used material from the same source area, but slightly

different composition, in thaw consolidation experiments. His data is summarized in Table 4.1

Several methods for freezing the soil sample were used.

1. The unfrozen sample on top of a bentonite paste were placed in a plastic sample holder and allowed to freeze in a cold room at -25 to -30 °C. Visible continuous ice lenses were formed in both the soil sample and the bentonite. Extrusion of the sample occurred due to expansion of the water within the sample. Ice polygons were observed and will be discussed in the next paragraph.
2. The unfrozen soil sample was placed in the sample holder and frozen in a cold bath at -25 °C in a plastic bag. Continuous ice lenses were formed. The bentonite paste was added just before the sample holder was placed in the electro-osmosis cell, and therefore frozen slowly, as a consequence large ice lenses were formed in the bentonite.
3. The sample was put in a plastic bag and hung in a cold bath at -50 °C. No continuous lenses were formed, but small expansion cracks were visible.

Upon inspection of samples prepared according to procedure 1 and procedure 2, small polygons were visible in the first centimeter adjacent to the end of the sample. Plate 4.1 illustrates the morphology of the polygons at the top of sample #4. Beneath the first centimeter no ice polygons were

detected. Pictures of the polygons showed a particular similarity with those reported by Chamberlain and Gow (1978), and Chamberlain and Blouin (1978); both size and shape agree well. Sample preparation with procedure 3 yielded polygons over the whole sample. They were not as regular as in the samples prepared according to 1 and 2. The sides of the samples were now clearly bulging, leading to the following mechanism for formation of these polygons. When the sample is frozen, an outer soil skin freezes first, this skin is cold and brittle. As time progresses the inside of the sample freezes, and as the sample is saturated, freezing is accompanied by expansion of the in situ water. The outside skin is forced to deform and cracks. When electo-osmosis was applied, these cracks became filled with water, leading to actual ice filled cracks. The pattern reported by Chamberlain and Gow (1978) may have originated in the same manner.

4.3 Test procedure and experimental results

After preliminary tests, the following procedure proved most satisfactory.

The soil sample was placed in a plastic bag, and hung in a cold bath at ≃ -50 °C. The soil sample was taken out of the bath after several hours and machined to a cylinder with a lathe in a cold room at ≃ -25 °C, such as to fit easily in the sample holder. The outside of the sample was greased and the sample was slid into the sample holder. A paste of

bentonite at a temperature of 0 °C filled the other half of the sample holder, and the completed sample was placed in the electro-osmosis cell.

Subsequently, the bath circulator, at the required temperature was switched on. The time required to reach thermal equilibrium, as illustrated by the LVDT readings indicating the expansion due to freezing of the water in the bentonite, was up to 24 hours.

When all the movement had ceased, the power source attached to the electrodes was switched on. During the experiment the voltage drop over the sample was constant and equal to 5 Volts. The temperature in the refrigerated bath circulator and the air temperature in the insulating box were monitored continuously and recorded on a data acquisition system. The heave of the sample as ice lenses formed was also measured continuously with the LVDT connected to the loading ram.

At the end of each experiment the sample and sample holder were taken out of the cell and cooled to -25 °C. The sample was taken out of the sample holder and pictures were taken, after which the sample was cut into pieces, and the water content of these pieces was measured gravimetrically.

The results for a typical experiment (#6) are presented in Fig. 4.3 to 4.5. The experimental results are compiled in Appendix D. Figure 4.3 shows the water content profile of the Athabasca Clay sample after the experiment was completed. The bottom of the figure corresponds with the

contact between the bentonite and the soil sample. The original water content was 28.5 %, as determined from the soil cuttings collected during preparation of the sample. Heave, measured with an LVDT, as a function of time is displayed in Fig. 4.4. Figure 4.5 illustrates the typical decrease of the electrical current through the sample with time.

4.4 Discussion of experiments

The measurement of the temperature and applied current was not a problem. Measurement of the heave, however, turned out to be rather difficult.

The purpose of the heave measurement was to find the variation of water intake into the soil sample throughout the experiment. As described previously, the sample was seated on a rim to allow upward movement only when water was taken up from the bentonite. To facilitate this movement the circumference of the sample was greased before placement in the sample holder. A continuous record of the displacement of the top of the sample was obtained with an LVDT.

At the end of each experiment the water content profile of the sample was determined. As the initial water content of the sample was known the heave due to the addition of water to the sample could be calculated.

Since the water intake into the sample was determined by two independent measurements, heave and water content comparison was possible. Water content data consistently

showed a higher uptake than the heave measurements. Heave measurements as shown in Fig. 4.4 were generally linear for some time (24 hours), after which the heave rate decreased. According to the theory, as presented later, this decrease should take place at a much later stage. When the linear portion of the heave measurement is extrapolated for the whole testing period, it is found that the agreement with the heave from the water content data is quite good. Most likely the heave measurements became disturbed in the later stages when the bentonite, which supports the soil sample partially, consolidated. When the bentonite was placed in the sample holder its temperature was between 0 and -1 °C. Freezing of unfrozen water in the bentonite caused it to expand, and to push the soil sample upward until thermal equilibrium was reached. As a consequence however, the soil sample was lifted off the rim, such that there was a small space between the rim and the sample. The water taken in by the soil sample was withdrawn from the bentonite, and created an empty space close to the positive electrode. Settling of the bentonite and consequent lowering of the soil sample probably counteracted the heave of the soil sample in the later part of the experiment. As a consequence the total heave measured with the LVDT is less than the heave resulting from ice lens formation in the sample.

4.5 Finite difference model

In order to interpret the experimental results, a theoretical analysis of the electro-osmotic consolidation problem was made. A finite difference program for a two soil (bentonite and soil sample) system was written. The principles on which the program is based are outlined in the Section 3 and the finite difference program is presented in Appendix A.

Some additional information is required for the case of a two-soil system and this is outlined below.
Continuity of flow between the bentonite and the soil sample requires:

k_{eB} = electro-osmotic conductivity of bentonite;
k_{eS} = electro-osmotic conductivity of soil;
q = rate of water flow
t = time
u = pore pressures
V = electric potential across sample
γ_w = density of water
ΔV_B = voltage drop over bentonite
ΔV_S = voltage drop over soil sample

1. The system is closed on both ends, leading to the boundary condition:

$$\frac{\partial \xi}{\partial x} = 0 \text{ , for all t, at both ends of the sample.}$$

2. $q_B = q_S$ [4.1]

at the interface of the bentonite and the soil sample.

3. $u = 0$,at $t = 0$, for all x

Thus, from 3.

$\frac{\partial u}{\partial x} = 0$, at $t = 0$, for all x

And in general:

$$q = - \frac{k}{\gamma_w} \frac{\partial u}{\partial x} - k_e \frac{\partial V}{\partial x} \qquad [4.2]$$

and at the interface of the bentonite and soil sample:

$$- k_{eB} \frac{\Delta V}{\Delta x_B} = - k_{eS} \frac{\Delta V}{\Delta x_S}$$

If one choses $\Delta x_B = \Delta x_S$, and assumes that V_B and V_S are linear through the bentonite and the soil sample respectively.

$$k_{eB} \Delta V_B = k_{eS} \Delta V_S$$

$$\Delta V_B = \frac{k_{eS}}{k_{eB}} \Delta V_S \qquad [4.3]$$

With these boundary conditions the program for the two-soil system was written as presented in Appendix C.

However, a contradiction in the theory becomes apparent when Ohm's law is considered:

I : electric current through bentonite and soil sample

R_B : electrical resistance of bentonite

R_S : electrical resistance of soil sample

$$\Delta V_B = R_B I \qquad [4.4]$$

$$\Delta V_S = R_S I \qquad [4.5]$$

$$I = \frac{\Delta V_B}{R_B} = \frac{\Delta V_S}{R_S}$$

$$\Delta V_B = \frac{R_B}{R_S} \Delta V_S \qquad [4.6]$$

Equations 4.3 and 4.6 combined yield:

$$\frac{R_B}{R_S} = \frac{k_{eS}}{k_{eB}} \qquad [4.7]$$

While the specific conductivity of soils may vary a hundredfold, Casagrande (1948) reported that values of k_e are remarkably constant, and equal to 5×10^{-5} cm^2/s V. However, Mitchell and Gray (1967) concluded that the electro-osmotic conductivity is not constant, but varies with moisture content (for instance, for a soil at w = 30 % they reported values of $k_e = 0.5 - 1.5 \times 10^{-5}$ cm^2/s V). They provide values that allow the relationship represented by

equation 4.7 to be verified. Also these values are not compatible with equation 4.7. The problem therefore remains unresolved, and makes the introduction of the boundary conditions in the finite difference program somewhat ambiguous. A solution for this problem is presented below.

4.6 Exploration of electro-osmosis problem

Figures 4.6 to 4.10 are results of the computer modelling of the electro-osmosis problem for different combinations of k_B/k_S and V_B/V_S. The bottom of each figure coincides with the contact between the bentonite and the soil sample. The horizontal axis indicates the amount of water accumulated at each level in the sample at time constants T_c varying from 0 to 0.02. The actual values derived from the computer program are valid for a sample (bentonite and soil) of height 1, hydraulic conductivity 1, and compressibility 1, while $\xi = 100$. In the following section the proper scaling techniques to interpret the results for a real soil will be discussed.

A physical explanation of the peculiar shape of the curves in Figs. 4.6 to 4.10 is presented in Appendix F.

Published results of the unfrozen water content in soils at temperatures below 0 °C (e.g. Anderson and Morgenstern, 1973) show that the amount of water that remains unfrozen in bentonite is significantly greater than in any other soil. It has been demonstrated that a good correlation exists between the unfrozen water content at a

temperature and the plasticity index of the soil (e.g. Anderson and Andersland, 1978). Based upon this observation it may be inferred that the hydraulic conductivity of bentonite at temperatures below 0 °C is greater than for other soils.

If the hydraulic conductivity of the bentonite is considerably higher than that of the Athabasca Clay, and the electro-osmotic conductivity do not differ, it follows that the exact value of the hydraulic conductivity of the bentonite does not influence the flow of water in the soil sample. The bentonite then just acts as a reservoir of unfrozen water for the soil sample to draw from during the experiment. The finite difference program illustrates the justification of this statement.

A glance through the experimental results shows that in all experiments water was accumulated at the interface between the bentonite and the soil sample (Fig. 4.3). If the value of k_B/k_S is smaller than 1, this can never be the case; only values larger than 1 are considered.

Comparison of Figs. 4.6, 4.7, and 4.8 shows that for a constant value of V_B/V_S the distribution of water as well as the rate of flow in the soil sample is quite insensitive to the variation of k_B/k_S, as long as k_B is larger than five times k_S.

Comparison of Figs. 4.7, 4.9, and 4.10 shows that for a constant value of k_B/k_S, the value of V_B/V_S determines the distribution of water in the soil sample. Therefore, in

order to determine which theoretical profile should be used for comparison with a set of experimental data, only the shape of the water content distribution needs to be considered.

Another point of interest is the variation of the amount of water stored in the soil sample with time. The total amount of water flowing from the bentonite into the soil sample as a function of the time constant T_c is examined in Fig. 4.11 for $k_B/k_S = 10.$ and $k_{eB}/k_{eS} = 1.$ For values of T_c smaller than 0.02 this relationship is virtually linear. In the following it will be shown that the time constant in the experiments was of the order of $T_c = 0.01$. For this reason the amount of water accumulated in the soil sample: $(\Sigma q\Delta t)_1$ varies linearly with T_c:

$$\frac{T_c}{(\Sigma q\Delta t)_1} = \text{Constant} \qquad [4.8]$$

Taking the previously dicussed factors into account, it may be deduced that this "Constant" is only a function of V_B/V_S.

However, study of the variation of the ratio of T_c over $(\Sigma q\Delta t)_1$ with changing V_B/V_S shows that the relationship is rather insensitive. When three values of V_B/V_S are considered: 0.33, 1., and 3., and constant ratio of the hydraulic conductivities (=10.); the variation of T_c over $(\Sigma q\Delta t)_1$ is approximately 2 % (the values were: 0.00559, 0.00563, 0.00570; the value of $(\Sigma q\Delta t)_1$ for $T_c = 0.01$ is represented by the shaded area in Fig. 4.6, and can be

deduced similarly for Figs. 4.8 and 4.9.) As a consequence, the calculated value of the electro-osmotic conductivity of the soil is quite insensitive to the values inserted in the computer program, which certainly enhances the reliability of the finite difference method.

4.7 Dimensional analysis

For quantitative analysis it is thought easiest to compare the experimental water content profiles with the amount of water stored according to the computer program. In order to do this, a dimensional analysis of the electro-osmotic consolidation problem was carried through, which is presented below.

$i = \frac{h}{H}$ hydraulic gradient

k = hydraulic conductivity

k_e = electro-osmotic conductivity

m_v = compressibility of soil

A = area of sample

H = height of sample

Δt = time increment

γ_w = density of water

$\int_0^t q\, dt = \Sigma q \Delta t$: flow over some period of time

$\Sigma q \Delta t = \Sigma (A\ k\ i\ \Delta t)$

The amounts of water moving into or out of two samples with different geometry (Fig. 4.12), are compared at the moment that the time constants for the two cases are equal, which means that they are at the same stage of consolidation. This comparison enables the identification of the relevant factors which should be taken into account when an actual sample is compared with the results from the computer simulation.

$$\frac{(\Sigma q \Delta t)_1}{(\Sigma q \Delta t)_2} = \frac{(k\ i\ \Delta t)_1}{(k\ i\ \Delta t)_2} \qquad [4.9]$$

assuming $\gamma_1 = \gamma_2 = 1\ g/cm^2$, and

$$T_1 = T_2 \qquad [4.10]$$

$$\frac{\Delta t_1}{\Delta t_2} = \frac{\left[\frac{k}{m_v \gamma_w H^2}\right]_2}{\left[\frac{k}{m_v \gamma_w H^2}\right]_1} \qquad [4.11]$$

inserting $\frac{\Delta t_1}{\Delta t_2}$ from Equation 4.11 in Equation 4.9:

$$\frac{(\Sigma q \Delta t)_1}{(\Sigma q \Delta t)_2} = \frac{(h\ H\ m_v)_1}{(h\ H\ m_v)_2} \qquad [4.12]$$

Applying this result to electro-osmotic consolidation, in which the maximum pore pressure can be expressed as:

$$h = \xi = \frac{k_e}{k} \gamma_w V \qquad [4.13]$$

$$\frac{(\Sigma q \Delta t)_1}{(\Sigma q \Delta t)_2} = \frac{(\xi\ H\ m_v)_1\ c_{v2}}{(k_e\ H\ V)_2} \qquad [4.14]$$

In program described in Appendix C:

$\xi_1 = 100\ (g/cm^2)$

$H_1 = 1\ (cm)$, H is the height of the whole sample

$m_{v1} = 1\ (cm^2/g)$

$$\frac{(\Sigma q \Delta t)_1}{(\Sigma q \Delta t)_2} = \frac{c_{v2}\ 100}{k_{e2}\ H_2\ V} \qquad [4.15]$$

$$\frac{k_{e2}}{c_{v2}} = \frac{(\Sigma q \Delta t)_2}{(\Sigma q \Delta t)_1}\ \frac{100}{H_2\ V} \qquad [4.16]$$

It is now possible to determine the electro-osmotic conductivity and the consolidation constant from the experimental data presented previously. To illustrate the analysis an example is worked out. Test data for experiment #6 on Athabasca clay are presented in Fig. 4.3.
In experiment:

$H_2 = 8$ cm (H is the height of the sample holder)

c_{v2} = unknown

k_{e2} = to be determined

$V = 5$ Volts

$$k_{e2} = c_{v2}\ \frac{(\Sigma q \Delta t)_2}{(\Sigma q \Delta t)_1}\ 2.5 \qquad [4.17]$$

As presented previously,

$$\frac{T_c}{(\Sigma q \Delta t)_1} = \text{Constant}$$

for each set of values of V_B/V_S, and k_B/k_S.
As a consequence, the estimate of k_{e2} is entirely independent of c_{v2}.

$$k_{e2} = \frac{T_c}{(\Sigma q \Delta t)_1} \frac{H_2^2}{t_2} (\Sigma q \Delta t)_2 \; 2.5 \qquad [4.18]$$

Calculation of $(\Sigma q \Delta t)_2$ based on moisture content data:

w = water content, g H_2O/g Soil;
W_w = weight of water;
W_s = weight of soil;
γ_w = density of water;
γ_s = density of soil solids;
H_w = equivalent height of water;
H_s = equivalent heigth of solids;
Δw = change in water content;
Δh = change in equivalent height of water;

$$w = \frac{W_w}{W_s} = \frac{\gamma_w H_w}{\gamma_s H_s} = \frac{H_w}{2.65 H_s}$$

$$H_s + H_w = 4.0 \text{ cm}$$

$$w + \Delta w = \frac{\gamma_w (H_w + h_w)}{\gamma_s H_s}$$

$h_v = (\Sigma q \Delta t)_2 = 2.65\ H_s\ \Delta w$

$w = 27.5\ \%$

$H_s = 2.31$ cm

$h_v = 6.13\ \Delta w$

Average increase of the moisture content in experiment #6, after 4000 minutes = 240,000 seconds:

$\Delta w = (33.2 - 27.5)\ \% = 5.7\ \%$

$h_v = 6.13\ 0.057 = .35$ (cm)

$k_{e2} = 0.0056\ \frac{64}{240{,}000}\ 0.35\ 2.5 = .13 \times 10^{-5}$ ($cm^2/s\ V$)

Or based on the straight part of the heave data, after 1200 minutes = 72,000 seconds:

$h_v = 0.12$ (cm)

$k_{e2} = 0.0056\ \frac{64}{72{,}000}\ 0.12\ 2.5 = .18 \times 10^{-5}$ ($cm^2/s\ V$)

These two numbers compare reasonably well, and indicate the accuracy of the measurements.

The same procedure was used to calculate the k_e from the other experiments. As it was difficult to obtain water content data for experiments conducted at low temperatures the heave data were used to calculate the water intake in those cases. The data are summarized in Table 4.2 and Fig 4.13.

It is also possible to express the electro osmotic conductivity of a soil in terms of charge transfer (e.g. Mitchell, 1976, p. 359-363). It can then be defined as:

I = electric current

q = hydraulic flow rate

$$q = k_i I \qquad [4.19]$$

k_i is expressed in moles Water/Faraday. It can be shown that (Mitchell, 1976, eq. 15.64)

$$k_i = 5600 \frac{k_e}{\sigma} \qquad [4.20]$$

k_e in $cm^2/s\ V$; and σ in mhos/cm.

Ice lenses formed in the soil sample, and as a consequence σ changed through the testing period. For this reason it was thought reasonable to calculate an average value of σ. Experiment #6 will be used as an example. The average current through the sample is calculated:

$$\bar{I} = \frac{28.4\ 10^{-3}\ \text{amp hr}}{67\ \text{hr}} = 0.42 \times 10^{-3}\ \text{amp}$$

Using Ohm's law to calculate the electrical resistance of the soil sample, assuming that the electrical resistance of the bentonite is neglegible compared to that of the soil sample, which is a reasonable assumption (Hoekstra and McNeil, 1973).

ΔL : length of the sample

A = area of the sample

R = electrical resistance of soil sample

$$R = \frac{5 \text{ Volts}}{0.42 \times 10^{-3} \text{ amp}} = 11.8 \times 10^{3} \text{ ohm}$$

$$\sigma = \frac{\Delta L}{A\ R} \qquad [4.21]$$

$$\sigma = \frac{4 \text{ cm}}{10 \text{ cm}^2\ 11.8 \times 10^{3} \text{ ohm}} = 34 \times 10^{-6} \text{ mhos/cm.}$$

$1/\sigma$ = 294 ohm m which is its resistivity

$$k_1 = 5600 \cdot \frac{0.13 \times 10^{-5}}{34 \times 10^{-6}} = 209 \qquad \text{in moles Water/Faraday.}$$

A summary of the results is given in Table 4.3

The resistivity data are of interest as a check on the quality of the experiments. It is well established that the resistivity decreases rapidly as the temperature decreases in frozen soil, Hoekstra and McNeil (1973). The results presented here show this decrease, however, experiments #5 and #6 do not follow the trend. This probably indicates an inaccuracy in the temperature measurements during these experiments.

An estimate of the coefficient of consolidation of the frozen soil can be obtained by comparison of the shapes of the water content profiles after the experiments with the theoretical water storage diagrams (Figs. 4.6 to 4.10).

The computation is carried out for experiment #6, using the water content profile presented in Fig. 4.3, and the theoretical water storage diagram which fits best is Fig. 4.10. For comparison, the relative increases of the water contents are used, i.e. increase in the middle of the sample compared with top and bottom.

By superposition of the theoretical diagram over the water content profile, one can deduce that the general shape of the water content profile falls between the theoretical curves for $T_c = 0.01$ and 0.02, but closer to $T_c = 0.01$. A value of $T_c = 0.012$ seems appropriate. Therefore:

$$c_v = \frac{T_c H^2}{t} = \frac{0.012 \times 64.}{2500 \times 60} = 5.1 \times 10^{-6} \text{ cm}^2/\text{s}$$

The same technique was applied for the water content diagrams, summarized in Table 4.4.

4.8 Summary and discussion of results

Values of the electro-osmotic conductivity k_e of frozen Athabasca clay at temperatures above -0.5 °C are the same as for unfrozen Athabasca Clay. Between -0.5 °C and -1.5 °C the electro-osmotic conductivity decreases rapidly from 0.2×10^{-5} to 0.002×10^{-5} $\text{cm}^2/\text{s V}$.

The electro-osmotic conductivity k_i, which expresses the efficiency of the electro-osmotic process, is the same for frozen and unfrozen Athabasca Clay, and equal to 45 moles of Water/Faraday, except for temperatures close to

-0.5 °C when a maximum of 230 moles of Water/Faraday is recorded.

It should be noted that the experiments were not conducted under ideal conditions, which may be reflected by the values of the electro-osmotic conductivity deduced. The value of k_e for the unfrozen soil is quite low, experiments conducted by Gray and Mitchell (1967) suggest a value of 0.5 - 1.5 x 10^{-5} cm^2/s V. However, their values were based on streaming potential data, and as a consequence virtually ideal conditions were obtained. When actual electro-osmosis experiments are carried out the flow of electric current through the sample does not remain uniform through the sample, as discussed by Miller (1955), and this phenomenon influences the measurements. The determination of the electro-osmotic conductivities also requires the electro-osmotic theory proposed by Esrig (1968) to be valid for the experimental conditions. Since many of the assumptions are only partially fulfilled some inaccuracy is introduced. Taking these circumstances into account it may be recommended to consider the values of the electro-osmotic conductivities as showing trends rather than absolute values.

When electric current flows through soil, cations in the pore water move towards the cathode and anions move towards the anode. Drag on water by the ions causes it to move along with these ions. As soil particles carry a negative charge, the pore water contains a significantly

higher number of cations than anions (the size of the cations and anions is also of importance). As a consequence more water is moved towards the cathode than towards the anode, resulting in a net flow of water towards the cathode.

Gray and Mitchell (1967) proposed a theory to calculate the electro-osmotic conductivity k_i. The theory is based on the Donnan distribution of ions in soil. The pore water of a soil is divided in an internal and an external solution. The ion distribution fulfills the requirements of electric neutrality of the external solution, and of the internal solution together with the charged soil skeleton, and chemical equilibrium of the external and internal solutions. It does not account for the actual double layer distribution in the soil. According to this theory k_i increases when the difference in concentration of the cations and anions increases, because the drag on the water in the direction of the cathode becomes greater.

Experimental results for unfrozen soils confirm the validity of the theory. k_i decreases with increasing concentration of the soil solution, and decreasing water content. In freezing soil this does not seem to work. As the temperature decreases the unfrozen water content decreases, (k_i is expected to decrease), and due to solute rejection, the soil solution becomes more concentrated (k_i is expected to decrease), however, k_i remains constant for decreasing temperatures. Moreover, k_i displays a maximum at -0.5 °C. The results seem to be contradictory to the model proposed

by Gray and Mitchell, unless the occurrence of ice in the pores of the soil skeleton causes an increase in the ratio of concentrations of cations and anions.

Gray and Mitchell (1967) and Mitchell (1976) reported extensive electro-osmosis experiments. Their conclusion, differs from Casagrande (1948), that the electro-osmotic conductivity k_e is not constant for all soils, and depends on the water content of a particular soil. They suggested that k_e approaches zero for soils with water contents approaching zero, and reaches 5. x 10^{-5} cm^2/s V at water contents in the order of 70 % depending on the soil type and pore water composition.

There is a direct relationship between unfrozen water content and temperature in frozen soils (Anderson and Morgenstern, 1973). If the unfrozen water is responsible for the movement of water in frozen soil due to electro-osmosis, the relationship suggested by Gray and Mitchell (1967) may be recovered.

The relationship between unfrozen water content and temperature of any soil can be approximated based on measurement of the liquid limit at blow counts of 25 and 100, as established by Tice et al. (1976). Anderson and Tice (1972) found that a power relationship could represent the amount of unfrozen water in a soil as a function of temperature quite well. The relationship is given by:

w_u = unfrozen water content, g H_2O/g Soil;

θ = temperature below 0 °C;

m and n = parameters determined on the basis of the water contents corresponding with blow counts of 25 and 100.

$$w_u = m\ \theta^n \qquad [4.22]$$

Athabasca Clay has a water content of 44.8 % corresponding with a blow count of 25 and of 37.8 % with a blow count of 100. The formula for the unfrozen water content at -1 °C and -2 °C from Tice et al. (1976):

$w_{u,(\theta=1)}$ = unfrozen water content at -1. °C;

$w_{u,(\theta=2)}$ = unfrozen water content at -2. °C;

$w_{(N=25)}$ = water content at blow count 25

$w_{(N=100)}$ = water content at blow count 100.

$$w_{u,(\theta=1)} = 0.346\ w_{(N=25)} - 3.01 \qquad [4.23]$$

$$w_{u,(\theta=2)} = 0.338\ w_{(N=100)} - 3.72 \qquad [4.24]$$

From these numbers one can easily deduce the values for m and n. It may be noted that equation 4.34 also expresses the freezing point depression of the soil at a given water content. For Athabasca Clay with a water content of 29 % the

freezing point depression is equal to -0.16 °C. Figure 4.15 contains the data for Athabasca Clay.

At -0.5 °C a considerable part of the water is frozen, however, k_e remained constant for temperatures between 22 °C and -0.5 °C. This observation does not seem to agree with the behavior as extrapolated from unfrozen soils.

When soil freezes ice initially forms in the largest pores of the soil skeleton (Pusch, 1978; Miller, 1980; Colbeck, 1985). Figures 4.15 and 4.16 show approximate distributions of anions and cations in the pores of frozen and unfrozen soil based on electric double layer considerations. As water is dragged along by the cations, most water will be moved in the region of the double layer where the difference in the concentration between cations and anions is the greatest. In the middle of the pores, the number of anions and cations is almost the same, the drag of the cations is cancelled out by the drag of the anions, resulting in, roughly speaking, no net movement of water. The ice crystals initially form in this region where electro-osmosis does not cause a net flow of water, but where electric energy is dissipated. Overall the electro-osmotic efficiency is enhanced by the initial formation of ice in the larger pores. The effect is only efficient until a certain point, however. Due to the exclusion of ions from the ice the overall concentration of the ions increases, which decreases the the ratio of cations over anions (compare Mitchell, 1976; Fig. 7.8). Also, the

increase of the electro-osmotic efficiency due to the formation of ice is more pronounced for large pores than for small pores. In the centre of a wide pore the influence of the double layer is extinguished, and the ratio of concentrations of cations over anions approaches one. In a small pore the ratio is well above one, and formation of ice will not increase the overall ratio of the concentrations.

The ice formation affects the distribution of ions in the internal solution, and as a consequence, its influence can 't be predicted by the Donnan theory. The theory of Gray and Mitchell does not consider the actual double layer distribution; it only considers the number of ions in the internal and external solutions.

It is difficult to quantify the effect of ice formation in the pores, since double layer tables (e.g. van Olphen, 1963) do not include the influence of an uncharged surface at some distance from the charged surface as would occur when ice fills part of the pores.

According to this mechanism, the electro-osmotic conductivity k_e would remain constant when large pores are filled with ice. A region where no water is transported between two double layers is filled with ice, and the flow of water with a given potential difference remains the same. The efficiency of electro-osmosis, expressed by k_i, would attain a maximum, because a region where energy is dissipated but no water is transported, is removed.

Another consideration leads to a similar conclusion. The electro-osmotic conductivity of the soil is probably mainly determined by the most restricted regions in the soil skeleton, such that the partial filling of the larger pores does not affect the overall electro-osmotic conductivity.

The same argument is also valid for the relationship between the hydraulic conductivity and temperature, and it should be reflected in the measurement of hydraulic conductivity as a function of temperature. Williams and Burt (1974) and Horiguchi and Miller (1980) conducted experiments to establish this relationship. Horiguchi and Miller conducted hydraulic conductivity experiments on a silt fraction (4-8 μm) at temperatures between 0 °C and -0.2 °C. The hydraulic conductivity and unfrozen water content of samples were measured simulaneously in cooling and warming cycles. In these experiments both the hydraulic conductivity and the unfrozen water content dropped at the same temperature (-0.10 °C), indicating that the initial formation of ice had a dramatic impact on the hydraulic conductivity. Therefore the previously proposed mechanism does not apply for the silt fraction used in this investigation.

A remaining problem is the sudden drop of k_e at temperatures just below -0.5 °C. To discuss this point it is of interest to visualize the microstructure of Athabasca Clay. The Athabasca Clay, as used in the experiments, was consolidated from a slurry, and its structure probably

corresponds to that of a fresh-water silty clay. The microstructure of a similar deposit is shown in Collins and McGown (1974). Their Fig. 14 is a microphotograph of an alluvial, fresh water silty clay with LL=67 % and PL=28 %. A soil of this nature is built up of domains with different packing and pore sizes. Pusch (1970) provided pore size diagrams for marine deposits deduced from microphotographs. The pore sizes were typically concentrated about a predominant diameter. A similar study was conducted on a consolidating Canadian sensitive clay by Delage and Lefebvre (1985), who also found that the pore sizes were concentrated about a predominant size. It can be concluded that also Athabasca Clay must have a structure with one or more predominant pore sizes.

The microstructure has direct bearing on the freezing behavior of the soil. Freezing of ice in a pore is determined not only by the concentration of the pore water, but also by the size of the pore (Miller, 1980, p. 269-272). If the pore size distribution is not even, but concentrated about one or more maxima, the unfrozen water content will drop suddenly when the temperature corresponding with these pore sizes is reached. In Athabasca Clay it appears that this temperature is -0.5 °C. At temperatures below -0.5 °C all the large pores are filled with ice, and the pore solution becomes highly concentrated to such a degree that the further formation of ice causes a decrease of the ratio of the concentrations of cations over anions and a

consequent decrease of the electro-osmotic flow.

Examples of irregular drops in the relationship between temperature and unfrozen water content are reported by Anderson and Tice (1972) for kaolinite (at -1.7 °C) and rust, and for montmorilllonite at temperatures between -30 and -60 °C by Anderson and Tice (1971). In this last example the authors referred explicitly to the existence of domains.

The two phenomena, increased ratio of concentrations of cations and anions due to freezing and a predominant pore size in the Athabasca Clay corresponding to a temperature of -0.5 °C seem to account for the observed temperature influence on the conductivities.

The ice lens morphology of the frozen soil after the electro-osmosis experiment seems to be the same as after a frost heave experiment (Plate 4.2). Athabasca Clay displayed "conchoidally shaped occluded particles and an undulating freezing front" (Andersland and Anderson, 1978, p. 81-82). In preliminary electro-osmosis experiments with Devon Silt (a slightly less plastic clay) the ice lenses were thick (up to 2 mm) and more widely spaced. A difference between the ice lenses formed due to frost heave and electro-osmosis was that the lenses due to electro-osmosis seemed to be more randomly oriented (the majority was close to horizontal, however).

Of considerable interest is the fact that the behavior of the bentonite - Athabasca Clay system could be modelled with a simple electro-osmotic theory. The theory required a

linearly elastic, homogeneous material. Some conclusions pertaining to the hydraulic characteristics of the frozen soil can be deduced.

Ice lenses were formed in the early stages of the experiments. This did not stop water from being transported continuously during the experiments. Proof of this is the accumulation of ice at the top of the sample. It can be concluded that when an electric gradient is applied to a frozen soil (containing ice lenses) the ice lens morphology of the soil does not affect the further distribution of water in the soil to a large degree. The soil behaves like a continuous medium.

It is also of interest that ice lenses form in frozen soil due to electro-osmosis whenever water is expected to accumulate. The increase of the ice content leads to segregated ice, not to an overall increase of the ice content in the pores. This observation may be explained with the reasoning presented by Konrad and Morgenstern (1980, p. 474-475) related to frost heaving. Initial formation of a thin ice lens results in stress relief at the bottom of the lens, and consequent accumulation of water.

However, in electro-osmosis the argument is different than in frost heaving. In electro-osmosis ice lenses form whenever water accumulates, in frost heave it is often argued that water accumulates because an ice lens is present, which supposedly constitutes an impermeable barrier once it is formed (Mageau and Morgenstern, 1980; Konrad and

Morgenstern, 1980).

Table 4.1 Properties of unfrozen Athabasca Clay (modified from Smith, 1972)

Properties of Athabasca Clay consolidating between 140 kPa and 280 kPa. A freeze thaw cycle consisted of freezing in a cold room at -15°C, and subsequent thawing.

Property	Not subjected to freezing	Subjected to one freeze-thaw cycle
k	$.16\ 10^{-7}$ cm/s	$.26\ 10^{-7}$ cm/s
c_v	$.36\ 10^{-3}$ cm^2/s	$.85\ 10^{-3}$ cm^2/s
m_v	$.04\ 10^{-3}$ cm^2/g	$.03\ 10^{-3}$ cm^2/g

The Atterberg limits for this material were:

LL = 40.3

PL = 20.3

and G_s = 2.65.

Table 4.2 Summary of electro-osmosis experiments, I

EXPERIMENT	TEMPERATURE °C	k_e 10^{-5} $cm^2/s\ V$	DATA derived from (1) water content, (2) heave
#4	- 0.79	0.018	1
#5	- 0.59	0.22	1
		0.16	2
#6	- 0.46	0.13	1
		0.18	2
#7	- 1.16	0.004	2
#8	- 0.79	0.025	1
#9	+ 22.	0.2	1
#10	+ 22.	0.06	1
#11	- 1.64	0.002	2
#12	- 0.97	0.030	2

Table 4.3 Summary of electro-osmosis experiments, II

Summary of electro-osmosis experiments on Athabasca clay consolidated to 210 kPa.

Experiment	T °C	Resistivity ohm-m	k_i Moles Water per Faraday
#4	-0.79	390	53
#5	-0.59	192	232
#6	-0.46	294	209
#8	-0.79	455	45
#9	22.	33	37
#11	-1.64	1075	47

Table 4.4 Coefficient of consolidation of Athabasca Clay

Coefficient of consolidation for Athabasca Clay consolidated to 210 kPa, at the given temperatures.

EXPERIMENT	TEMPERATURE °C	c_v 10^{-6} cm^2/s
#4	- .79	2.0
#5	- .59	3.7
#6	- .46	5.1
#8	- .79	1.1

Values for unfrozen Athabasca Clay consolidated between 140 and 280 kPa, from Smith (1972):

c_v = 0.36 to 0.85 10^{-3} cm^2/s.

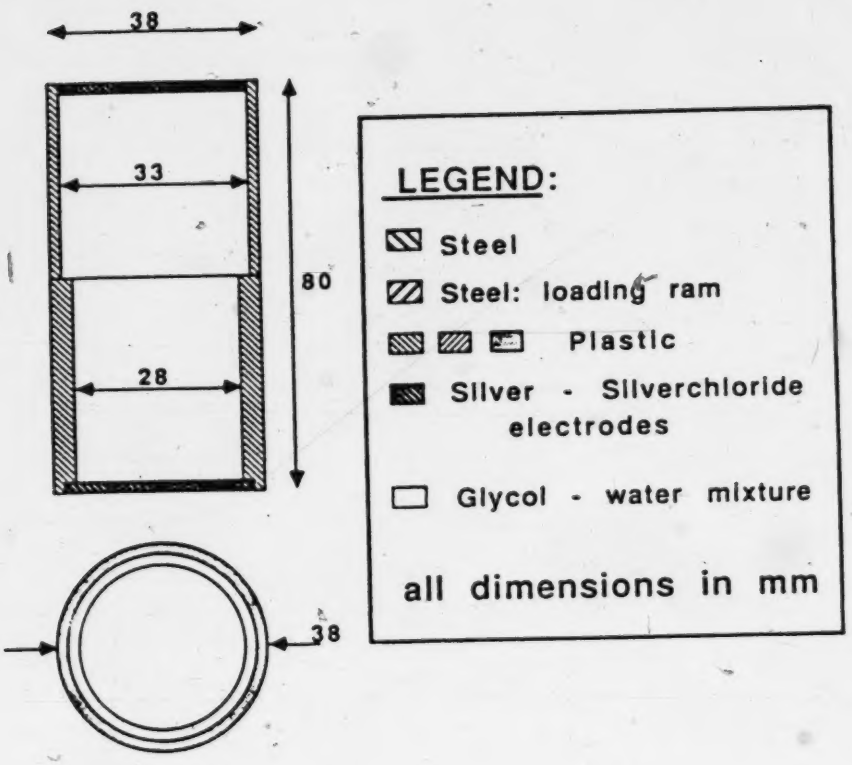

Figure 4.1 Sketch of sample holder

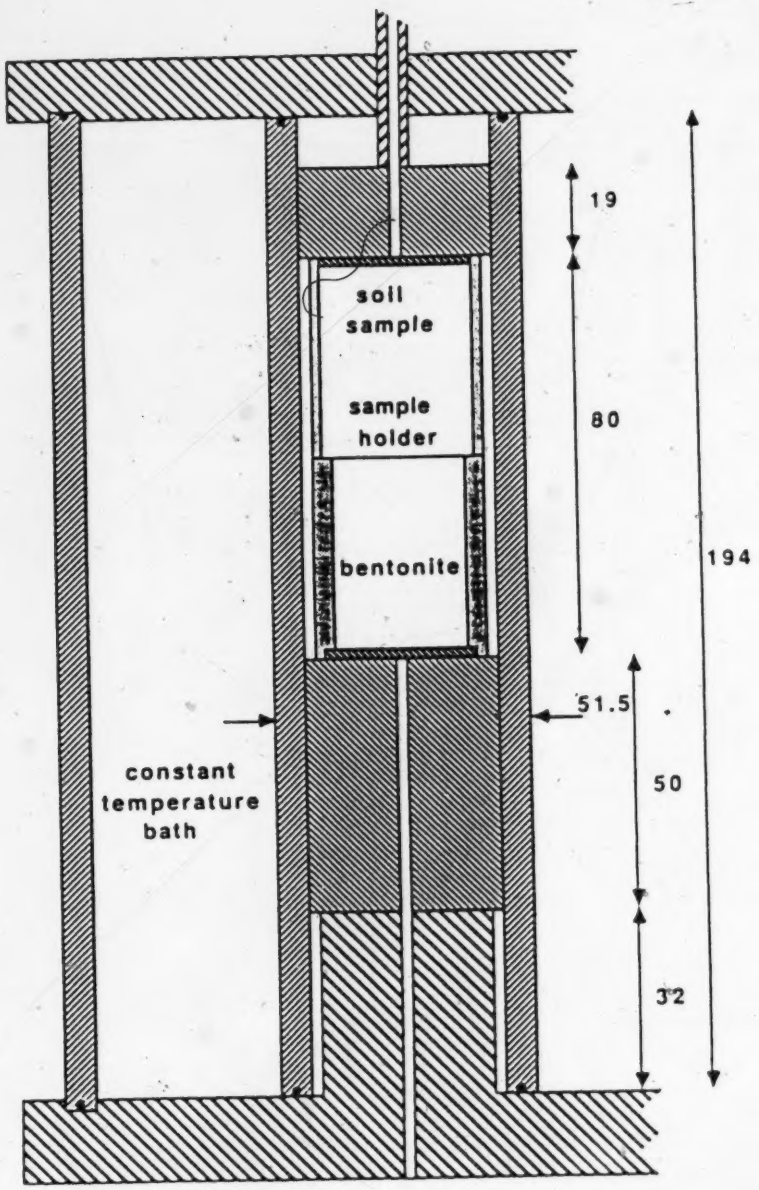

Figure 4.2 Sketch of experimental apparatus

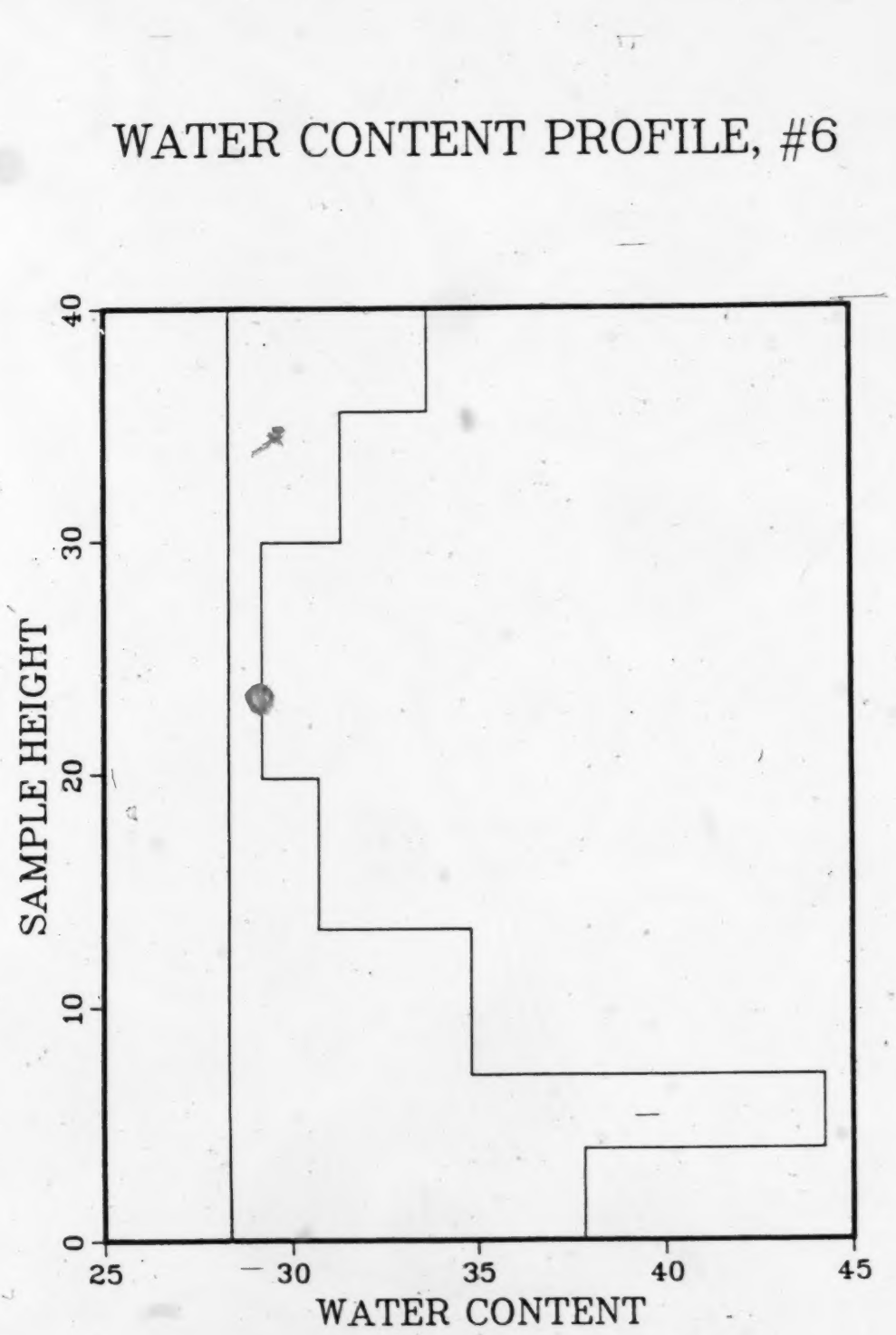

Figure 4.3 Water content profile, experiment #6

EXPERIMENT #6

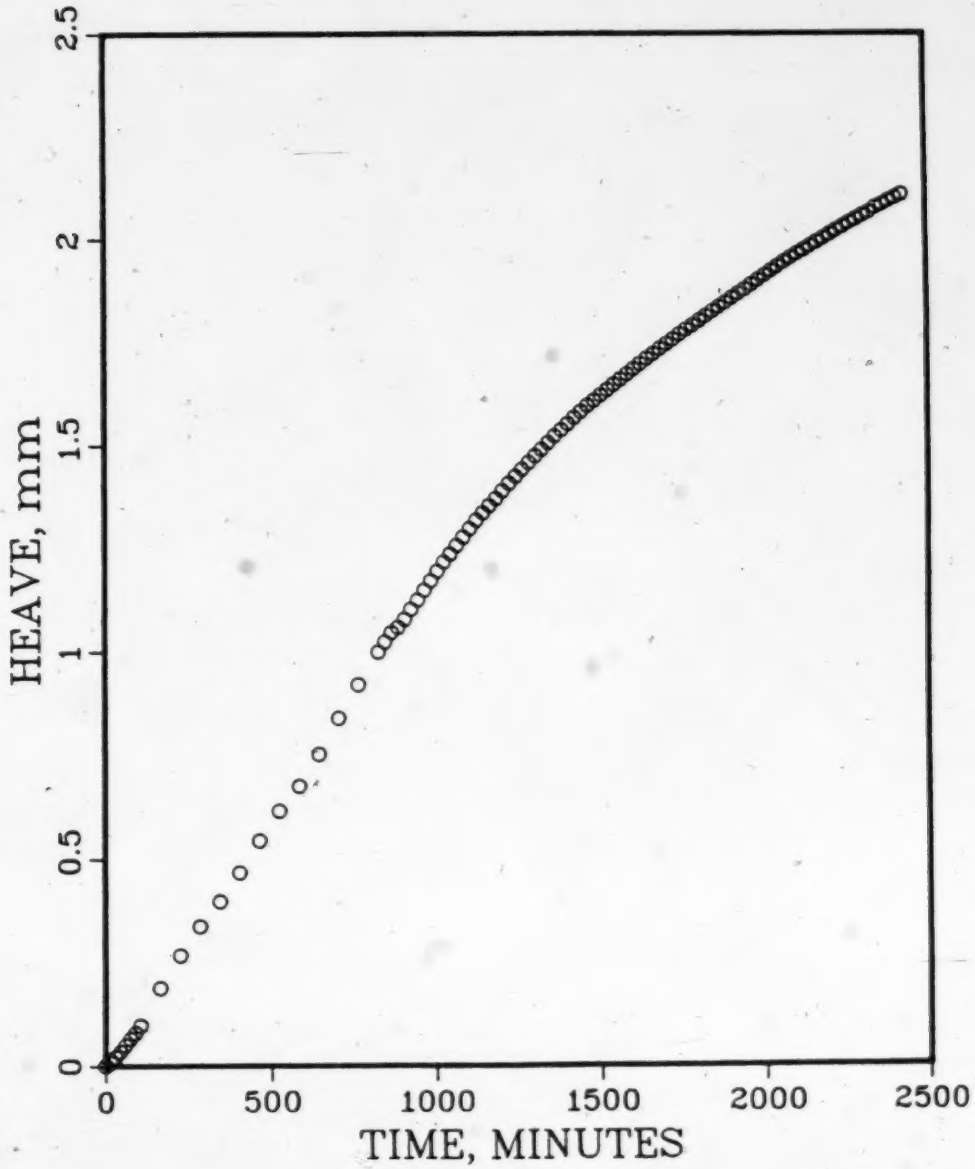

Figure 4.4 Heave of soil sample, experiment #6

EXPERIMENT #6

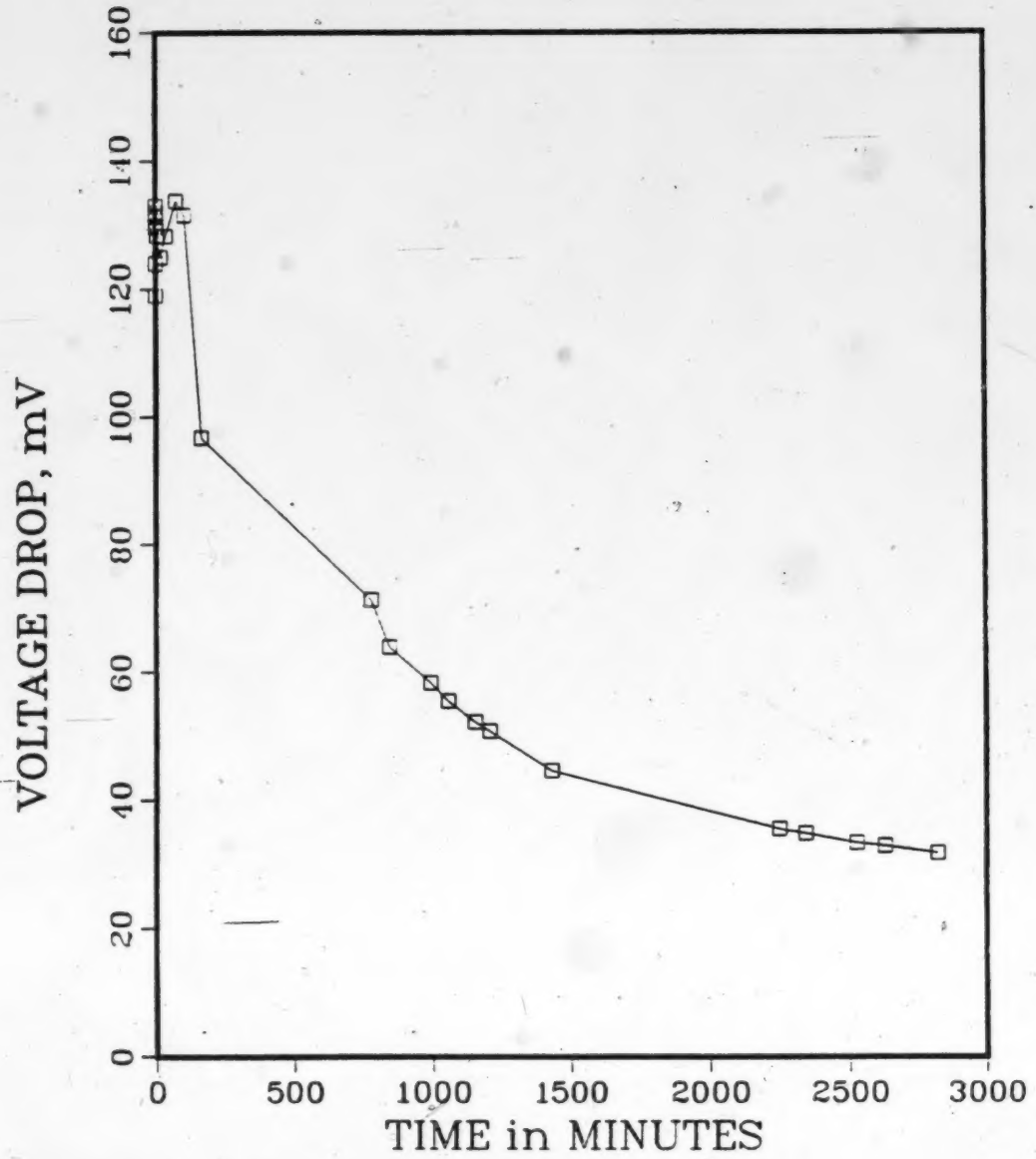

Figure 4.5 Electrical current through resistance in series with sample, experiment #6

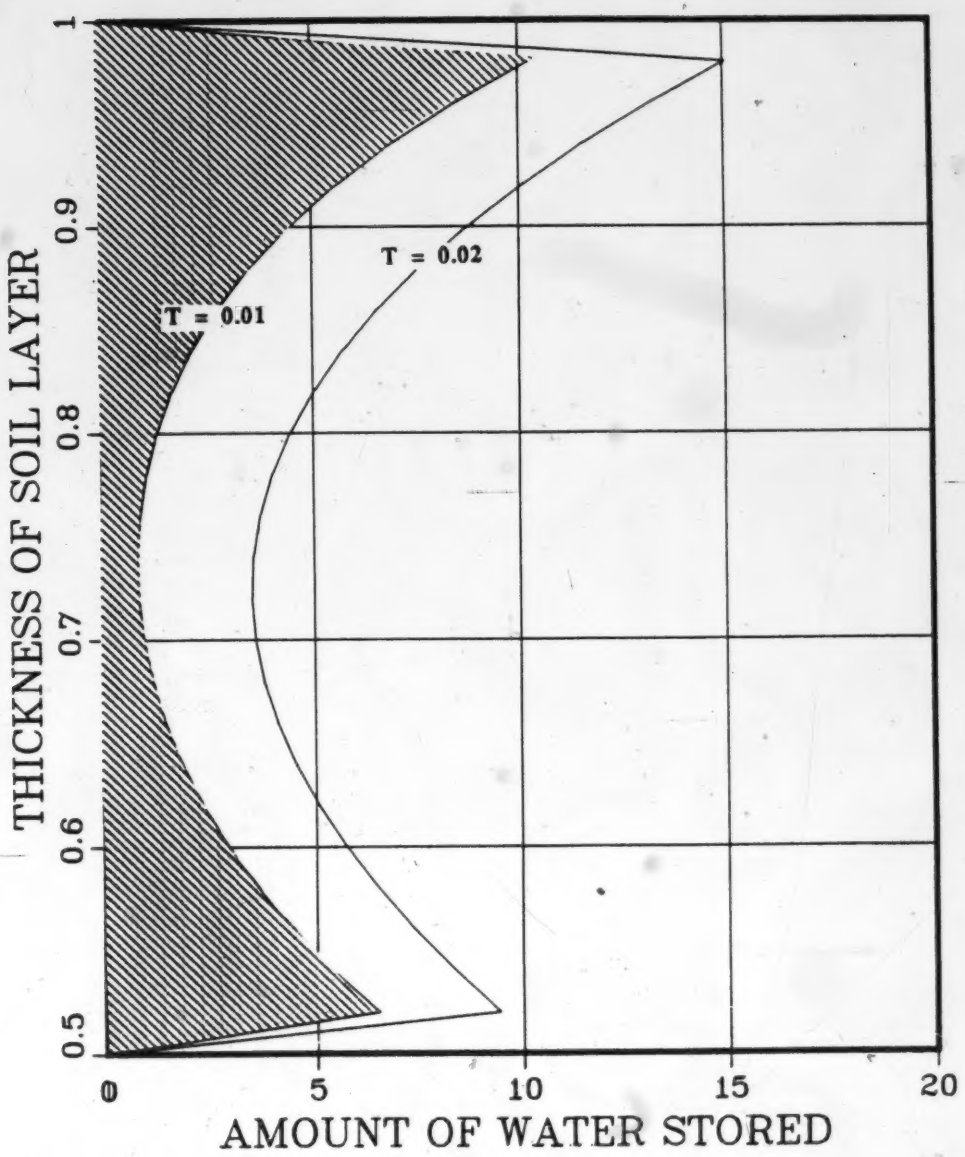

Figure 4.6 Accumulation of water in soil sample according to numerical analysis, $k_B/k_S=5.$, $V_B/V_S=1.$

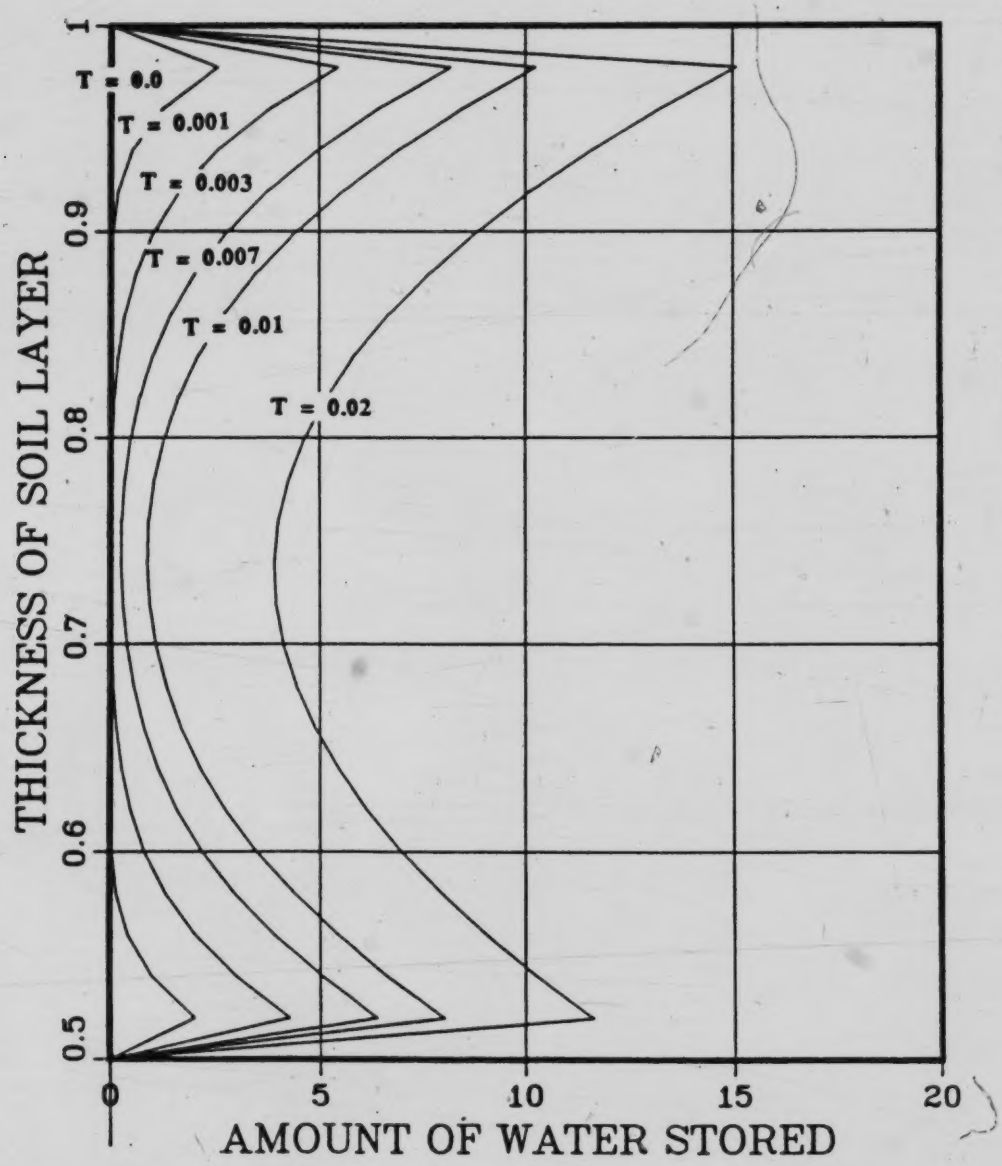

Figure 4.7 Accumulation of water in soil sample according to numerical analysis, $k_B/k_S=10.$, $V_B/V_S=1.$

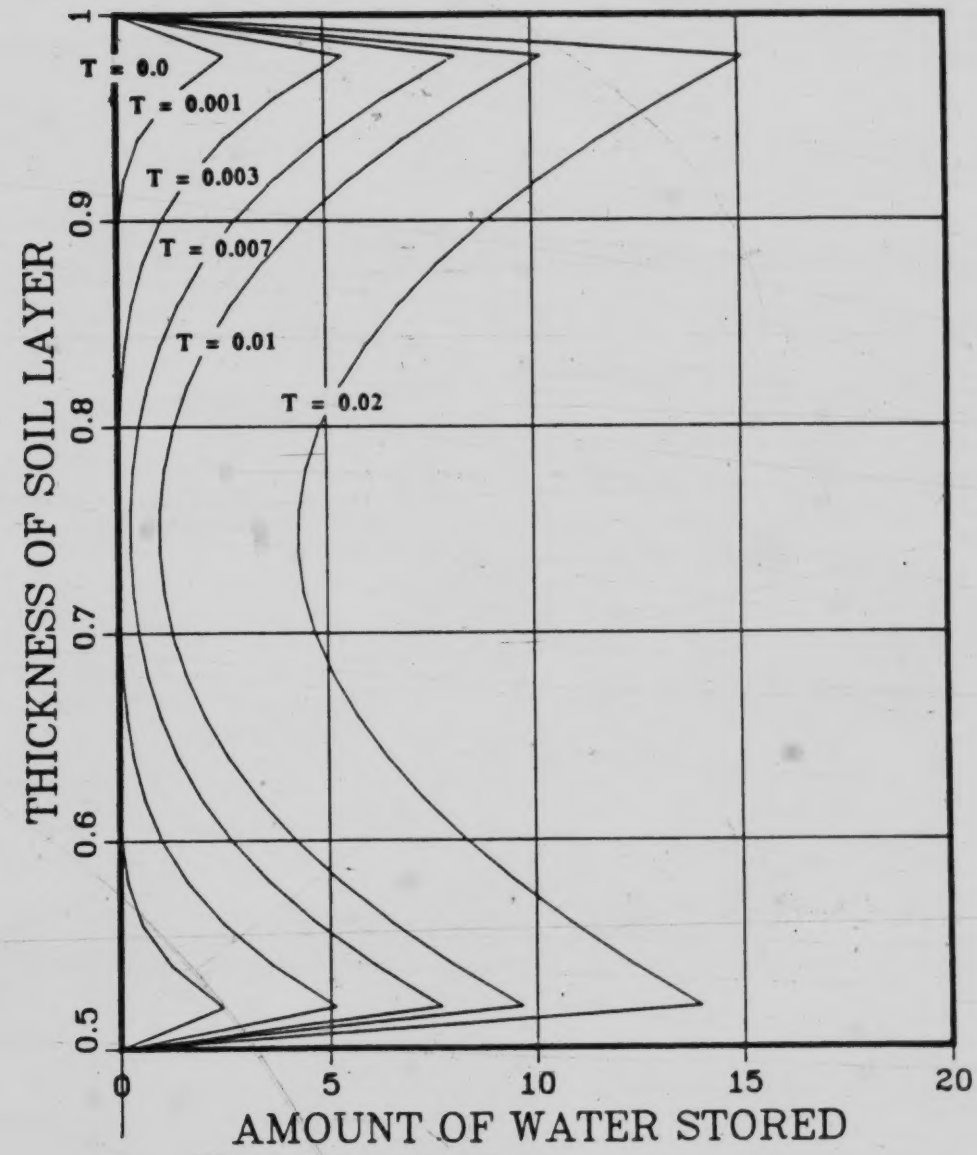

Figure 4.8 Accumulation of water in soil sample according to numerical analysis, $k_b/k_s=100.$, $V_b/V_s=1.$

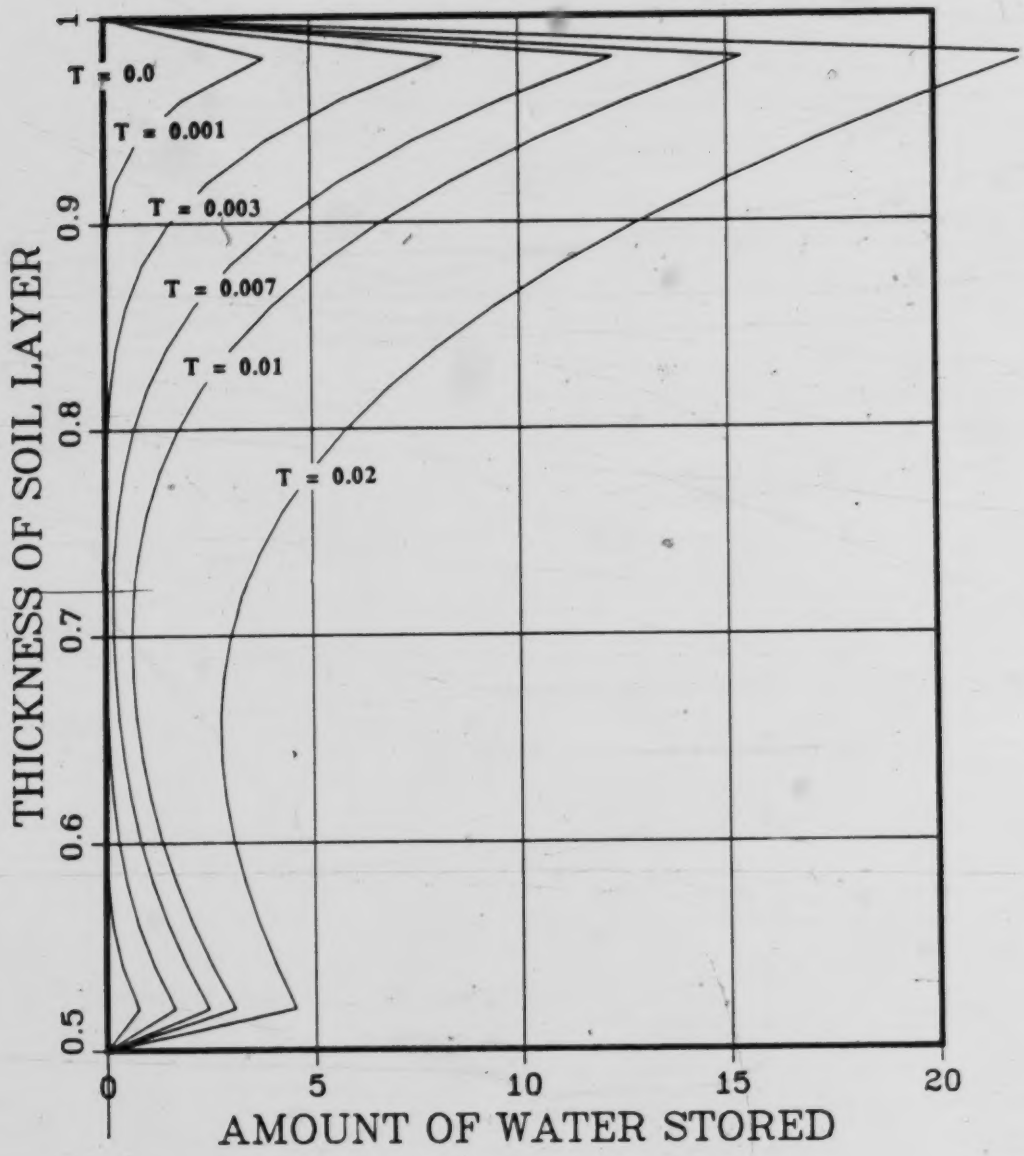

Figure 4.9 Accumulation of water in soil sample according to numerical analysis, k_b/k_s=10., V_b/V_s=3.

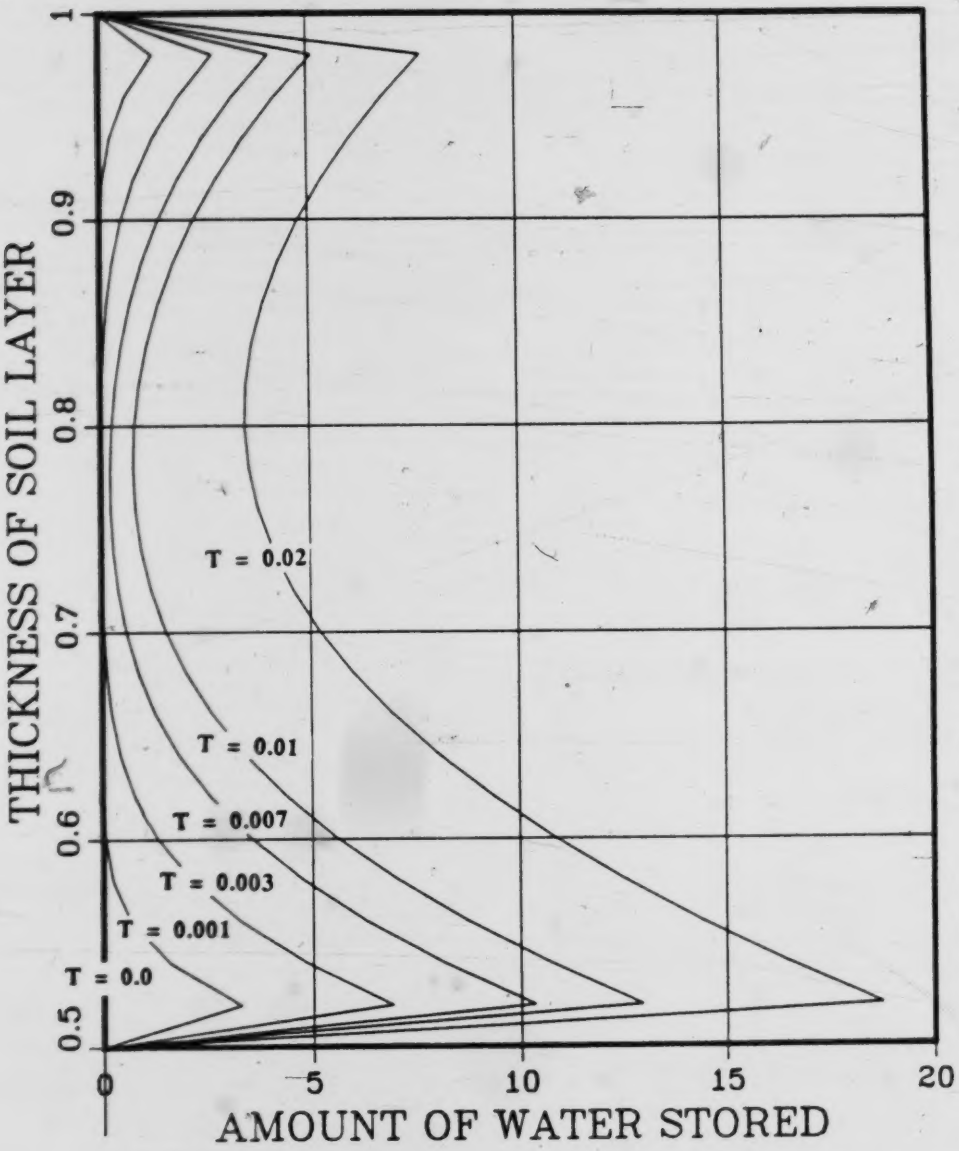

Figure 4.10 Accumulation of water in soil sample according to numerical analysis, $k_B/k_S=10.$, $V_B/V_S=0.33$

ACCUMULATED WATER INTAKE

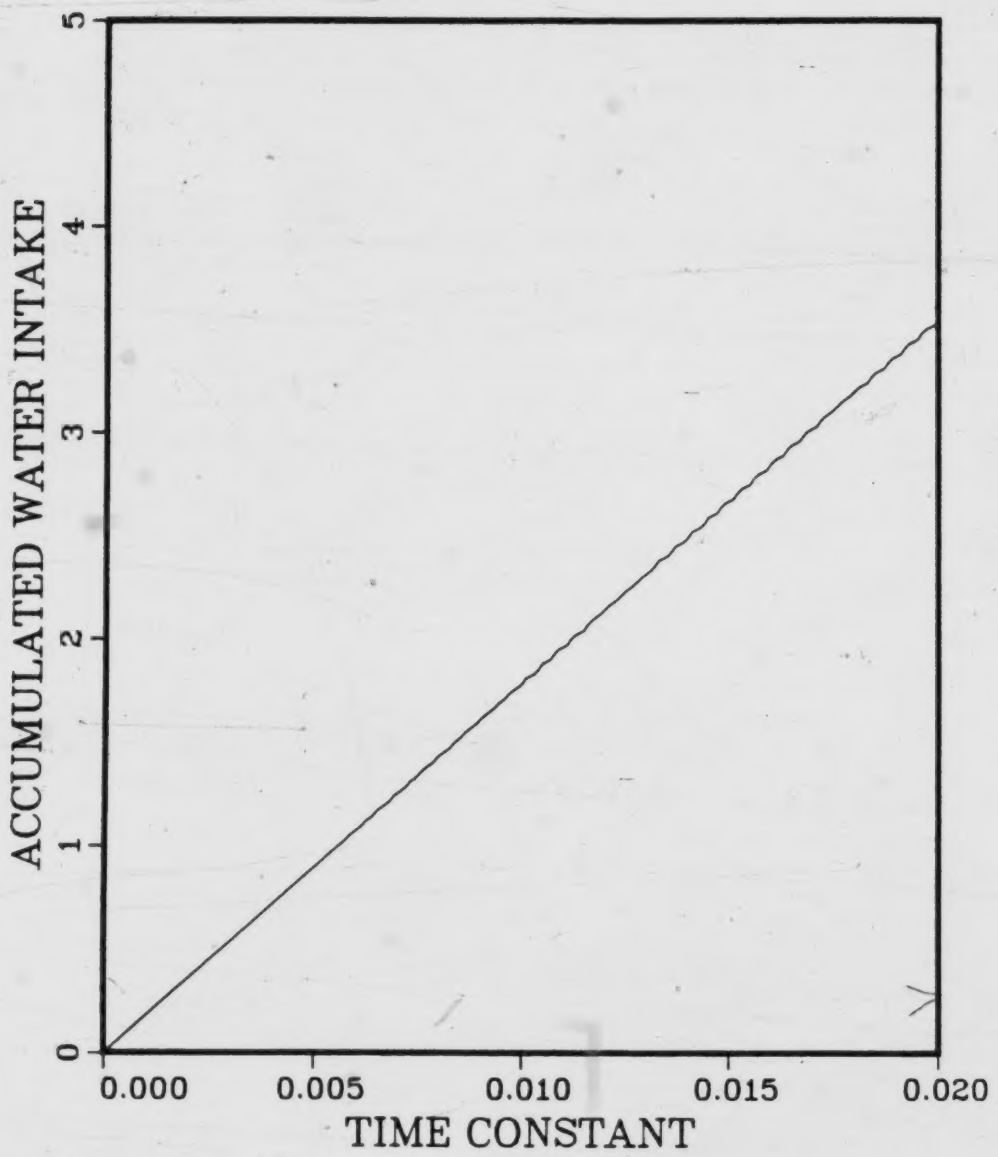

Figure 4.11 Water flow entering the soil sample as a function of time, $k_B/k_S=10$, $V_B/V_S=1$.

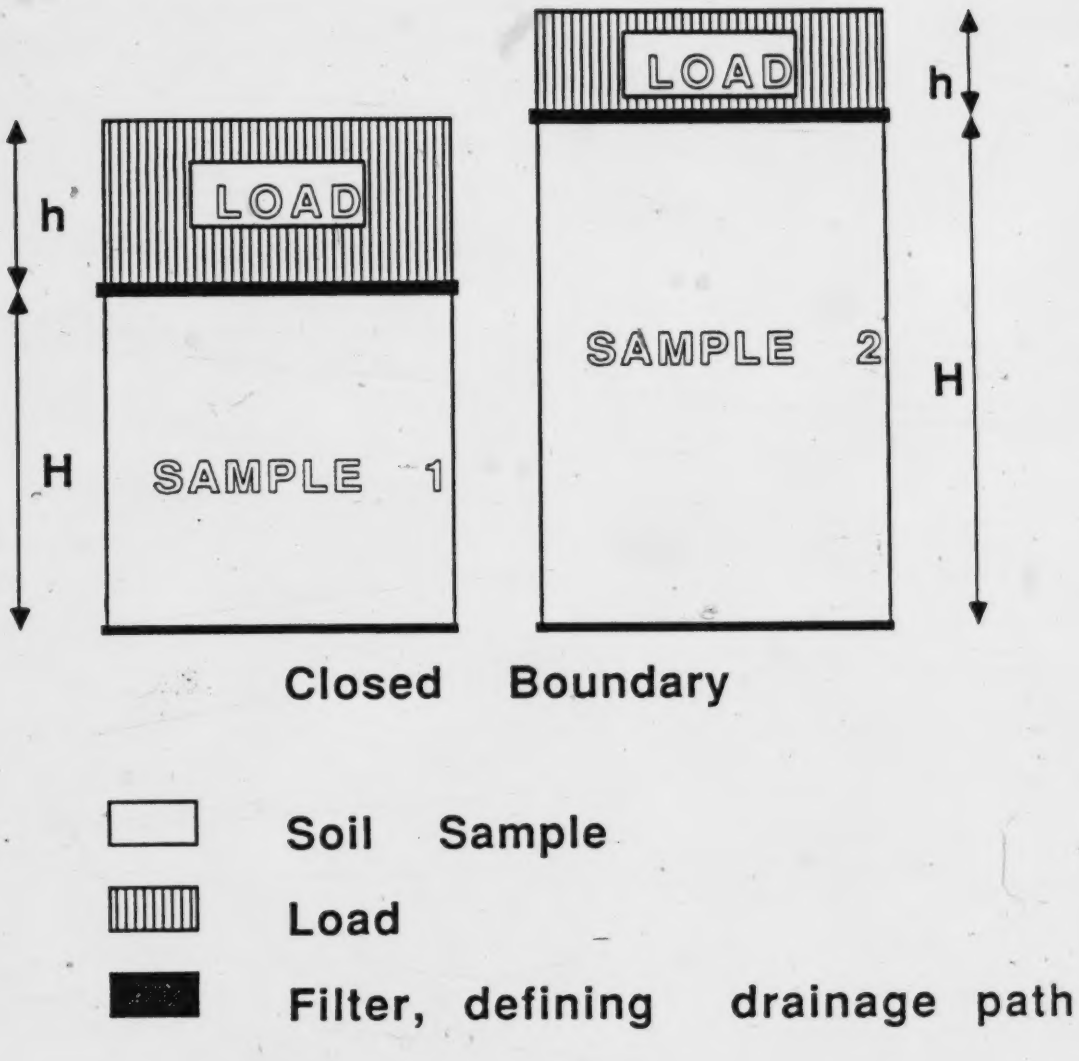

Figure 4.12 Consolidation of samples with different geometry

ELECTRO–OSMOTIC CONDUCTIVITY

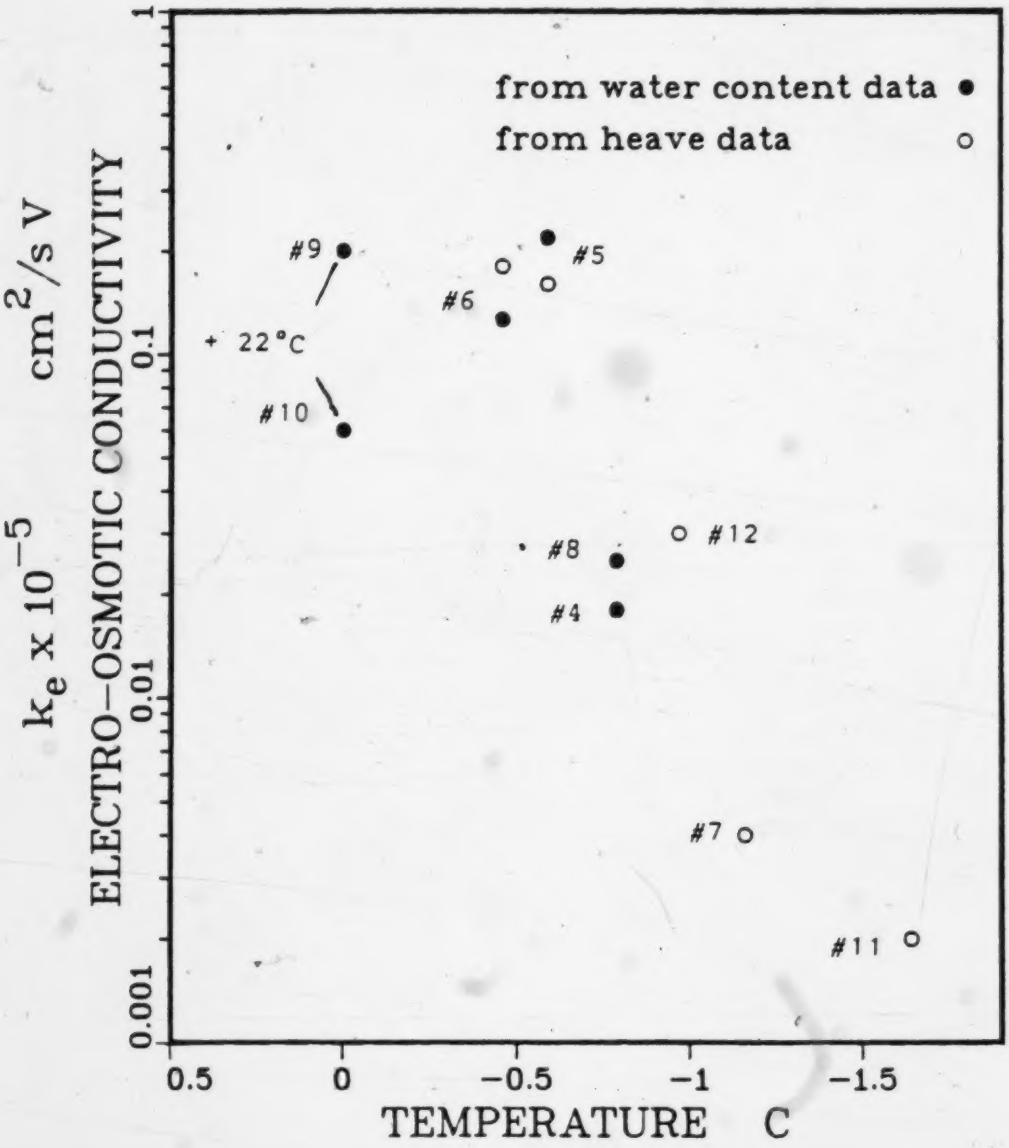

Figure 4.13 Electro-osmotic conductivity k_e of Athabasca Clay as a function of temperature.

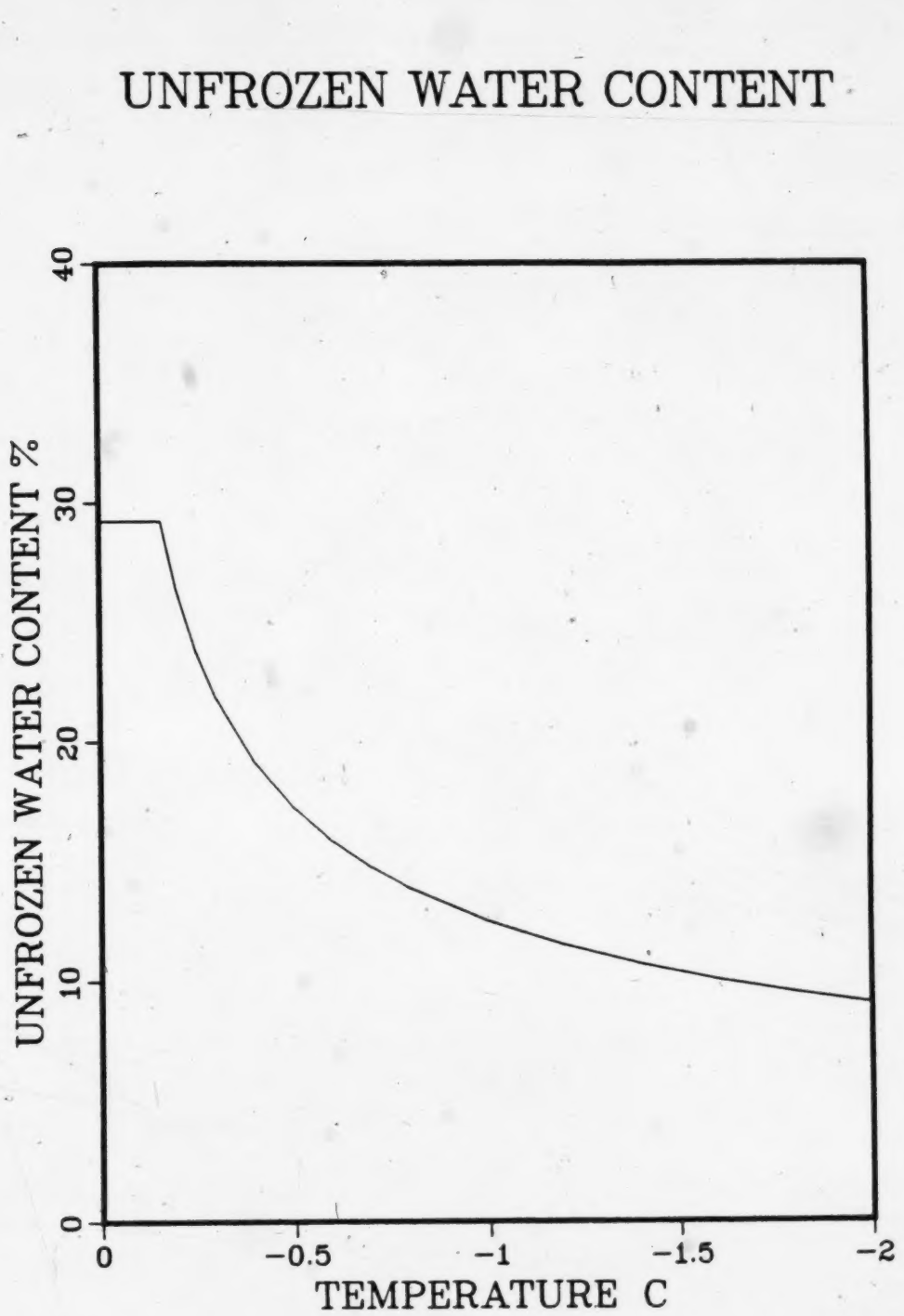

Figure 4.14 Unfrozen water content of Athabasca Clay as a function of temperature

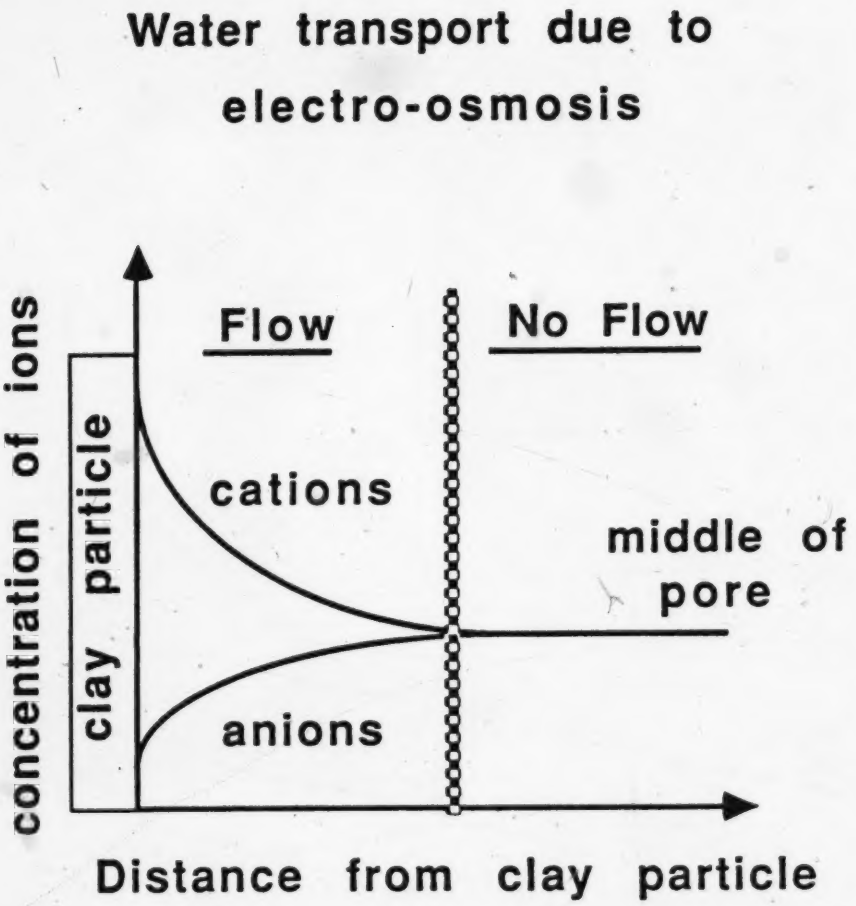

Figure 4.15 Relationship between distance from pore wall and electro-osmotic transport.

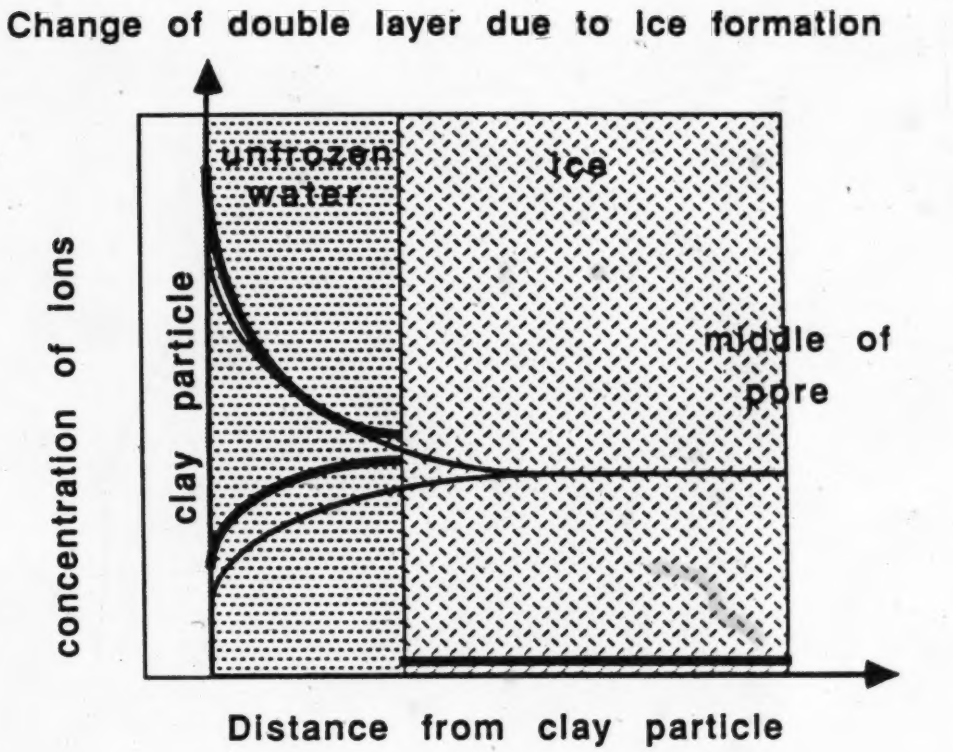

Figure 4.16 Influence of formation of ice in pores on distribution of ions.

Plate 4.1 Athabasca Clay frozen confined in a sample holder, #4

Plate 4.2 Ice structure after electro-osmosis experiment, #5

5. Concluding remarks

In the thesis freezing potentials have been reviewed. No unequivocal explanation of the phenomenon can be given. Most likely freezing potentials are partially induced by a charge imbalance between the frozen and unfrozen soil analogous to freezing solutes, however, this is not definitely proved.

It was postulated that this charge imbalance does exist and some aspects of electro-osmosis due to this imbalance were investigated.

Since the charge imbalance is thought to occur in a very small zone, the effect of the limited extent of the power source on the amount of water transported in a saturated soil was studied. Here it was found that this geometrical condition does not adversely affect the transport of water.

It has been recognized that freezing and thawing of a soil may cause overconsolidation. However, the magnitude of the overconsolidation has not been quantified in the past. An attempt was made to quantify the observed overconsolidation stresses with the Clausius-Clapeyron equation. However, it was found that the Clausius-Clapeyron equation failed to account for the high consolidation stresses in some soils. Electro-osmosis was postulated in order to account for these high consolidation stresses; it was shown that electro-osmosis may induce very high pore pressures, and thus cause high stresses which will overconsolidate the soils.

In the experimental programme the electro-osmotic conductivity of a frozen silty clay as a function of temperature was investigated. It was found that the electro-osmotic conductivity k_e of frozen Athabasca Clay is the same as for unfrozen soil down to a temperature of -0.5 °C. Below this temperature k_e drops quickly by a factor 100. k_i, which indicates the efficiency of electro-osmosis, reaches a maximum at a temperature of -0.5 °C.

This behavior may be explained by the fact that the ratio of cations over anions increases when ice forms initially in the large pores of the soil skeleton. When the temperature drops below -0.5 °C, smaller pores fill with ice, the concentration of the pore water increases to such an extent that the ratio of cations over anions increases, causing a decrease of the electro-osmotic conductivity.

5.1 Conclusions

From the consolidation characteristics of soils due to freezing and thawing one can deduce that the Clausius-Clapeyron equation, even when modified for solutes, does not account for the pore pressures which develop in a freezing soil. Examples of soils consolidated to high stresses due to freezing and thawing were discussed. In montmorillonite the collapse of the interlaminar spacing during freezing is proof that very high stresses are induced. This conclusion has bearing on our understanding of freezing of soils and frost heave.

An important issue is the use of the Clausius-Clapeyron equation in frost heave models. All frost heave models that are currently available and able to predict frost heave are based on the balance of two flows: heat and water flow. Heat flow does not constitute a theoretical problem, water flow does. In these theories water flow is calculated using the Clausius-Clapeyron equation, to determine the pressure difference between the ice and the water. It is important to note that the Clausius-Clapeyron equation does not provide the absolute pore water pressures, only the difference. It is customary to choose the ice pressure and calculate the resulting pore water pressure. However there is still discussion in the literature as to the validity of this concept (e.g. Martin, 1980; Miller, 1980; Williams and Wood, 1985). It was shown herein that the collapse of the interlaminar spacing in montmorillonite is accompanied by stress differences between the water and the ice higher than predicted by the Clausius-Clapeyron equation. Although some of the models that have been proposed do predict frost heave with some success this indicates that the assumptions on which they are based may be incomplete.

5.2 Recommendations for future research

For some time to come engineering theories like the Segregation Potential theory, as discussed in Appendix E, will be used in practice. However, the theory of frost heave and freezing soils needs improvements and probably some

dramatic developments in order to offer congruent explanations of the observed phenomena. Construction of major projects in the North requires a thorough understanding of the processes involved.

In the thesis the electro-osmotic characteristics of Athabasca Clay are determined. A remaining problem is the determination of the charge transfer which takes place between the frozen and unfrozen soil. Charge transfer may be slightly more complex to determine than freezing potentials, but its interpretation in terms of water movement is straight forward. Charge transfer may be determined by embedding two electrodes in a freezing soil sample on either side of a freezing front. The charge transfer can then be measured with a shunt similarly as in dilute solutions. As a result it would be possible to assess the importance of electro-osmosis on the migration of water in freezing soil.

Little gain can be expected from the measurement of electric freezing potentials as their interpretation is too complex.

References

Ad Hoc Study Group on Ice Segregation and Frost Heaving, 1984. Ice segregation and frost heaving. National Academy Press, Washington D.C., 72 p.

Ahlrichs J.L., and White J.L., 1962. Freezing and lyophilizing alters the structure of bentonite gels. Science, 136, pp. 1116-1118.

Andersland, O.B., and Anderson, D.M., 1978. **Geotechnical Engineering for Cold Regions**. McGraw-Hill, New York, 566 p.

Anderson, D.M., and Hoekstra, P., 1965. Migration of interlamellar water during freezing and thawing of Wyoming bentonite. Soil Science Society of America Proceedings, 29, pp. 498-504.

Anderson, D.M., Low, P.F., and Hoekstra, P., 1968. Some thermodynamic relationships for soils at or below the freezing point. Journal of Water Resources Research, 4, pp. 379-394.

Anderson, D.M., and Morgenstern, N.R., Physics, chemistry, and mechanics of frozen ground. Proceeding 2nd International Conference on Permafrost, North American Contribution, Yakutsk, U.S.S.R., pp. 257-288.

Anderson, D.M., and Tice, A.R., 1971. Low-temperature phases of interstitial water in clay-water systems. Soil Sience Society of America Proceedings, 35, pp. 47-54.

Anderson, D.M., and Tice, A.R., 1972. Predicting unfrozen water contents in frozen soils from surface area measurements. Highway Research Record, 393, pp. 12-18.

Anderson, D.M., and Tice, A.R., 1985. Thawing of frozen clays. In: Anderson D.M. and Williams P.J., **Freezing and Thawing of soil-water systems**. Technical Councel on Cold Regions Engineering Monograph, A.S.C.E., pp. 1-9.

Arctic Construction and Frost Effects Laboratory, 1951. Frost Investigations, Fiscal Year 1951, Cold Room studies, Volumes 1 and 2.

Arctic Construction and Frost Effects Laboratory, 1958. Cold room studies. Third Interim Report, with Appendices A & B. Technical Report 43.

Arctic Construction and Frost Effects Laboratory, 1958. Cold room studies. Third Interim Report, Mineral and Chemical studies, Appendices C & D. Technical Report 43.

Bishop, A.W., and Blight, G.E., 1963. Some aspects of effective stress in saturated and partly saturated soils. Géotechnique, 13, pp. 177-197.

Bjerrum, L. 1972. Embankments on soft ground. Proc. A.S.C.E. Specialty Conference on Performance of Earth and Earth-Supported Structures, Vol. 1, pp. 1-54.

Bjerrum, L., Moum, J., and Eide, O., 1967. Application of electro-osmosis on a foundation problem in Norwegian quick clay. Géotechnique, 17, pp. 214-235.

Boikess, R.S., and Edelson, E., 1978. **Chemical principles.** Harper & Row, New York, 742 p.

Bolt, G.H., and Peech, M., 1953. The application of the Gouy theory to salt-water systems. Soil Science Society of America Proceedings, 17, pp. 210-213.

Bolt, G.H., and Miller, R.D.,1956. Compression studies of illite suspensions. Soil Science Society of America Proceedings, 19, pp. 285-288.

Booth, D.B., 1982. Macroscopic behavior of freezing saturated silty soils. Cold Regions Science and Technology, 4, pp. 163-174.

Campbell, C.A, Ferguson, W.S., and Warder, F.G., 1970. Winter changes in soil nitrate and exchangeable ammonium. Canadian Journal of Soil Science, 50, pp.151-162.

Cary, J.W., and Mayland, H.F., 1972. Salt and water movement in unsaturated frozen soil. Soil Science Society of Amererica Proceedings, 36, pp. 549-555.

Cary, J.W., Papendick, R.I., and Campbell, G.S., 1979. Water and salt movement in unsaturated frozen soil: principles and field observations. Soil Science Society of America Proceedings, 43, pp. 3-8.

Casagrande, A., 1936. The determination of the preconsolidation load and its practical significance. Proceedings 1st International Conference Soil Mechanics and Foundation Engineering Cambridge, Mass., 60 pp.

Casagrande, L., 1948. Electro-osmosis in soils. Géotechnique, 1, pp. 159-177.

Chamberlain, E.J., 1980. Overconsolidation effects of ground freezing. Ground Freezing, Preprints 2nd International Symposium, Trondheim, Norway. pp. 325-337.

Chamberlain, E.J., 1984. Frost heave of saline soils.

Proceedings 4th International Conference on Permafrost, Fairbanks, Alaska, pp. 121-126.

Chamberlain, E.J., and Blouin, S.E., 1978. Densification by freezing and thawing of fine material dredged from waterways. Proceedings 3rd International Conference on Permafrost, Edmonton, Alberta, pp. 622-628.

Chamberlain, E.J., and Sellman, P.V., Blouin, S.E., Hopkins, D.M., and Lewellen, R.I., 1978. Engineering properties of subsea permafrost in the Prudhoe Bay region of the Beaufort Sea. Proceeding 3rd International Conference on Permafrost, Ottawa, Ontario, pp.629-635.

Chamberlain, E.J., and Gow, A.J., 1978. Effect of freezing and thawing on the permeability and structure of soils. Proceedings 1st International Symposium on Ground Freezing, Bochum, Germany, pp. 73-92.

Christian, H., 1985. Stress history of surficial Beaufort Sea sediments. Unpublished M.Sc. thesis, University of Alberta, 334 p.

Colbeck, S.C., 1985. A technique for observing freezing fronts. Soil Science, 139, pp. 13-20.

Collins, K., and McGown, A., 1974. The form and function of microfabric features in a variety of natural soils. Géotechnique, 21, pp. 211-222.

Delage, P., and Lefebvre, G., 1985. Study of the structure of a sensitive clay and its evolution during consolidation. Canadian Geotechnical Journal, 22, pp. 21-35.

Edlefsen, N.E., and Anderson, A.B.C., 1943. Thermodynamics of soil moisture. Hilgardia, 15, pp. 31-298.

Elrick, D.E., Smiles, D.E., Baumgartner, N., and Groenevelt, P.H., 1976. Coupling phenomena in saturated homo-ionic montmorillonite: I. Experimental. Soil Science Society of America Proceedings, 40, pp. 490-491.

Esrig, M.I., 1968. Pore pressures, consolidation, and electrokinetics. Journal of the Soil Mechanics and Foundation Division, 94, pp. 899-921.

Gairon, S., and Schwartzendruber D., 1975. Water flux and electrical potentials in water saturated bentonite. Soil Science Society of America Proceedings, 39, pp. 811-817.

Gray, D.H., and Mitchell, J.K., 1967. Fundamental aspects of electro-osmosis in soils. Journal of the Soil Mechanics Division, 93 pp. 209-236, 1969. Closure Disussion: 95,

pp. 875-879.

Gray, D.M., and Granger, R.J., 1986. In situ measurement of moisture and salt movement in freezing soil. Canadian Journal of Earth Sciences, 23, pp. 696-704.

Gross, G.W., 1968. Some effects of inorganics on the ice-water system. In: Gould, R.F., **Trace inorganics in water.** Advances in Chemistry Series, 73, pp. 23-97.

Haley, J.F., and Kaplar,C.W., 1952. Cold room studies of frost action in soils. Highway Research Board, 213, pp. 246-267.

Hallet, B., 1978. Solute redistribution in freezing ground. Proceedings 3rd International Conference on Permafrost, Edmonton, Alberta, pp. 85-91.

Hanley, T.O'D., and Rao, S.R., 1982. Electrical freezing potentials and the migration of moisture and ions in freezing soils. Proceedings 4th Canadian Permafrost Conference, pp. 453-458.

Hanley, T.O'D., 1985. Electrical freezing potentials and corrosion rates in clay sludge. Canadian Geotechnical Journal, 22, pp. 599-604.

Harlan, R.L., 1973. Analysis of coupled heat-fluid transport in partially frozen soil. Water Resources Research, 9, pp. 1314-1323.

Hobbs, P.V., 1974. **The physics of ice.** Clarendon Press, Oxford, p. 837.

Hoekstra, P., and Chamberlain, E.J., 1964. Electro-osmosis in frozen soil. Nature, 203, pp.1406-1407.

Hoekstra, P., and McNeil, D., 1973. Electromagnetic probing of permafrost. North American Contributions 2nd Int. Conf. Permafrost, Yakutsk, USSR, National Academy of Sciences, Washington, pp. 517-527.

Horiguchi, K., and Miller, R.D., 1980. Experimental studies with frozen soil in an ice sandwich permeameter. Cold Regions Science and Technology, 3, pp. 177-183.

Hopkins, D.M., 1982. Aspects of paleogeography of Beringia during the Late Pleistcene. In: Hopkins D.M., Matthews, J.V., Schweger, C.E., and Young, S.B., **Paleaecology of Beringia.** pp. 3-28.

Ishizaki, T., Yoneyama, K., Nishio, N., 1985. X-ray technique for observation of ice lens growth in partially frozen, saturated soil. Cold Regions Science

and Technology, 11, pp. 213-221.

Iskandar, I.K., Osterkamp, T.E., and Harrison, W.D., 1978. Chemistry of interstitial water from subsea permafrost, Prudhoe Bay, Alaska. Proceedings 3rd International Permafrost Conference, Edmonton, Alberta, pp. 92-98.

Jumikis, A.R., 1958. Some concepts pertaining to the freezing soil sysstem. Highway Research Board Special Report, 40, pp. 178-190.

Jumikis, A.R., 1960. Concerning a mechanism for soil moisture translocation in the film phase upon freezing. Highway Research Board Proc., 39, pp. 619-639.

Kaplar, C.W., 1974. Freezing test for evaluating relative frost susceptibility of various soils. CRREL, Technical Report, 250, 40 p.

Katz, W.J., and Mason, D.G., 1970. Freezing methods used to condition activated sludge. Water and Sewage Works, 117, pp. 110-114.

Kay, B.D., and Groenevelt, P.H., 1984, The redistribution of solutes in freezing soil: exclusion of solutes. Proceedings 4th International Conference on Permafrost, Fairbanks, Alaska, pp. 584-588.

Konrad, J.-M.,1980. Frost heave mechanics, Ph.D. Thesis, University of Alberta, 472 p.

Konrad, J.-M., and Morgenstern, N.R., 1980. A mechanistic theory of ice lens formation in fine-grained soils. Canadian Geotechnical Journal, 17, pp. 473-486.

Konrad, J.-M., and Morgenstern, N.R., 1981. The segregation potential of a freezing soil. Canadian Geotechnical Journal, 18, pp. 482-491.

Konrad, J.-M., and Morgenstern, N.R., 1982. Prediction of frost heave in the laboratory during transient freezing. Canadian Geotechnical Journal, 19, pp. 250-259.

Lambe, T.W., and Martin, R.T., 1953-1957. Composition and engineering properties of soil. Highway Research Board Proceedings, I-1953, II-1954, III-1955, IV-1956,V-1957.

Lambe, T.W., and Whitman, R.V., 1969. Soil mechanics. Wiley, New York, 553 p.

Lessard, G., and Mitchell, J.K., 1985. The causes and effects of aging in quick clays. Canadian Geotechnical Journal, 22, pp. 325-346.

Low, P.F., Anderson, D.M., and Hoekstra, P., 1968a. Some thermodynamic relationships for soils at or below the freezing point 1 Freezing point depression and heat capacity. Water Resources Research, 4, pp. 379-394.

Low, P.F., Hoekstra, P., and Anderson, D.M., 1968b. Some thermodynamic relationships for soils at or below the freezing point 2 Effects of temperature and pressure on unfrozen soil water. Water Resources Research, 4, pp. 541-544.

Mackay, J.R., 1974. Reticulate ice veins in permafrost, Northern Canada. Canadian Geotechnical Journal, 11, pp. 230-237.

Mageau, D., and Morgenstern, N.R., 1980. Observations on moisture migration in frozen soils. Canadian Geotechnical Journal, 17, pp 54-60.

Martin, R.T., 1980. A comment on "pressure melting". Cold Regions Science and Technology, 3, pp. 89.

Miller, R.D., 1955. Neglected aspects of electroosmosis in porous bodies. Science, 122, pp. 373-374.

Miller, R.D., 1978. Frost heaving in non-colloidal soils. Proceedings 3rd International Conference on Permafrost, Ottawa, Ontario, pp. 708-720.

Miller, R.D.,1980. Freezing phenomena in soils. In: Hillel, D., **Applications of soil physics.**, pp. 254-299.

Mitchell, J.K., 1976. **Fundamentals of soil behavior.** Wiley, New York, 420 p.

Mitchell, J.K., Greenberg, J.A., Witherspoon, P.A., 1973. Chemico osmotic effects in fine grained soils. Journal of the Soil Mechanics Divison , A.S.C.E., 99,, pp. 307-322. 8, pp. 558-565.

Nacci, V.A., Kelly, W.E., Wang, M.C., and Demars, K.R., 1974. Strength and stress-strain characteristics of deep-sea sediments. In: Interbitzen, A.L.,Deep Sea Sediments: physical and mechanical properties. Plenum Press, New York, pp. 129-150.

Nixon, J.F., 1987. Thermally induced heave beneath chilled pipelines in frozen ground. Canadian Geotechnical Journal, 24, pp. 260-266.

Nixon, J.F., and Morgenstern, N.R., 1973. The residual stress in thawing soils. Canadian Geotechnical Journal, 10, pp. 571-580.

Olsen, H.W., 1969. Simultaneous fluxes of liquid and charge in saturated kaolinite. Soil Science Society of America Proceedings, 33, pp. 338-344.

Olsen, H.W., 1985. Osmosis: a cause of apparent deviations from Darcy's law. Canadian Geotechnical Journal, 22, pp. 238-241.

Parameswaran, V.R., and Mackay, J.R., 1983. Field measurements of electrical freezing potentials in permafrost areas. Proceedings 4th International Conference on Permafrost, Fairbanks, Alaska, pp. 962-967.

Parameswaran, V.R., Johnston, G.H., and Mackay, J.R., 1985. Electrical potentials developed during thawing of frozen ground. Proceedings 4th International Symposium on Ground Freezing, Sapporo, Japan, pp. 9-16.

Peech, M., Olson, R.A., and Bolt, G.H., 1953. The significance of potentiometric measurements involving liquid junction in clay and soil suspensions. Soil Science Society of America Proceedings, 17, pp.214-218.

Penner, E., 1986. Aspects of ice lens growth in soils. Cold Regions Science and Technology, 13, pp. 91-100.

Péwé, T.L., 1975. Quaternary geology of Alaska. Geological Survey Profesional Paper, 835, 150 p.

Pusch, R., 1970. Clay microstructure. National Swedish Building Research Document, D8:1970, 76 p.

Pusch, R., 1977. Ice formation in clays with reference to their microstructural constitution. Frost Action in Soils, International Symposium Proceedings Vol. 1, Lulea, Sweden, pp. 137-142.

Römkens, M.J.M., and Miller, R.D., 1973. Migration of mineral particles in ice with a temperature gradient. Journal of Colloid and Interface Science, 42, pp. 103-111.

Sellman, P.V., and Chamberlain, E.J., 1979. Permafrost beneath the Beaufort Sea near Prudhoe Bay, Alaska. 1979 Offshore Technology Conference. Houston, Alaska. Paper 3527.

Shainberg, I, and Kemper, W.D., 1972. Transport numbers and mobility of ions in bentonite membranes. Soil Science of America Proceedings, 36, pp. 577-582.

Skempton, A.W., and Henkel, D.J., 1953. The post-glacial clays of the Thames estuary at Tillburg and Shellhaven.

Proceedings 3rd International Conference on Soil Mechanics and Foundation Engineering, Vol. 1, pp. 30-53.

Smith, L.B., 1972. Thaw consolidation tests on remoulded clays. Unpublished M.Sc. thesis, University of Alberta, 157 p.

Terzaghi, K., 1943. **Theoretical soil mechanics.** Wiley, New York, 510 p.

Tice, A.R., Anderson, D.M., and Banin, A., 1976. The prediction of unfrozen water contents in frozen soils from liquid limit determinations. CRREL Report 76-8, 9 p.

van Olphen, H., 1963. **An introduction to clay colloid chemistry.** Wiley Interscience, New York. 301 p.

Tsytovich, N.A., 1975. **The mechanics of frozen ground.** McGraw-Hill, New York.

Veder, C., 1978. **Landslides and their stabilization.** Springer Verlag, New York, 247 p.

Wang, J.L., 1982. Geotechnical properties of Alaska OCS silts. Offshore Technology Conference, Houston, Texas, Paper 4412.

Warkentin, B.P., Bolt, G.H., and Miller, R.D., 1957. Swelling pressure of montmorillonite. Soil Science Society of America Proceedings, 21, pp. 495-497.

Williams, P.J., and Burt, P.T., 1974. Measurements of hydraulic conductivity in frozen soils. Canadian Geotechnical Journal, 11, pp. 647-650.

Williams, P.J., and Wood, J.A., 1985. Internal stresses in frozen ground. Canadian Geotechnical Journal, 22, pp. 413-416.

Workman, E.J., and Reynolds, S.L., 1950. Electrical phenomena occurring during the freezing of dilute solutions and their possible relationship to thunderstorm activity. Physical Review, 78, pp. 254-259.

Yarkin, I.G., 1978. Effect of natural electric potentials an water migration in freezing soils. Proceedings 2nd International Conference on Permafrost, U.S.S.R. Contribution, Yakutsk, U.S.S.R., pp. 359-361.

Yarkin, I.G., 1986. Natural electric potentials that arise when soils freeze. CRREL Special Report 86-12, 24 p.

Yong, R.N., Taylor, L.O., and Warkentin B.P., 1963. Swelling

pressure of sodium montmorillonite at depressed temperatures. Clays and Clay Minerals, 11, pp. 268-281.

Yong, R.N., Boonsinsuk, P., and Yin, C.W.P., 1985. Alteration of soil behavior after cyclic freezing and thawing. Proceedings 4th International Symposium on Ground Freezing, Sapporo, Japan, pp. 187-196.

APPENDIX A: Finite difference code

```
1     C ******************************************************************
2     C   Finite difference program for electro-osmosis in a soil
3     C   sample in which the spacing between cathode and anode can
4     C   be chosen. The theoretical development and boundary
5     C   conditions can be found in Esrig (1968) and in this thesis
6     C   (under heading: An Electric Source in Freezing Soil)
7     C
8     C   Variables and Constants:
9     C     U    : Matrix with dummy variable 'chi'
10    C            In the rows the distance is constant, in the
11    C            columns the time is constant.
12    C     UT   : Vector with percent consolidation
13    C     A, B : Vectors used to calculate UT.
14    C     IEL  : The spacing between the electrodes.
15    C            The spacing between the electrodes is given by
16    C            (50-IEL)/50. The height of the sample is 1.
17    C
18    C   Output unit 6: a matrix with pore pressures as time progresses
19    C   Output unit 5: consolidation as time progresses
20    C   Output unit 9: a consolidation diagram
21    C
22    C ******************************************************************
23          DIMENSION U(51,7500),UT(7500),X(51),Y(51),A(51),B(51)
24          CALL DSPDEV('PLOTTER ')
25          CALL PAGE(8.5,11.)
26          CALL SCMPLX
27          CALL MIXALF('GREEK')
28          CALL BASALF('STAND')
29          CALL INTAXS
30          CALL AREA2D(4.8,6.)
31          CALL HEADIN('ELECTRO-OSMOTIC CONSOLIDATION$',100,1.,1)
32          CALL HEIGHT(.16)
33          CALL XNAME('(x)$',100)
34          CALL YNAME('THICKNESS OF SOIL LAYER$',100)
35          CALL GRAF(0.,20.,100.,0.,.2,1.)
36          CALL THKFRM(0.03)
37          CALL FRAME
38              IEL=46
39            IELMA=IEL+1
40            IELMI=IEL-1
41            DO 7 I=1,51
42            DO 7 J=1,7500
43            U(I,J)=0.
44    7       CONTINUE
45          DO 1 I=IELMA, 51
46          U(I,1)=U(I-1,1) + 100./(51.-IEL)
47    1     CONTINUE
48          DO 2 J=1,7500
49          U(51,J)=100.
50    2     CONTINUE
51          DO 3 J=2,7500
52          DO 4 I=2,IELMI
```

```
53              U(I,J)=(U(I,J-1)+U(I-1,J-1)+U(I+1,J-1))/3.
54              U(1,J)=U(2,J)
55        4     CONTINUE
56              DO 5 I=IELMA,50
57              U(I,J)=(U(I,J-1)+U(I-1,J-1)+U(I+1,J-1))/3.
58        5     CONTINUE
59              U(IEL,J)=(U(IELMI,J)+U(IELMA,J))/2.
60        3     CONTINUE
61              DO 11 J=1,7500
62              IF(J.EQ.1) GOTO 12
63              IF(J.EQ.75) GOTO 12
64              IF(J.EQ.375) GOTO 12
65              IF(J.EQ.750) GOTO 12
66              IF(J.EQ.1500) GOTO 12
67              IF(J.EQ.3000) GOTO 12
68              IF(J.EQ.4500) GOTO 12
69              IF(J.EQ.6000) GOTO 12
70              IF(J.EQ.7500) GOTO 12
71              GOTO 11
72        12      UT(J)=0.
73                DO 21 I=1,51
74                A(I)=0.
75                B(I)=0.
76        21      CONTINUE
77                A(1)=U(1,J)-U(1,1)
78                B(1)=100.-U(1,1)
79                DO 14 I=2,51
80                A(I)=A(I-1)+U(I,J)-U(I,1)
81                B(I)=B(I-1)+100.-U(I,1)
82        14      CONTINUE
83                UT(J)=A(51)/B(51)
84              WRITE(6,101) J,(U(I,J),I=1,51,3)
85        101   FORMAT(I6,' * ',17F5.0,' * ')
86              WRITE(5,102) UT(J)
87        102   FORMAT(G15.5)
88              DO 19 I=1,51
89              X(I)=U(I,J)
90              Y(I)=(I-1)/50.
91        19    CONTINUE
92              CALL CURVE(X,Y,51,0)
93        11    CONTINUE
94              CALL ENDPL(0)
95              CALL DONEPL
96              STOP
97              END
```

APPENDIX B: Mode of consolidation of Beaufort Sea deposits.

The Beaufort Sea deposits are estimated to be less than 22,000 years old (Chamberlain et al., 1978), being Late Wisconsinan. Some uncertainty remains as to the exact dating of the deposits, but their age does not significantly alter any of the arguments presented below. The cause for the high overconsolidation stresses is not obvious, and will be discussed in detail in the following.

Overriding by glaciers is ruled out as the Northern part of Alaska has not been glaciated during the Quaternary (Péwé, 1975) Also unloading is excluded from the possible mechanisms, because no significant erosion has taken place.

A sea level fluctuation of 80 m may have occurred since the deposition of these sediments (Hopkins, 1982), which would have caused minor loading effects (up to 300 kPa).

Desiccation may have occurred during this period, but Sellman and Chamberlain (1979) argue that the same kind of ice-saturated clays have been observed on shore, and therefore desiccation is a doubtful process. More convincing however is the consideration that the maximal preconsolidation load that may be reached due to drying is given by:

$\bar{p}_s$: preconsolidation pressure

h_c : height of capillary rise

γ_w : density of water

$\bar{p}_s = h_c \gamma_w$, Terzaghi (1943, p. 333)

The height of capillary rise is less than 5 m for silts (Lambe and Whitman, 1969, p. 246) and may reach values of 20 m and more for clays. For instance the upper crust of London Clay (Liquid Limit = 106 %, Plastic Limit = 30 %), is consolidated to 200 kPa, and this is entirely attributed to drying (Skempton and Henkel, 1953).

Consolidation to 1600 kPa of the silty sand, which contains only 26 % clay and silt sized particles, can certainly not be explained by desiccation.

Secondary consolidation may have occurred when the sediments were loaded during the marine regression, which lasted several thousands of years. Bjerrum (1972) stated that the importance of secondary consolidation expressed as $\bar{p}_c/\bar{p}_o$ ($\bar{p}_c$: overconsolidation pressure, $\bar{p}_o$: overburden pressure) is dependent on the plasticity index. According to Bjerrum (1972) p_c/p_o is smaller than 1.5 for late glacial and post glacial clays with plasticity index smaller than 20 %. The plasticity index for the Beaufort silts is less than 20 %, and consequently secondary consolidation may only cause minor precompression.

Chemico-osmotic consolidation is the consolidation of a soil layer when it is brought in contact with an external solution with a high salt concentration. This process has been investigated by Mitchell et al. (1973) for a variety of soils and external solutions. They found that

chemico-osmosis was most effective in highly plastic clays (bentonite) surrounded by an external solution with a molecular weight of 6000. The void ratio of a bentonite layer consolidated to 100 kPa was reduced when placed in contact with a concentrated solution to a value corresponding to an overconsolidation pressure of 200 kPa, after which the bentonite began swelling.

In general the process can be described in the following way: after an initial decrease of the void ratio it increases again to its original value if the compression and swelling coefficients are identical. This happens because the process is twofold: an initial water flow out of the soil layer because the external solution has a higher concentration, followed by the migration of the salt into the soil accompanied by swelling of the soil layer. Since the compression and swelling coefficients are not equal for soils in general, some residual consolidation is expected to occur.

Assuming that the soils of the Prudhoe Bay region were fresh water deposits, or leached out in some later stage of their formation, chemico-osmosis may have occurred. Since they range from silty sand to silty clay chemico-osmotic consolidation would have been a minor effect. It is also of interest to note that the salt concentrations in the Prudhoe Bay soil water are higher than in the seawater. From the results presented by Mitchell et al. it seems very unlikely that chemico-osmotic consolidation would be responsible for

the observed overconsolidation of these deposits.

Another possibility to explain the (apparent) overconsolidation stresses is cementation. Cementation of sediments is discussed by Nacci et al. (1974) and Christian (1985). Two soil constituents may cause cementation: carbonates and iron oxide. Carbonate contents (as percent of dry weight) of the soil samples from Pruhoe Bay are given by Iskander et al. (1978) and range from less than .1 % to 25 %. Comparison of the $CaCO_3$ content with the (apparent) overconsolidation shows that there is no correlation whatsoever. The $CaCO_3$ content in borehole PB-2 varies between 1.2 % and 13.8 % within 3 m, while the measured overconsolidation pressure does not change significantly (Chamberlain and Sellman, 1978). Iron oxides may also cause cementation (Christian, 1985), but data on iron oxide is not given; it is reasonable to assume that it was not present in any large quantity, as a chemical analysis of the samples was conducted (Iskander et al., 1978).

Additional causes for apparent overconsolidation of soft sediments are discussed by Christian (1985).

Sellman and Chamberlain (1979) conclude that freezing and thawing has probably caused the overconsolidation of these sediments. It may be of interest to note that this is not an isolated example. Wang (1982) discussed the geotechnical properties of Alaskan silts, and found that significant overconsolidation was one of the typical properties, the values of the overconsolidation pressure

are, however, considerably lower than those from Prudhoe Bay. His conclusion was:

> " The freezing and thawing action has probably caused a highly variable "apparent" overconsolidation of the fine grained soils, particularly the frost susceptible silts."

APPENDIX C: Finite difference code

DIFF.2SOIL

```
C*****************************************************************
C   Program to calculate the movement of water in a two soil
C   system (bentonite and soil sample). The theory on which
C   the program is based is explained in the text.
C   Identification of the variables:
C     I         : stands for the location in the sample,
C                 I=1 corresponds to the bottom of the
C                 bentonite,
C                 I=51 corresponds to the top of the soil
C                 sample.
C     U(I,J)    : matrix containing the variable "chi" of the
C                 theory.
C     UT(J)     :
C     X(I)      :
C     STOR(I,J): contains the stepwise storage of water in
C                 the soil layer I.
C     Q(250)    : the total amount of water stored in the
C                 soil sample.
C*****************************************************************
      DIMENSION U(51,250),UT(250),X(51),Y(51),A(51),B(51),Q(250)
      DIMENSION R(250),T(250),STOR(51,250),ST(250)
      CALL DSPDEV('PLOTTER ')
      CALL PAGE(8.5,11.)
      CALL SCMPLX
      CALL NIXALF('GREEK')
      CALL BASALF('STAND')
      CALL INTAXS
      CALL AREA2D(4.8,6.)
      CALL HEADIN('ELECTRO-OSMOTIC CONSOLIDATION$',100,1.,1)
      CALL HEIGHT(.16)
      CALL XNAME('AMOUNT OF WATER STORED$',100)
      CALL YNAME('THICKNESS OF SOIL LAYER$',100)
      CALL GRAF(0.,5.,20.,.5,.1,1.)
      CALL GRID(1,1)
      CALL THKFRM(0.03)
      CALL FRAME
      READ(5,111) IEL,DVB,BKH
      WRITE(6,111) IEL,DVB,BKH
111   FORMAT(I6,2G10.3)
      IELNA=IEL+1
      IELNI=IEL-1
      DO 7 I=1,51
      DO 7 J=1,250
      U(I,J)=0.
      STOR(I,J)=0.
      R(J)=0.
7     CONTINUE
C*****************************************************************
C  Initial conditions: the pore pressures are zero, and chi is
C  determined by the voltage applied.
C  The voltage applied is linear in each soil element, but
C  the voltage drop over each soil element can be changed
C  through the variable DVB, which gives the I of the total
C  voltage dropped over the bentonite.
C  The voltage is zero at the bottom of the bentonite.
C*****************************************************************
      DO 1 I=1,IEL
      U(I,1)=DVB/IEL*I
```

DIFF.2SOIL

```
      1     CONTINUE
            DO 2 I=IEL,51
            U(I,1)=(I-IEL)*(100.-DVB)/(51.-IEL)+DVB
      2     CONTINUE
      C*****************************************************************
      C  Solution of the finite difference equations.
      C  In both the bentonite and the soil sample the same equations
      C  are used, the difference in properties is entirely introduced
      C  through the boundary between the two.
      C  At the boundary the continuity of flow is expressed.
      C*****************************************************************
            DO 4 J=2,250
            DO 4 I=2,50
            U(I,J)=(U(I,J-1)+U(I-1,J-1)+U(I+1,J-1))/3.
            U(1,J)=U(2,J)
            U(51,J)=U(50,J)
            U(IEL,J)=(BKH*U(IELMI,J)+U(IELMA,J))/(1.+BKH)
      4     CONTINUE
      C*****************************************************************
      C  In order to compute the amount of water stored in each soil
      C  layer in each time step, the flow in and out of each layer
      C  is calculated, the difference is the amount of water stored.
      C  The derivation of the time constant from I is found by
      C  dividing by 7500, as the height of the sample was divided
      C  in 50 layers, and beta is 1/3.
      C  The flow of water between two layers can be found from the
      C  difference between the two CHI values, *50 for the gradient
      C  layer thickness is 50.;/7500 for the time step, *50 for
      C  normalisation to a thickness of 1.
      C*****************************************************************
            DO 11 J=1,151
            DO 92 I=IELMA,50
            STOR(I,J)=STOR(I,J-1)-(U(I+1,J)-2.*U(I,J)+U(I-1,J))/150.*50.
      92    CONTINUE
            IF(J.EQ.1) GOTO 12
            IF(J.EQ.8) GOTO 12
            IF(J.EQ.25) GOTO 12
            IF(J.EQ.50) GOTO 12
            IF(J.EQ.75) GOTO 12
            IF(J.EQ.150) GOTO 12
            GOTO 11
      12    CONTINUE
            DO 19 I=1,51
            Y(I)=(I-1)/50.
            ST(I)=STOR(I,J)
      19    CONTINUE
            ST(51)=0.
            CALL CURVE(ST,Y,51,0)
      11    CONTINUE
            DO 333 J=2,151
      C*****************************************************************
      C  The total flow from the bentonite into the soil sample Q(J),
      C  is calculated from the gradient at the interface.
      C*****************************************************************
            Q(J)=(U(IELMA,J)-U(IEL,J))/150.+R(J)
            R(J+1)=Q(J)
            T(J)=(J-1)/7500.
            WRITE(7,222)T(J),Q(J)
      222   FORMAT(2G10.3)
      333   CONTINUE
            CALL ENDPL(0)
            CALL DONEPL
            STOP
            END
```

APPENDIX D: Experimental results

WATER CONTENT PROFILE, #4

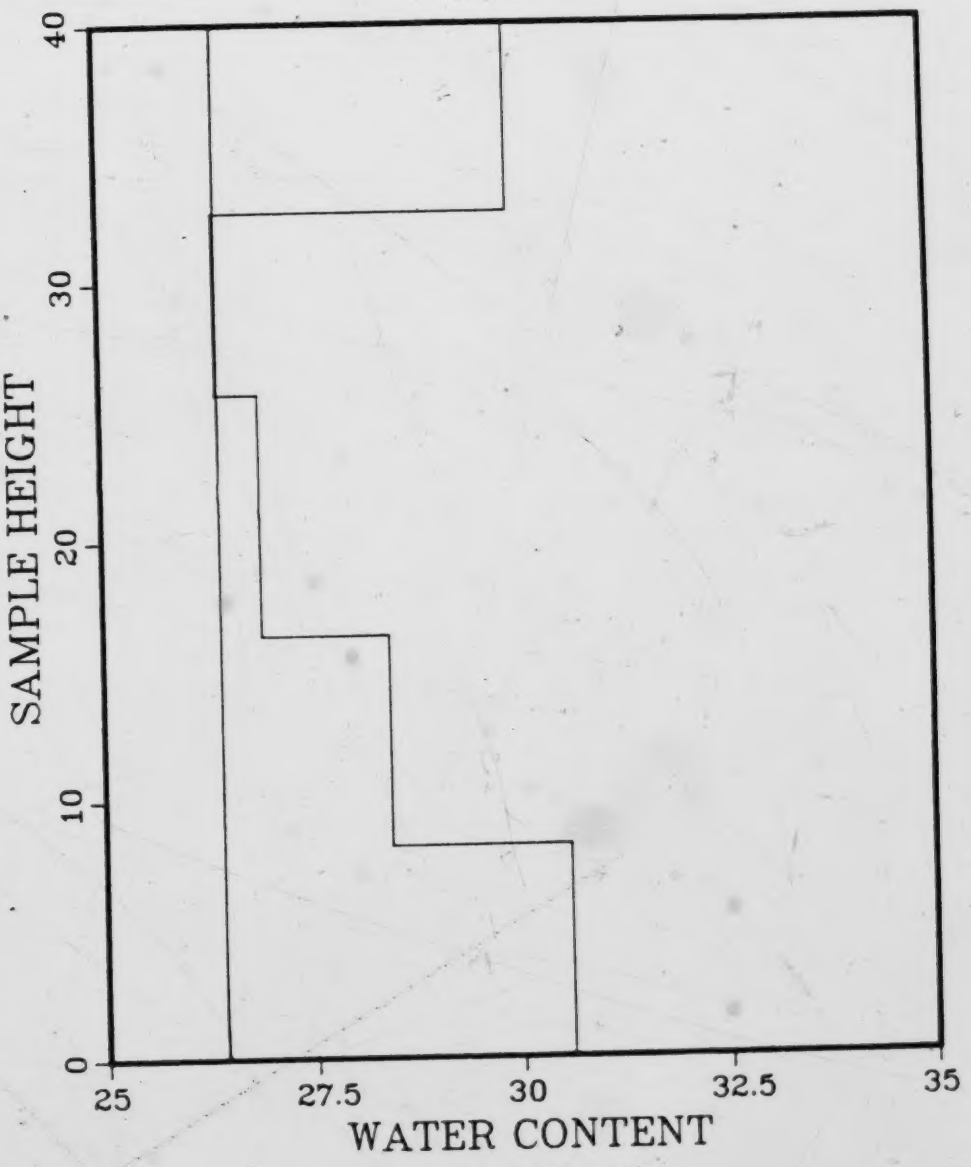

Figure D.1 Initial and final water content profiles, Exp. #4

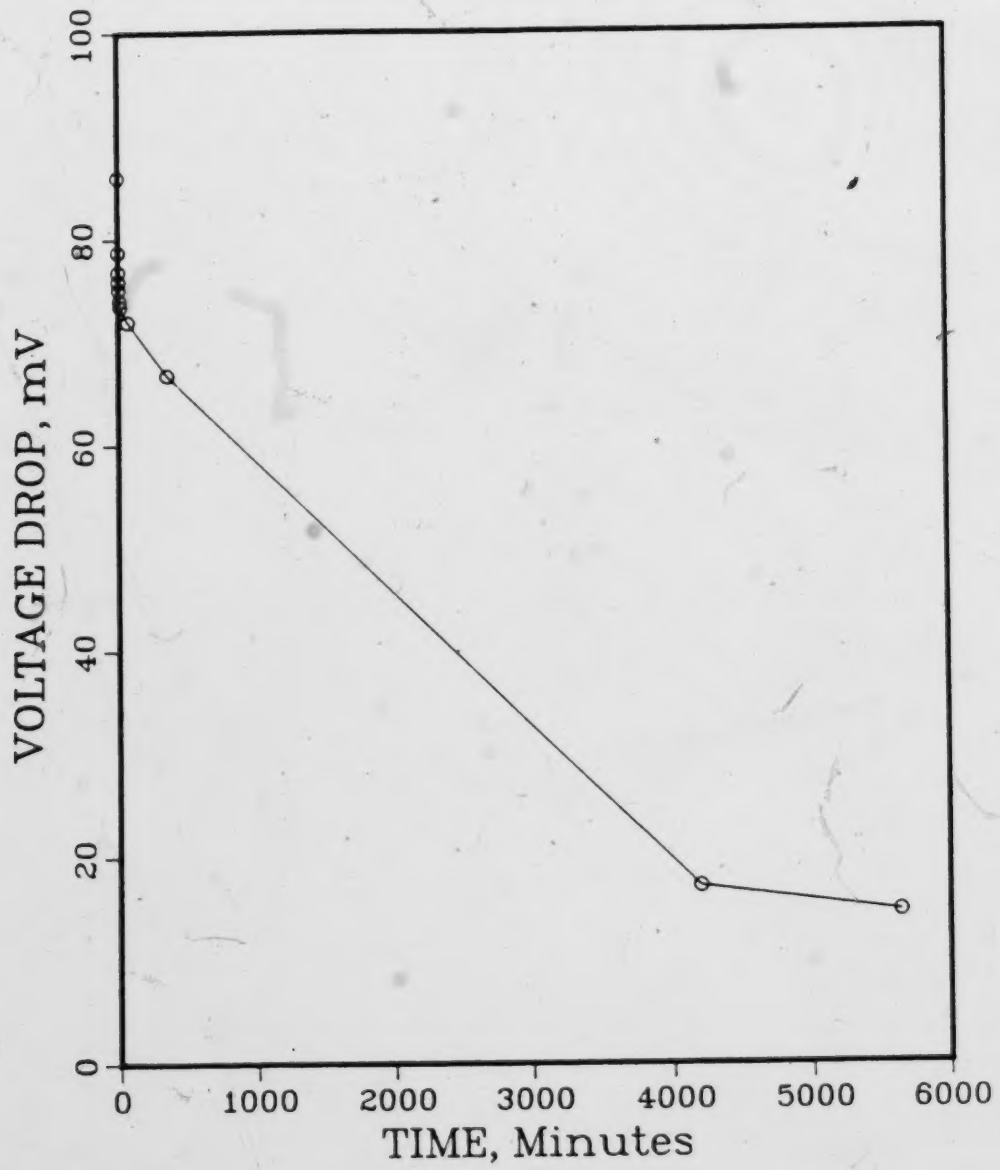

Figure D.2 Voltage drop across 120 Ohm resistor in series with the soil sample vs. time, Exp. #4

Figure D.3 Initial and final water content profiles, Exp. #5

EXPERIMENT #5

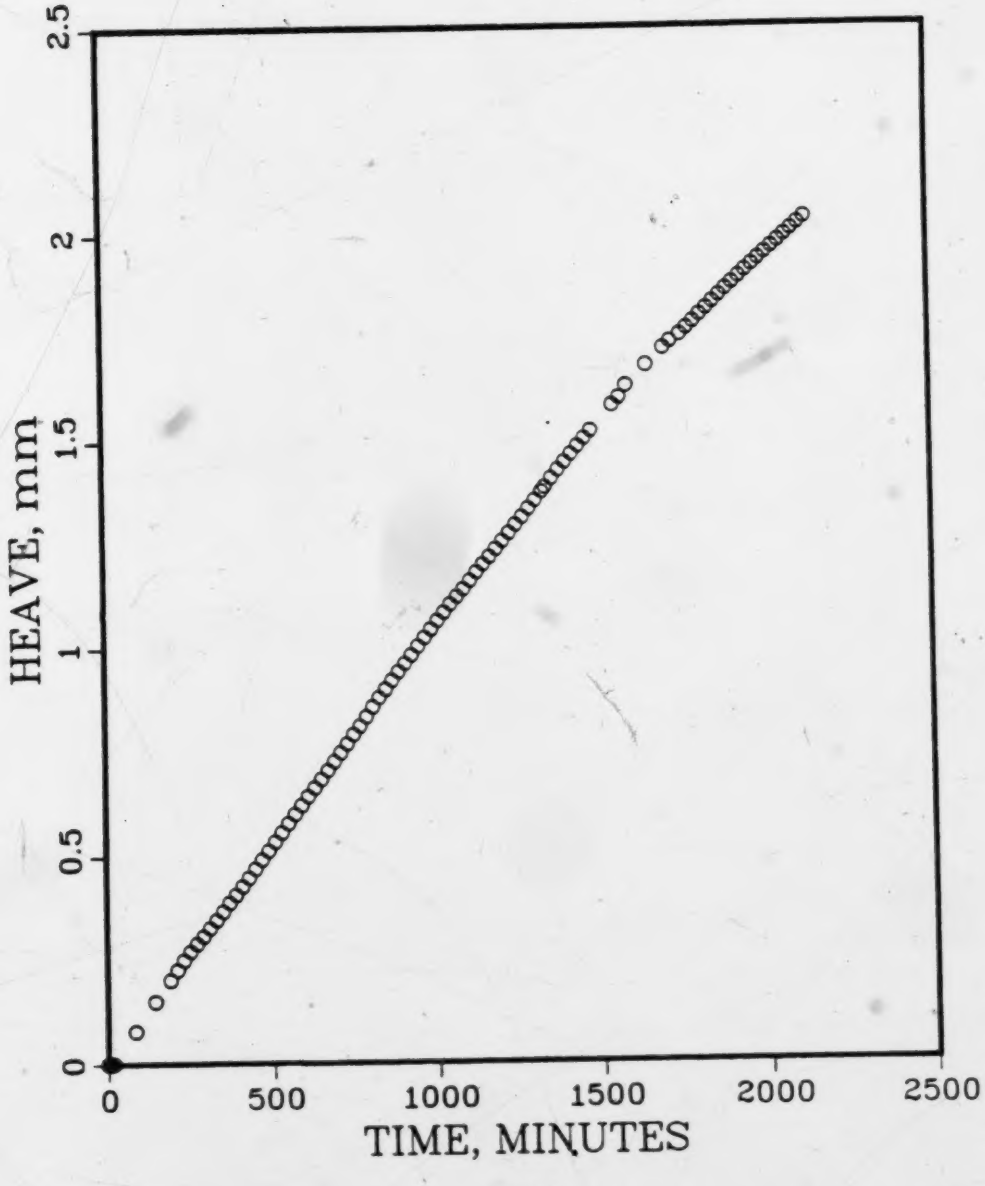

Figure D.4 Heave of top of soil sample vs. time, Exp. #5

EXPERIMENT #5

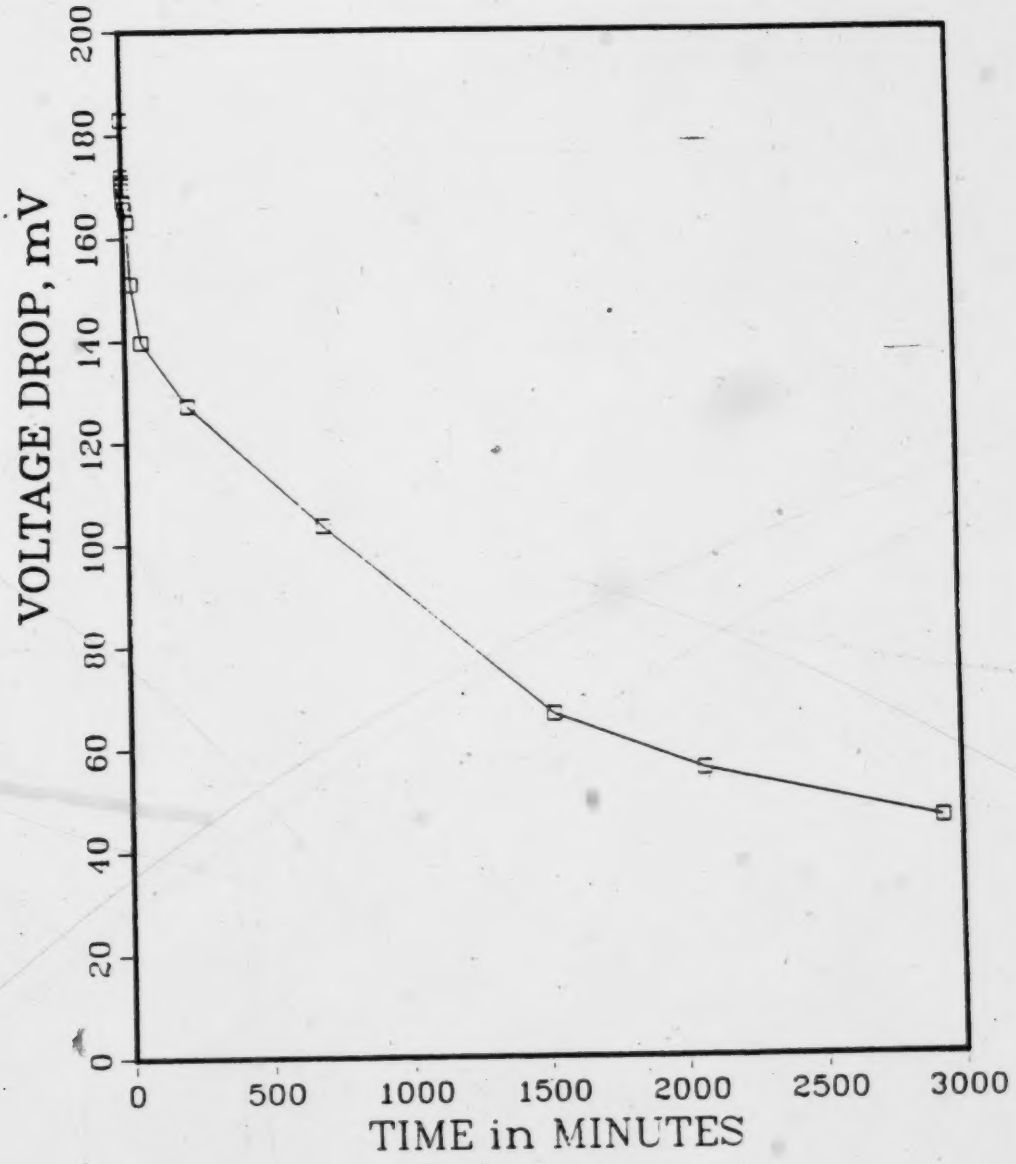

Figure D.5 Voltage drop across 120 Ohm resistor in series with the soil sample vs. time, Exp. #5

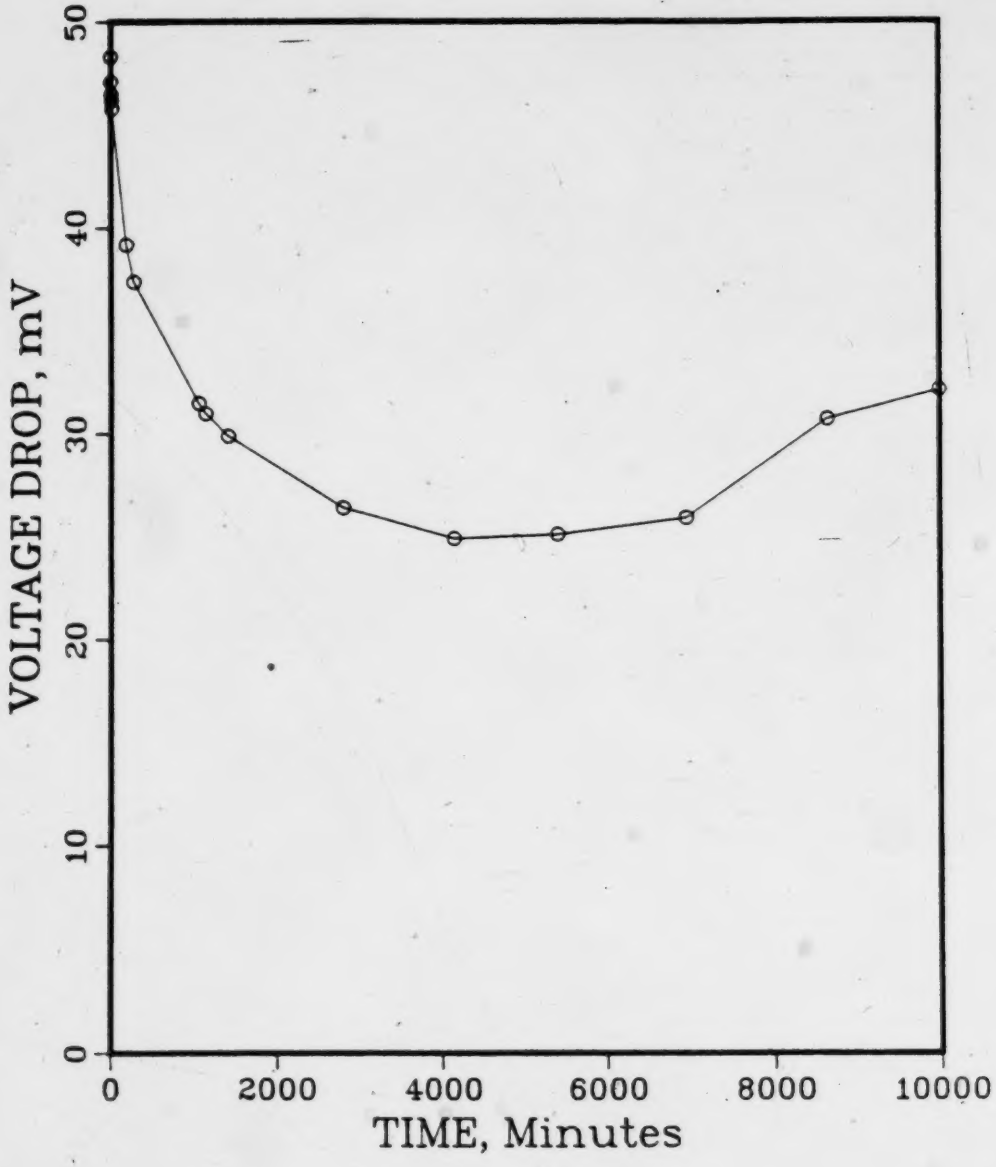

Figure D.6 Voltage drop across 120 Ohm resistor in series with the soil sample vs. time, Exp. #7

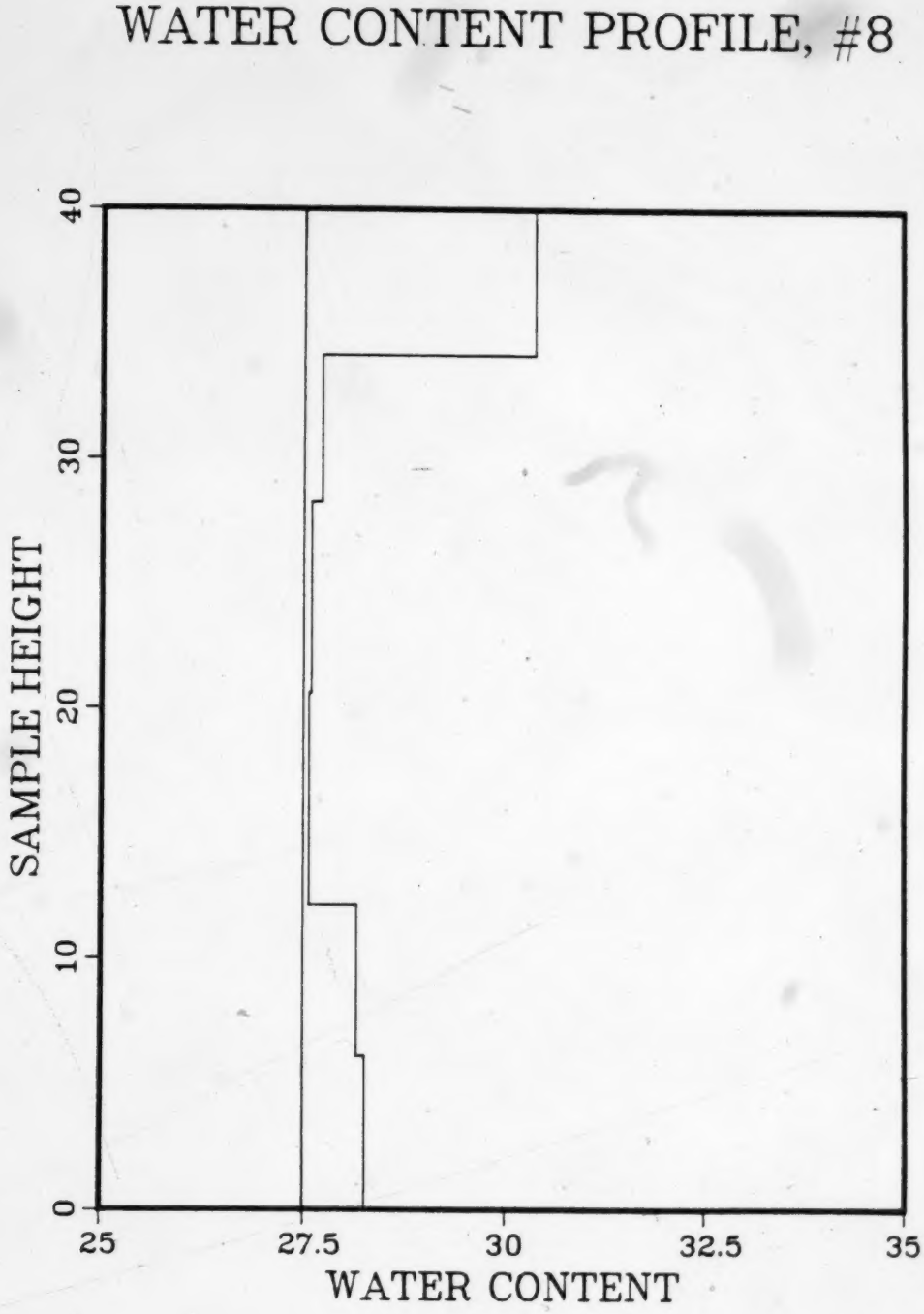

Figure D.7 Initial and final water content profiles, Exp. #8

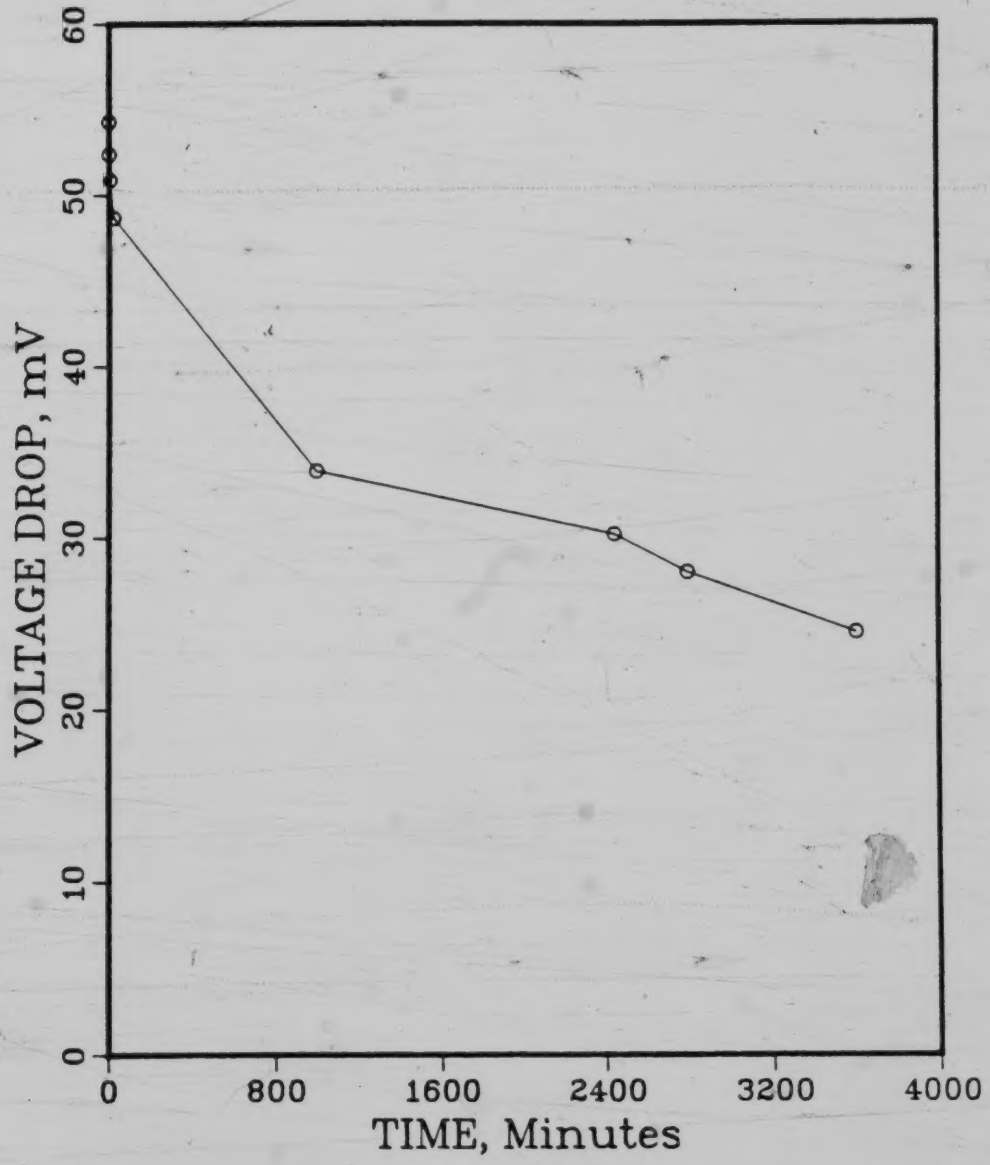

Figure D.8 Voltage drop across 120 Ohm resistor in series with the soil sample vs. time, Exp. #8

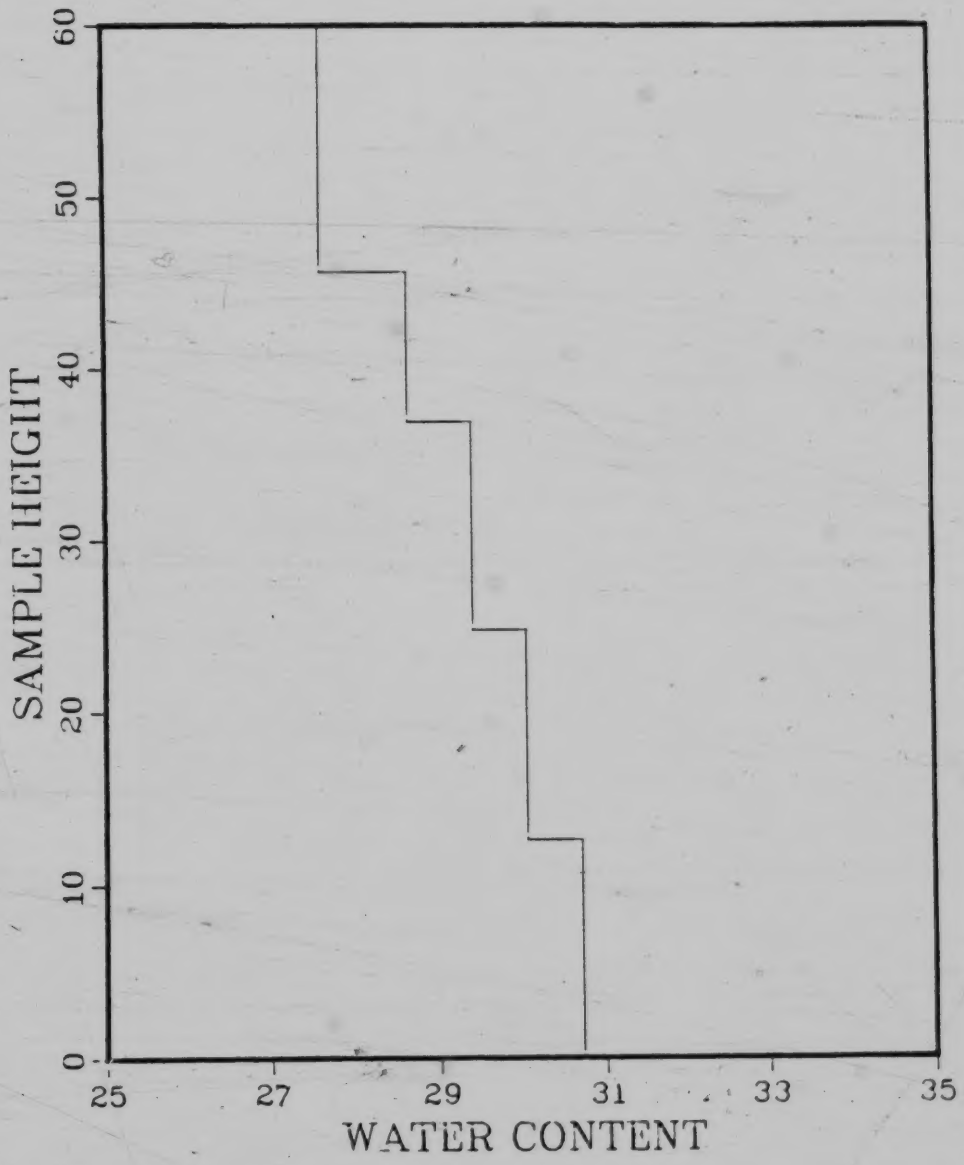

Figure D.9 Initial and final water content profiles, Exp. #9

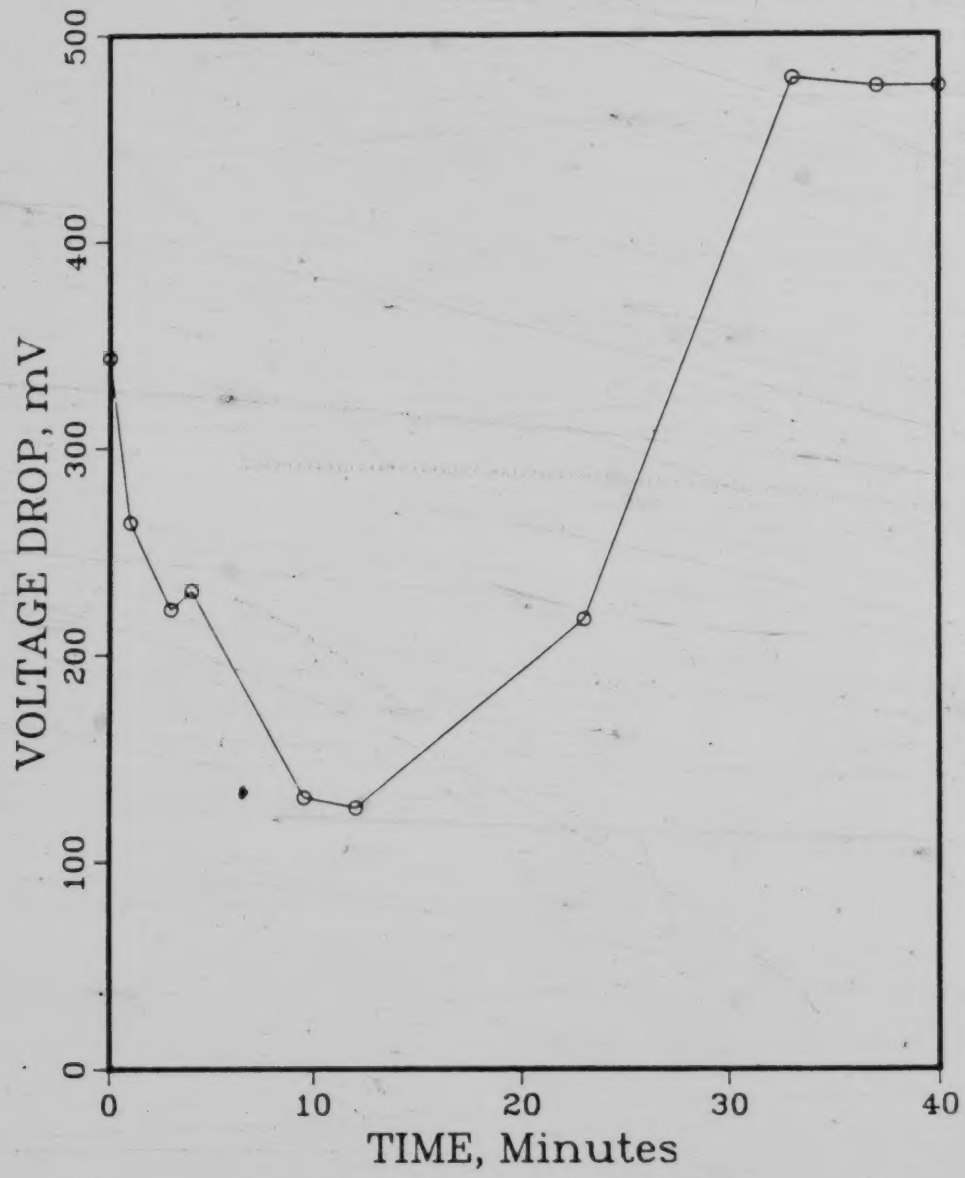

Figure D.10 Voltage drop across 120 Ohm resistor in series with the soil sample vs. time, Exp. #9

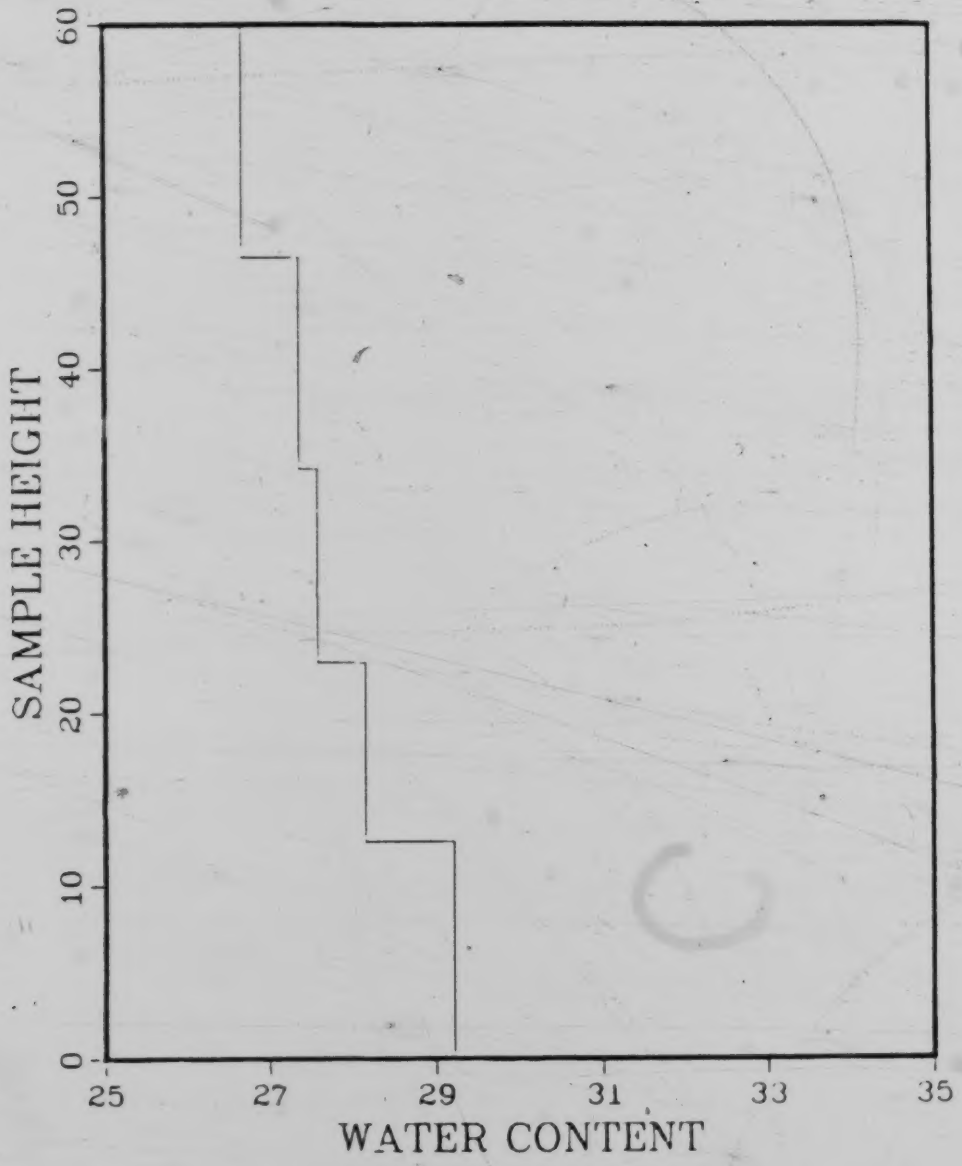

Figure D.11 Initial and final water content profiles, Exp. #10

EXPERIMENT #11

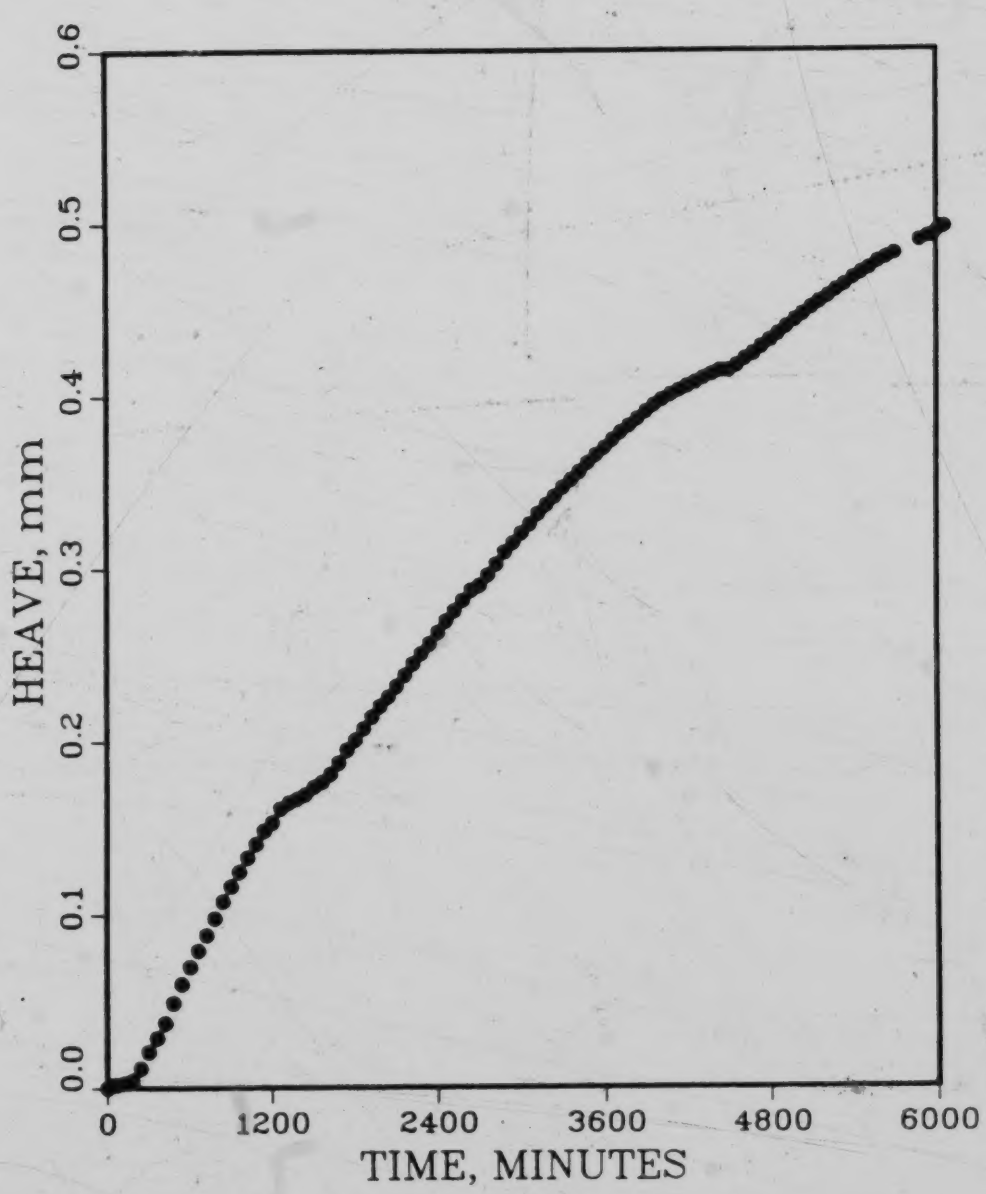

Figure D.12 Heave of top of soil sample vs. time, Exp. #11

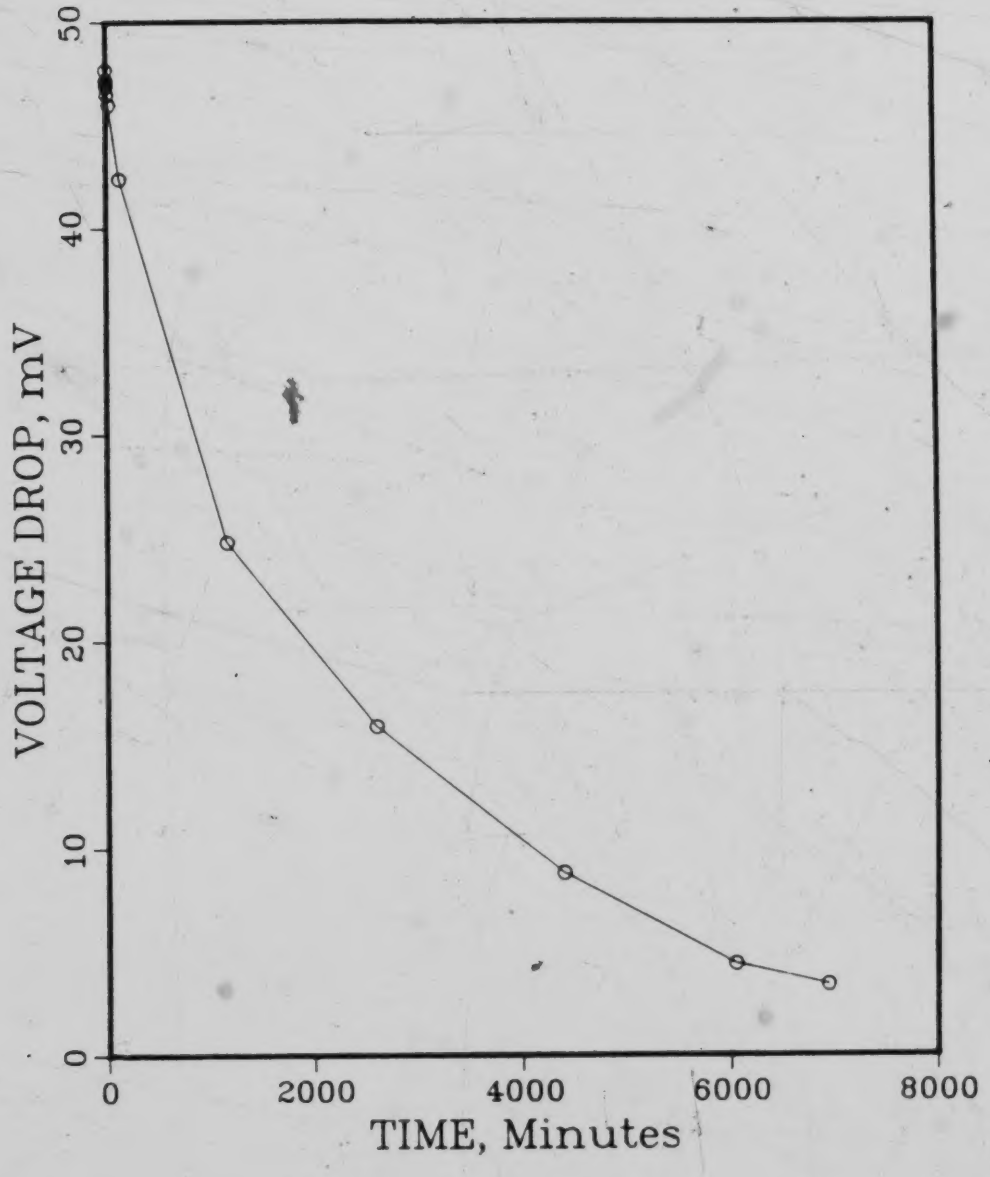

Figure D.13 Voltage drop across 120 Ohm resistor in series with the soil sample vs. time, Exp. #11

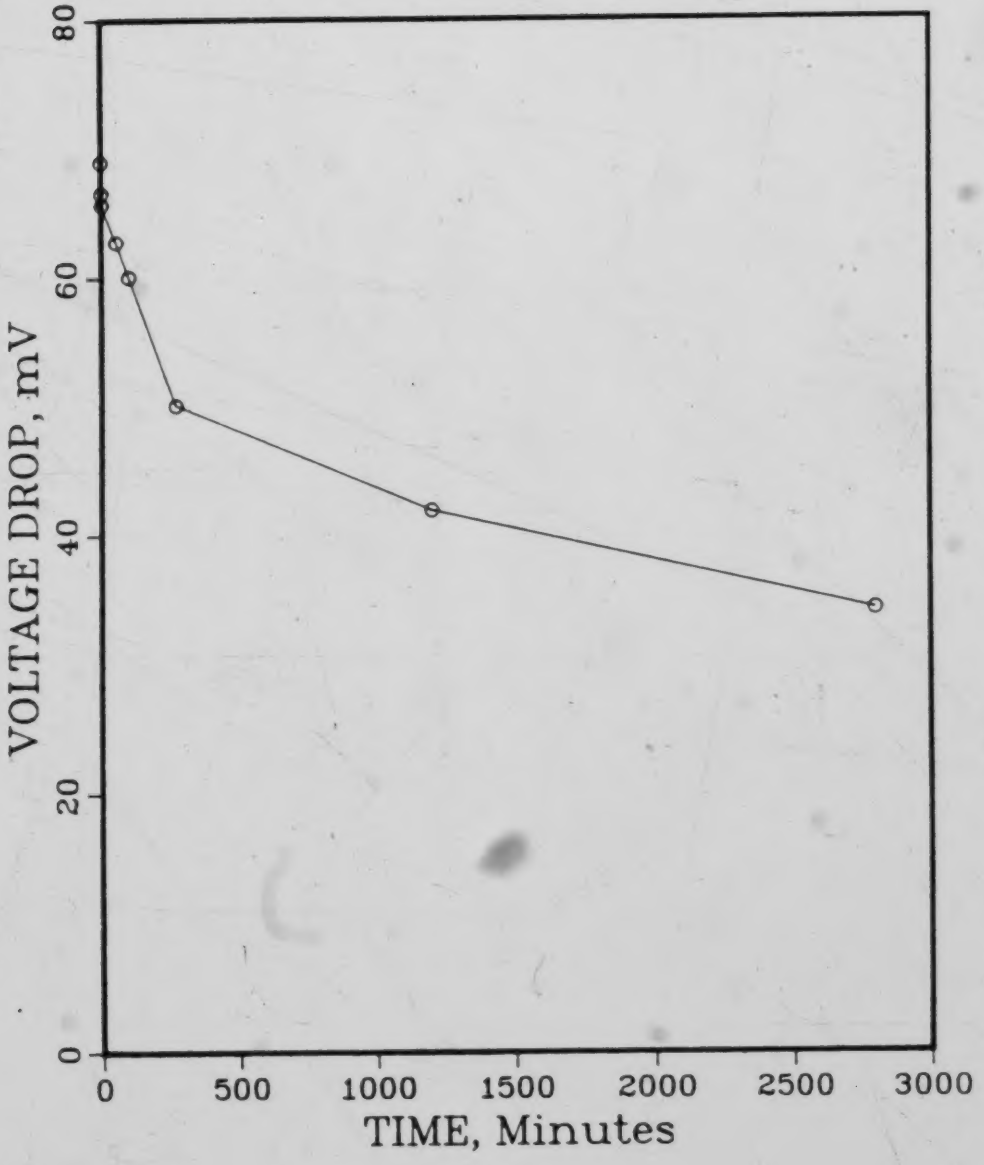

Figure D.14 Voltage drop across 120 Ohm resistor in series with the soil sample vs. time, Exp. #12

APPENDIX E: The Segregation Potential theory

E.1 Correlation of index properties and frost susceptibility

The original aim of this thesis was to correlate index properties of soils with their frost susceptibility. The method of frost heave analysis chosen was the Segregation Potential Theory as proposed by Konrad and Morgenstern (1980, 1981, 1982), and Konrad (1980).

A vast quantity of frost heave experiments has been conducted by the U.S. Army prior to establishing the U.S. Army Corps of Engineers Frost Susceptibility Criterion. These tests are described in ACFEL (Arctic Construction and Frost Effects Laboratory)(1951, 1958a and b) and Kaplar and Haley (1952). It was contemplated that the Segregation Potential Theory would enable a rational analysis of these data; thus leading to the objective.

Computer programs were written to automate the analysis. As a check on the calculations using the computer programs, Konrad's laboratory data was reanalysed. Each of the experiments reported in Konrad (1980) yielded a number of points in the SP - cooling rate - suction space. The data from the reanalysis of one test is illustrated in Fig. E.1. Compilation of points from several tests allowed a best fit surface to be derived. The surface chosen was a third order function in terms of both cooling rate and suction, the result is shown in Fig. E.2. Konrad arrived at his surface, shown in Fig. E.3, through analytical expressions between SP

and suction for five values of the cooling rate. SP values for intermediate values of the cooling rate are obtained by interpolation. This procedure introduces twenty-two (22) parameters. However, it is not felt that there is a conflict of principle between the two methods. The major difference between the two is that at a suction of 80 kPa Konrad's surface yields SP equal to zero; where Fig. E.2 has values different from zero. Konrad assumed that cavitation would occur at a suction of 80 kPa, and concluded that the water intake would be zero. However, occurrence of cavitation does not necessarily imply that the water intake ceases.

After this verification of the computational procedure the ACFEL-data were analysed. For each of the frost heave tests reported in their study three graphs are presented, namely:

1. time versus heave
2. time versus frost penetration
3. time versus temperature at cold side

According to Chapter 4 in Konrad (1980) these are necessary to calculate the relationship between SP, cooling rate, and suction. For this purpose the three graphs were digitized and cubic spline functions were fitted through the digitized points, yielding an analytical equation for each graph of the data.

The ACFEL frost penetration curves must be interpreted using a different approach than when using the curves from Konrad (1980). The thermocouples in the ACFEL experiments

were embedded in the soil sample, and therefore travelled together with the soil as it heaved during freezing. In Konrad's experiments the thermocouples were embedded in the side of the frost heave cell, and therefore they did not move with the soil. With some modifications in the programs the relationship between SP, cooling rate and pore pressure could be calculated, and presented graphically (Figs. E.5 to E.7). Figure E.5 allowed the relationship between SP, cooling rate and suction to be established at any time during the experiment. This yielded a high number of data points in the SP-cooling rate-suction space. A least square surface was fitted through these points; this surface is represented in Fig. E.6. As to graphically represent the goodness of fit, a cut through the surface is shown in Fig. E.7. The data points in this cut were corrected for the changed suction such that the value is given by:

SP(in Figure)= SP(calculated from data)

- SP(calculated from surface for original suction)

+ SP(calculated from surface for reported suction)

Another set is illustrated in Figs. E.8 to E.10.

After analysis of a number of experiments it became apparent that the scatter of the data was great. Some of it may be explained by non-ideal test conditions; however, it also called for a critical review of the basic assumptions of the Segregation Potential Theory. This will be dealt with in the next section.

To obtain the relationship between the index properties and frost susceptibility a single value for SP had to be chosen for each soil. Since there is no singular point on the SP-surface a rather artificial choice had to be made. It was decided to take the maximal SP corresponding with a suction equal to the maximum divided by eight. For Konrad's results this procedure would yield SP_o. Consequently Figs. E.11 to E.13 were prepared; the straight lines represent lines of best fit, the points were derived as described above. In general the fit is not good.

E.2 Review of Segregation Potential theory.

As the basic assumptions of the Segregation Potential Theory came in question it was decided to review its underlying principles.

A first point of contention was the confusion that exists as to which temperature gradients should be used for calculation of the SP from laboratory tests and to calculate the magnitude of heave. Konrad and Morgenstern (1980) used the temperature gradient from the unfrozen side, while Konrad and Morgenstern (1982) used the gradient from the frozen side. The same confusion exists in the original presetation by Konrad (1980).

In the paper by Konrad and Morgenstern (1980) they present Fig. E.14. This is indeed the key Figure on which the Segregation Potential Theory is based. The meaning of water intake velocity is clear, the temperature gradient is

less so. Grad T is conceptually the temperature gradient in the frozen fringe, but they actually used the warm side gradient. Both quantities are measured at the moment of initiation of the final ice lens in the freezing soil. In the Figure Grad T is provided with error bars, which are reasonable in magnitude. What, however, is the error of the intake velocity, and how does one determine the moment of initiation of the final ice lens ?

Konrad (1980, p. 70) states:

> "After freezing, the samples were carefully inspected, cut into two parts and water contents were taken from one.
>
> This permitted a check of the validity of the assumption that water flow to the ice lens is continuous with no accumulation within the frozen fringe. Further, those measurements allow one to back calculate very accurately the time at which the final ice lens was initiated. Finally, the position of the frost front obtained from thermistor readings could be compared with the measured height of unfrozen soil.

Errors involved in this procedure are summed up below:

1. Temperature measurement.(± 0.05°C)
2. Assumption for T_{so}= -.10°C (± 0.05°C)
3. Measurement of the height of unfrozen soil.(± 1 mm)

The frost penetration curve was derived from thermistors which were embedded in the wall of the frost heave cell,

their location was known. Konrad proposed an error of ±0.05°C for temperature readings, which is reasonable for the equipment used. The first point quoted above leads to a geometry shown in Fig. E.15.

$$x_1 = \frac{T_1 - \Delta T}{T_1 - T_2} L, \qquad x_2 = \frac{T_1 + \Delta T}{T_1 - T_2} L,$$

$$\Delta x_1 = x_2 - x_1 = \frac{2\ \Delta T}{T_1 - T_2} L$$

To get an idea of the importance of the error caused by an uncertainty of ± 0.05°C on the temperature measurement, consider:

Five thermistors in a sample with a height of 80 mm, with a temperature difference of $T_w - T_c = 4°C$.

Therefore,

1. $T_1 - T_2 \simeq 1°C$,
2. $L \simeq 20$ mm,
3. $\Delta T \simeq 0.05°C$

$$\Delta x_1 = \frac{2 \times 0.05°C}{1°C} \quad 20 \text{ mm} = 2.0 \text{ mm}$$

Now including the second source of error: an error of ≃ 0.05°C on T_{so}. Similar geometrical considerations, illustrated in Fig. E.16, lead to an accumulated error: $\Delta x_2 = 2 \times \Delta x_1 \simeq 4.0$ mm.

It may be of interest to note that the relationship between unfrozen water content and Atterberg limits as proposed by Tice et al. (1976) predicts a freezing point depression of just below -0.15 °C for Devon Silt. This would indicate that the error on the estimate of T_{so} is much larger than assumed here. It is expected to be in the order of 0.10 to 0.20 °C. However, assuming an error of ± 0.05 °C on the estimate of the segregation temperature, the first two sources of error would give an uncertainty in the location of the frost penetration line of 4.0 mm.

Including the third source of error, the error on the measurement of the height of the unfrozen soil, leads to the a situation as represented in Fig. E.17.

It is clear that the moment of initiation of the final ice lens can not be determined accurately. In a relatively short period of time the heave rate varies considerably. For example, Experiment NS-4, for which according to Konrad and Morgenstern (1980) the initiation of the final ice lens occured at t = 37 Hrs. and the intake velocity was 40 x 10^{-6} mm/s. An analysis using carefully digitized data yielded Table E.1.

The intake velocity exhibited a typically wavering pattern, also reported by Penner (1986). It shows that an error of Δt = 10 Hrs. would lead to a possible error in the intake velocity of 30 %.

In this simple analysis several factors, which would increase the magnitude of the estimated error, have not been

taken into account.

1. The exact location of the thermistors is difficult to determine, the finite dimensions of the sensor usually introduce an uncertainty larger than 1 mm.
2. The temperature measured by the thermistor is not equal to the temperature in the soil. This is especially valid for Konrad's data, because the thermistors were shielded from water by a rubber membrane surrounding the soil sample.
3. The measurement of the water intake velocity introduces a considerable error, as the intake velocity is calculated as the first derivative of the water intake, or, as the first derivative of the heave, including a correction for in situ freezing of water. Note that one actually needs to know the depth of frost penetration in the second case in order to calculate the intake velocity.
4. In the above it was assumed that one can estimate the temperature profile between two thermistors with a straight line; this introduces some error.

When all these factors are taken into account it transpires that the single value for SP_o is based on coincidence rather than on a law of nature.

E.3 Conclusion

The Segregation Potential theory, like many other frost heave theories (e.g. Harlan, 1973) is based on the balance of the heat flow equation and the Clausius-Clapeyron equation. Work by Miller (1980) suggests that the use of the Clausius-Clapeyron equation may not govern the frost heave behavior of a freezing soil. He proposed secondary heaving, which is based on the fact that a soil particle frozen in an ice sample which is subjected to a temperature gradient tends to migrate towards the warmer side of the ice sample (Römkens and Miller, 1973).

The driving force behind this movement is an osmotic or electro-osmotic gradient combined with heat flow and the Clausius-Clapeyron equation. It was for this reason thought of interest to study electro-osmosis is freezing and frozen soil.

Table E.1 Time versus Water Intake Velocity record for sample NS-4.

Time in Hrs.	Intake Velocity in 10^{-6}mm/s
32.	63.6
34.	59.6
36.	53.4
38.	56.1
40.	48.8
42.	45.0
44.	49.7

SP–DIAGRAM

TEST E–6

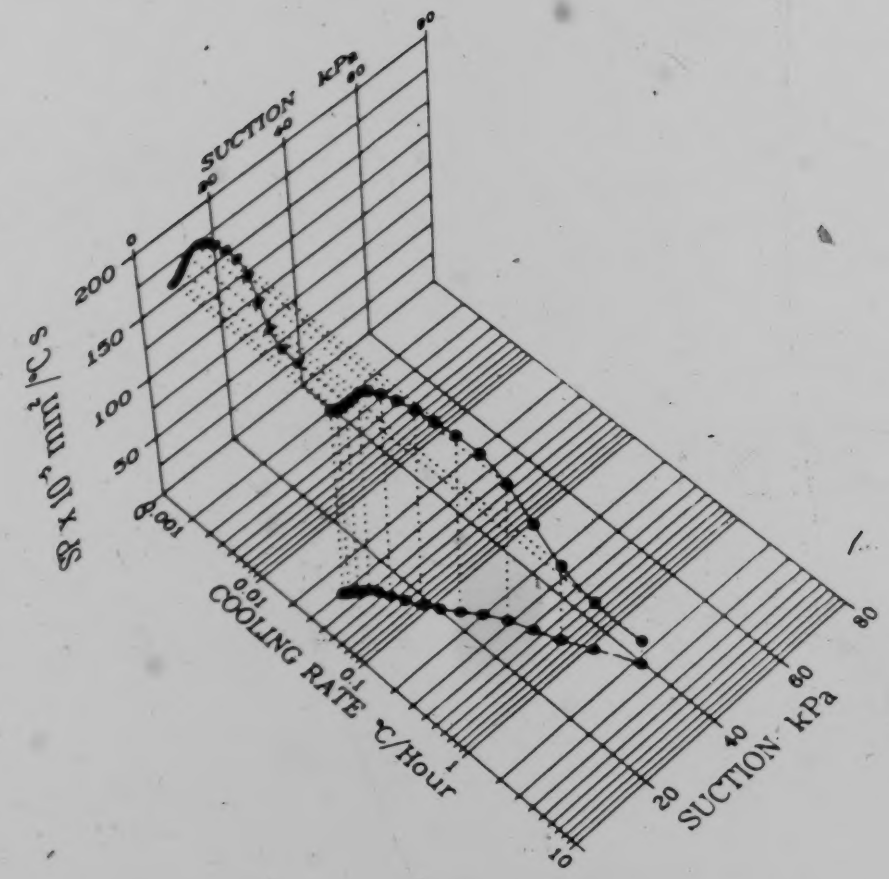

Figure E.1 Relationship between SP, suction at bottom of frost front and cooling rate for sample E-6.

SP–DIAGRAM

DEVON SILT

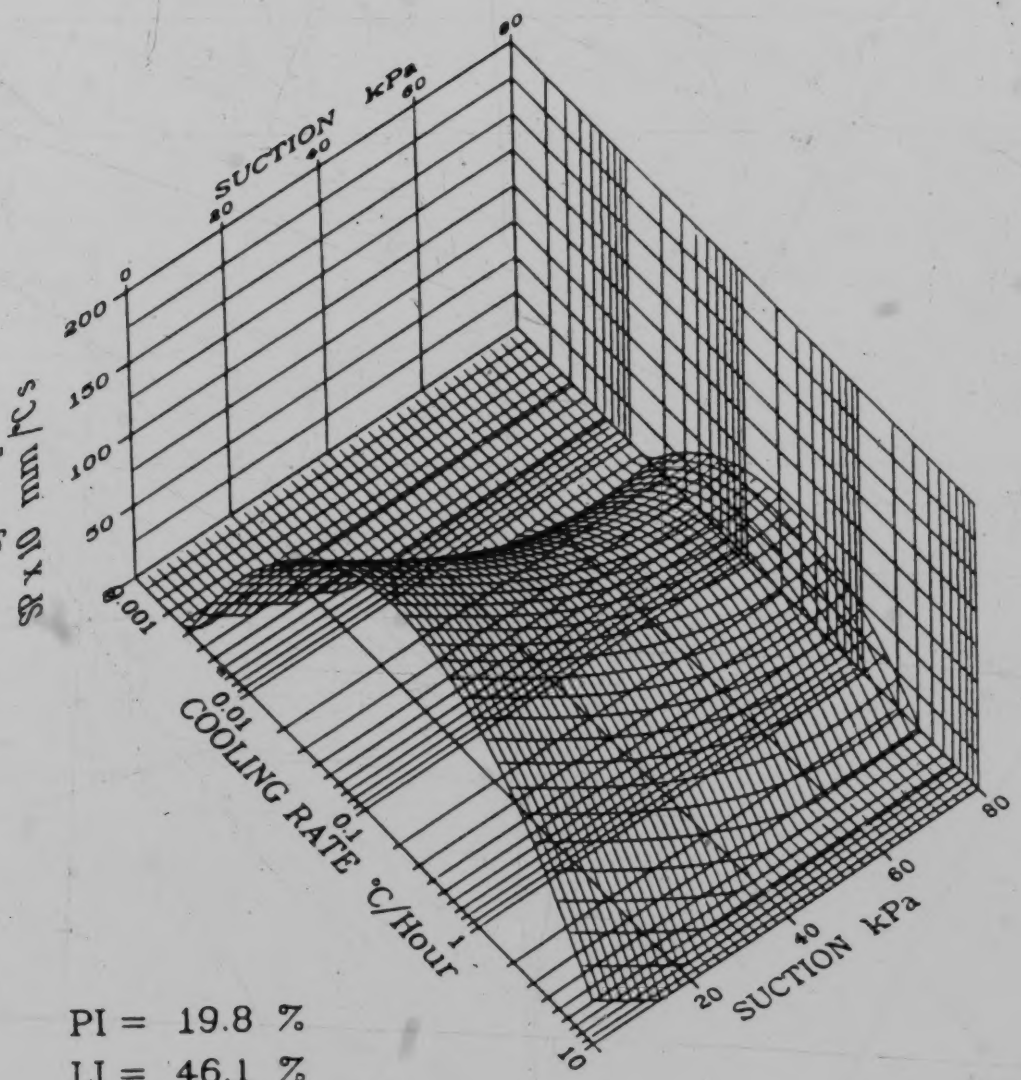

PI = 19.8 %
LI = 46.1 %
K = $10.0 * 10^{-10}$ m/s

Figure E.2 Relationship between SP, suction and cooling rate for Devon Silt.

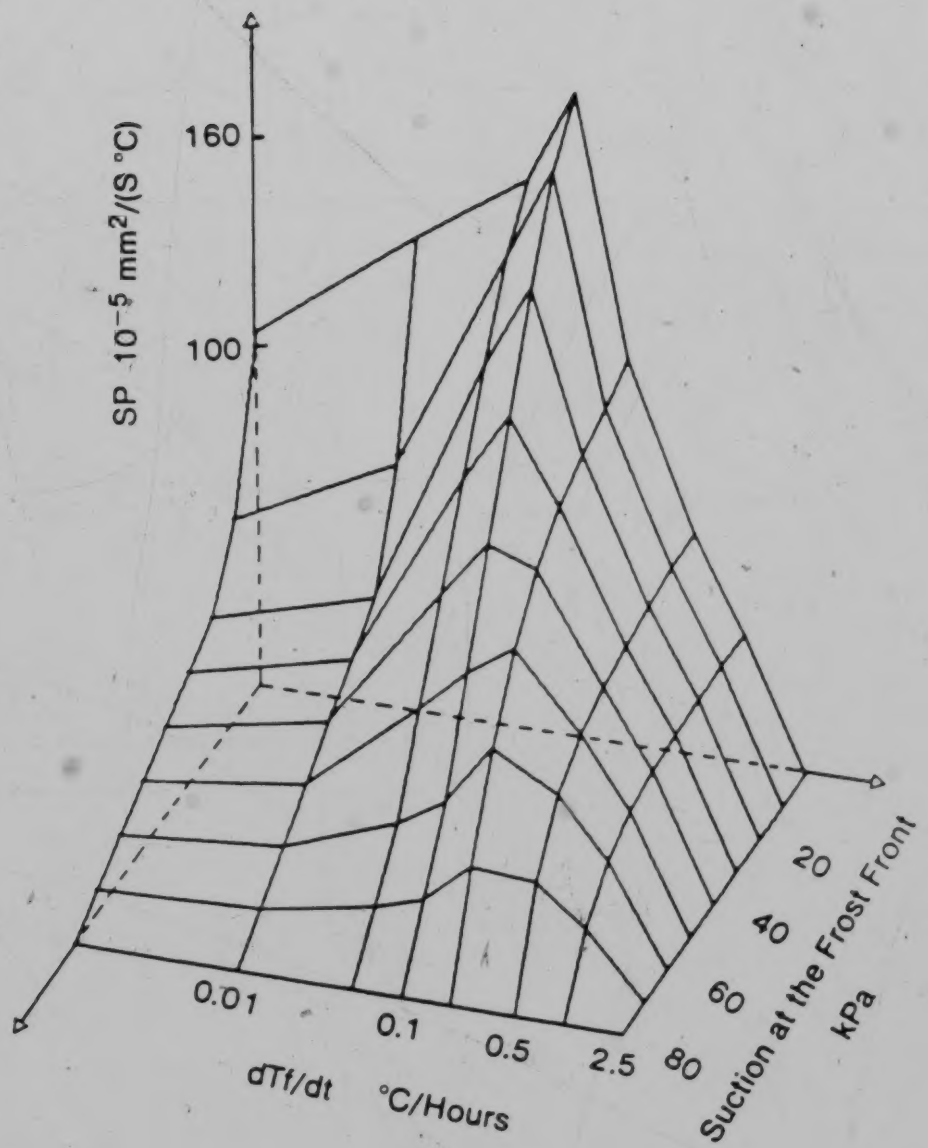

Figure E.3 Relationship between SP, suction and cooling rate for Devon Silt, (modified from Konrad, 1980)

SP–DIAGRAM

DEVON SILT

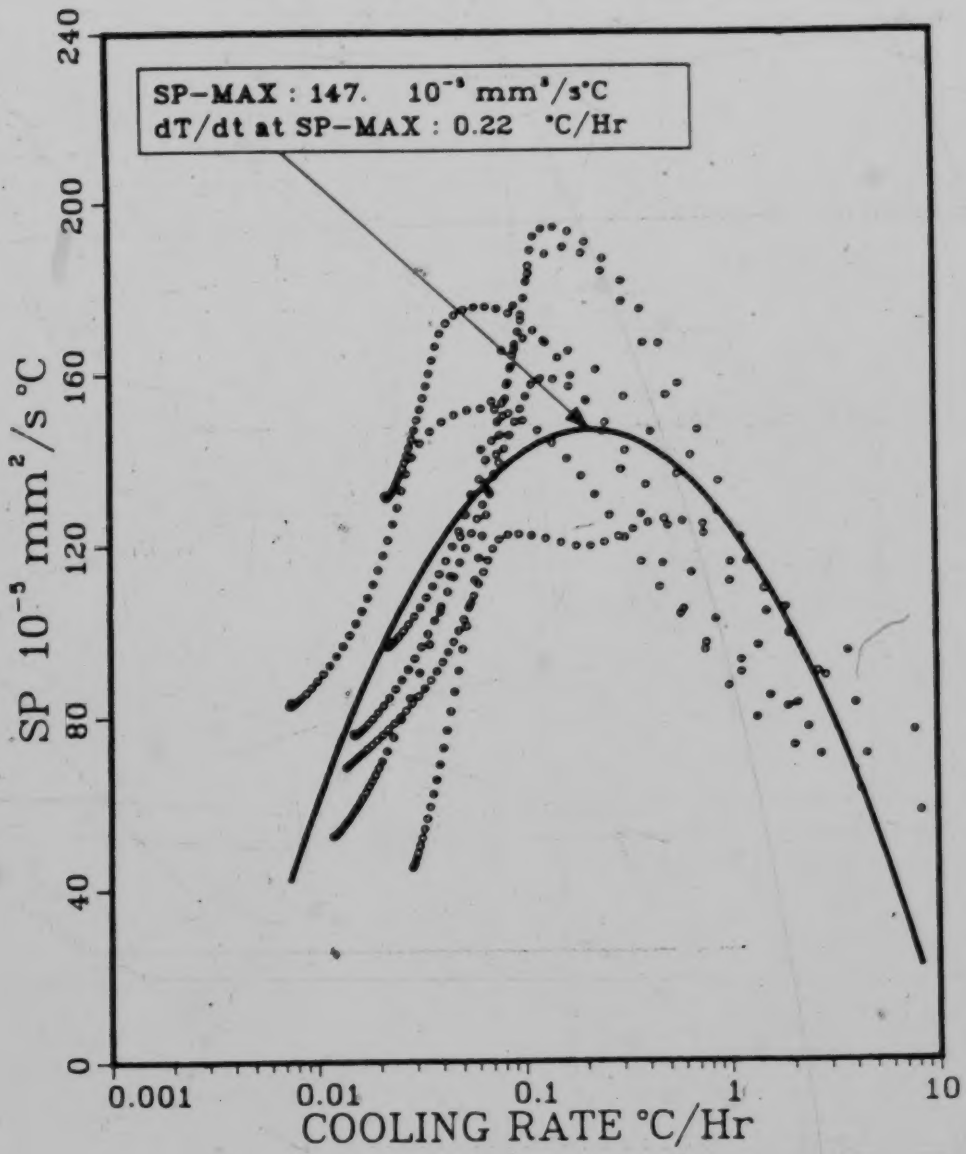

SUCTION : 10.00 kPA

Figure E.4 SP versus Cooling Rate for Devon Silt, the data points are plotted after correction for the changed suction.

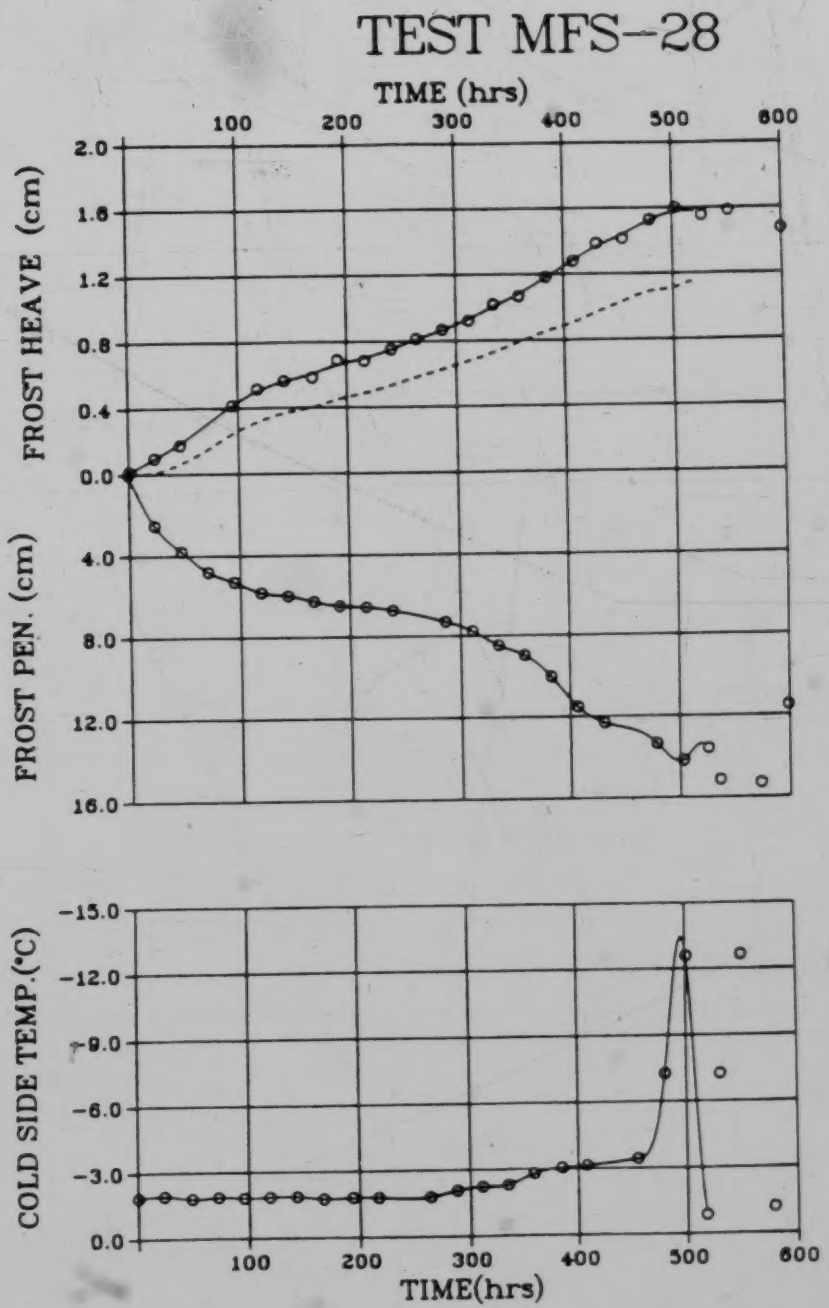

Figure E.5 Example of ACFEL data, MFS-28, (modfied from ACFEL ,1951)

SP–DIAGRAM

TEST MFS–28

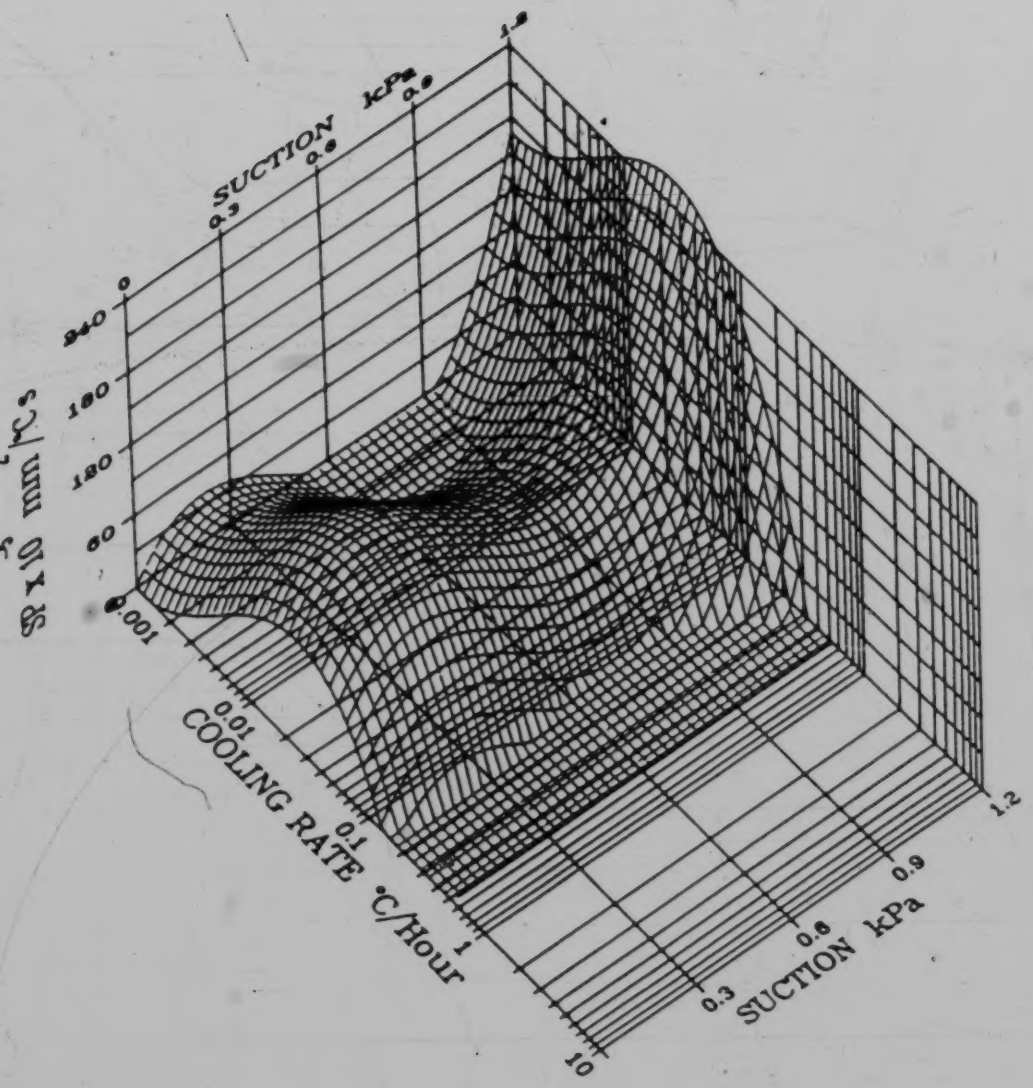

Figure E.6 Relationship between SP, cooling rate and suction for a typical test from ACFEL data, MFS-28.

SP–DIAGRAM

TEST MFS–28

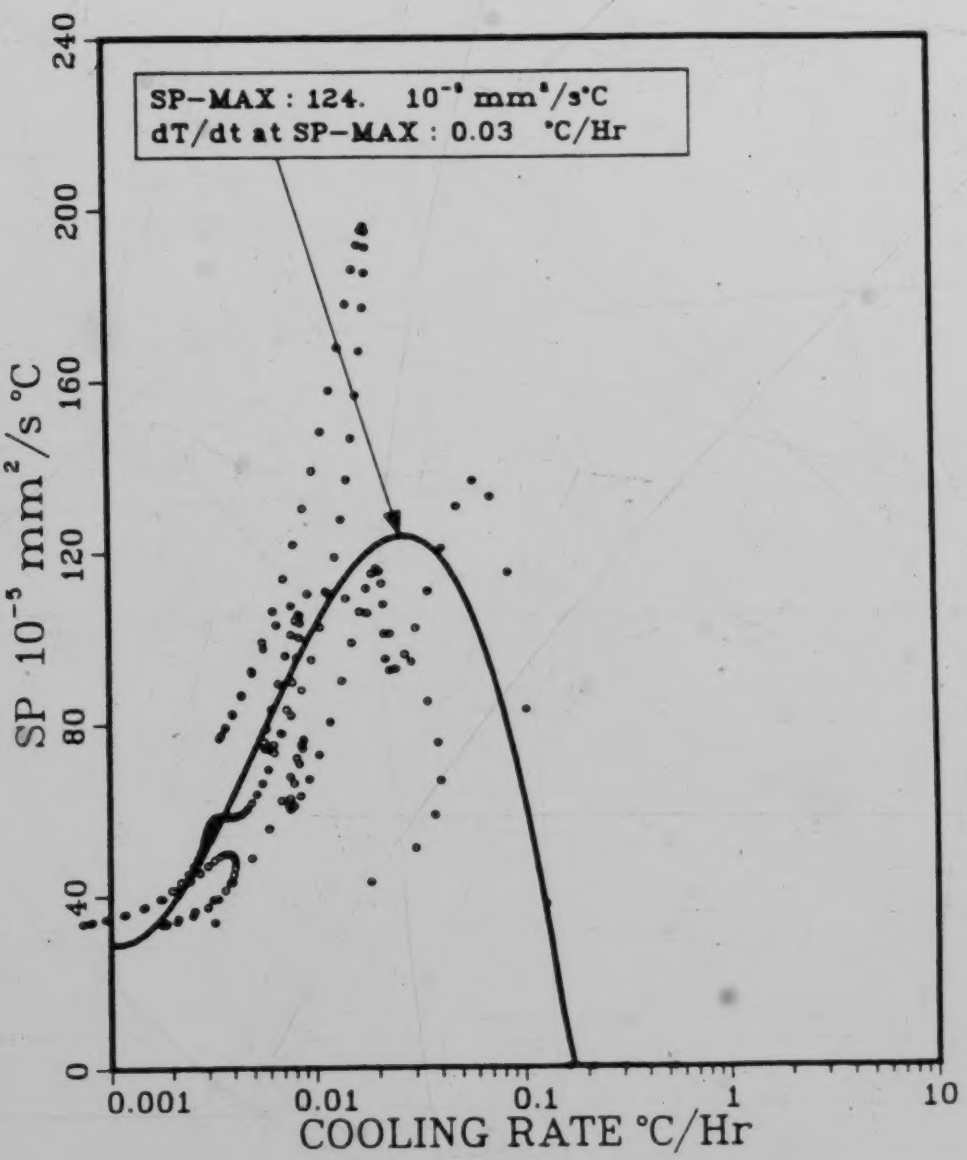

SUCTION : 0.10 kPA

Figure E.7 Relationship between SP and Cooling Rate for typical test from ACFEL data, MFS-28,data points are corrected for suction.

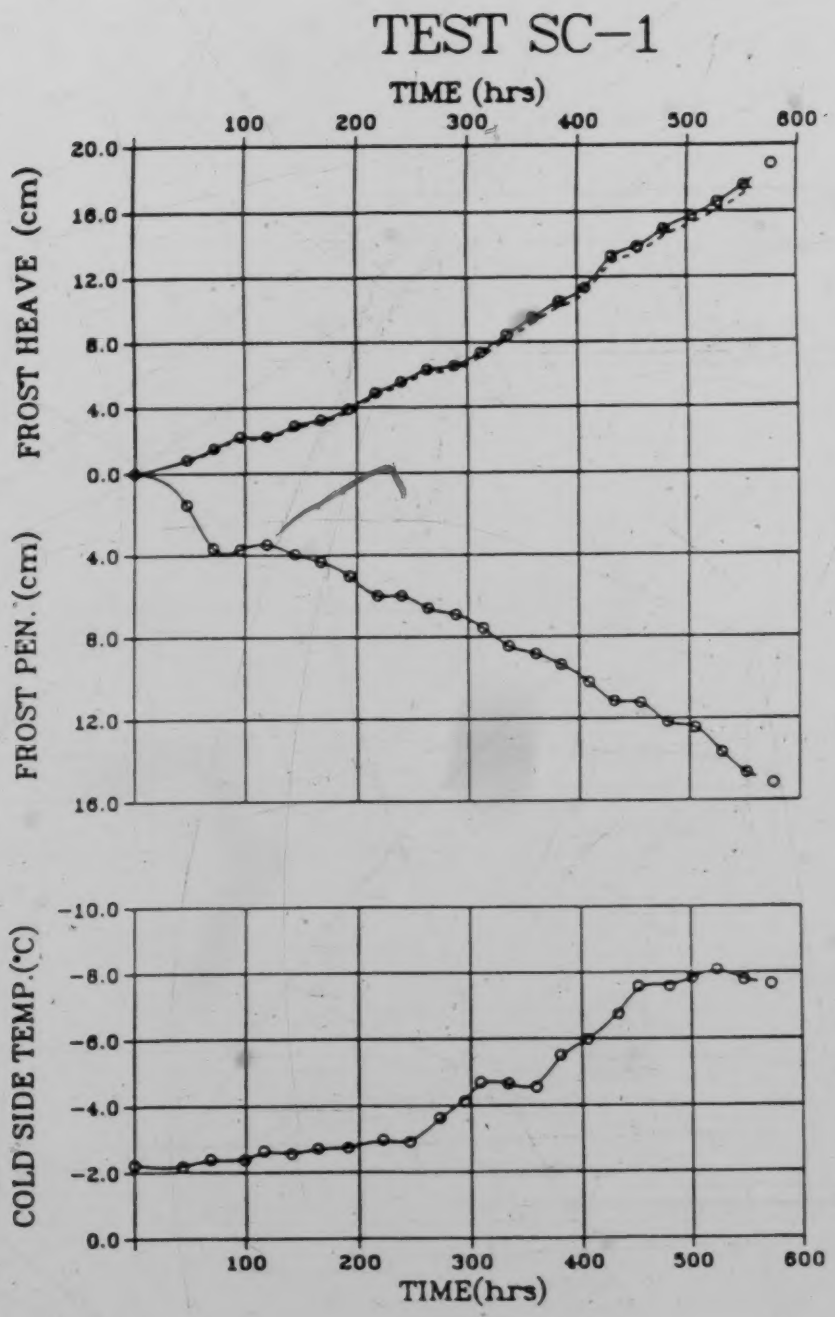

Figure E.8 Example of ACFEL data, SC-1, (modified from ACFEL, 1951)

SP–DIAGRAM

TEST SC–1

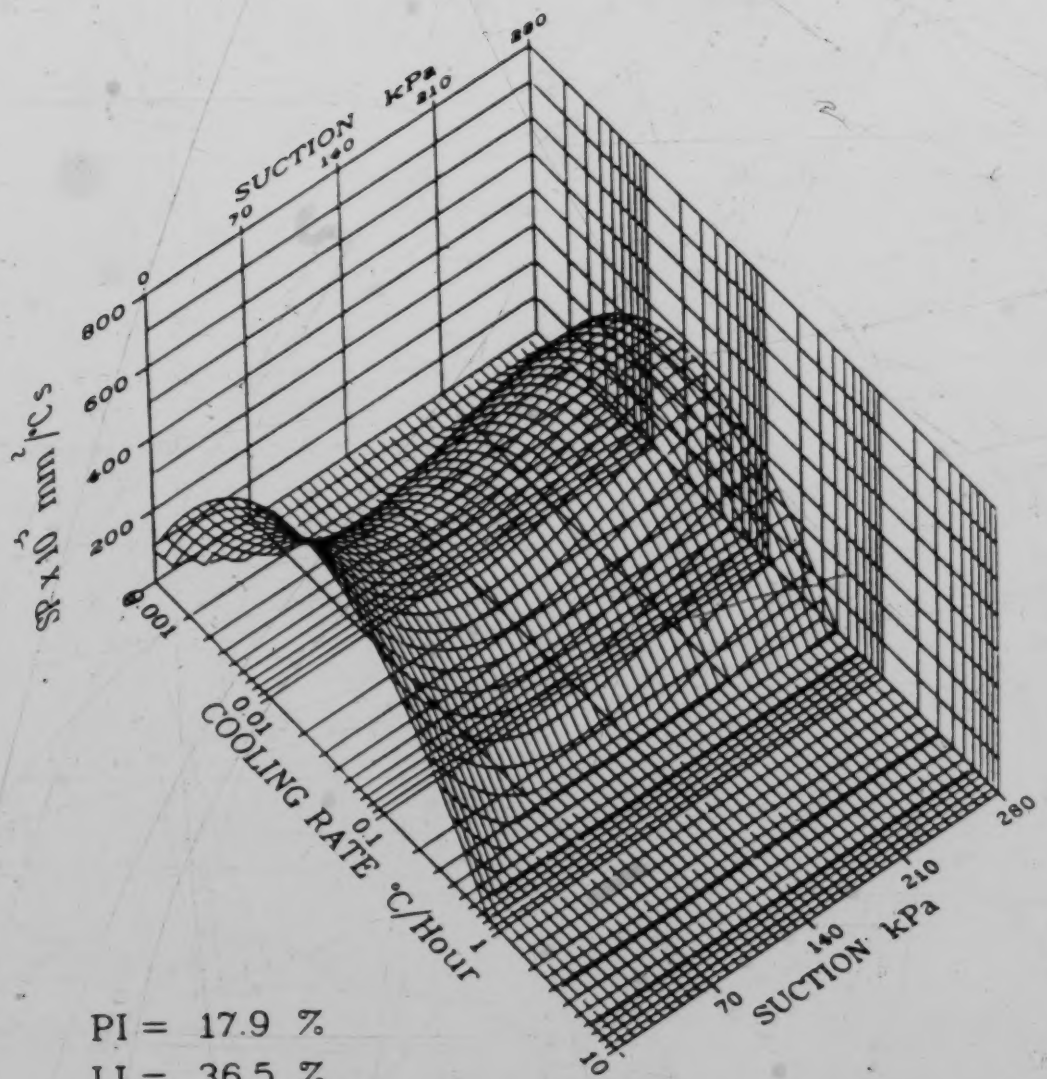

PI = 17.9 %
LI = 36.5 %
K = $3.6*10^{-10}$ m/s

Figure E.9 Relationship between SP, cooling rate and suction for a typical test from ACFEL data, SC-1.

SP–DIAGRAM

TEST SC–1

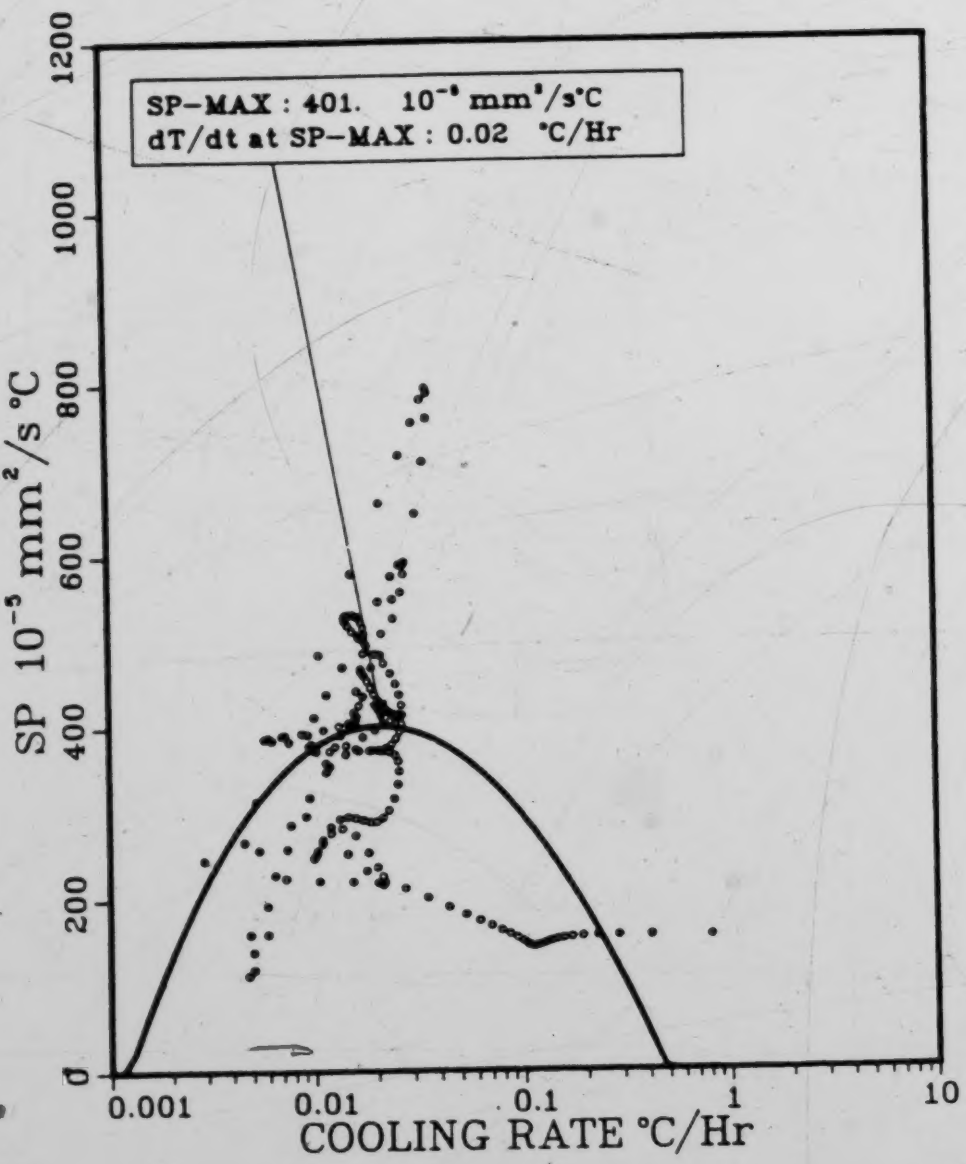

SUCTION : 27.78 kPA

Figure E.10 Relationship between SP and Cooling Rate for typical test from ACFEL data, SC-1, data points are corrected for suction.

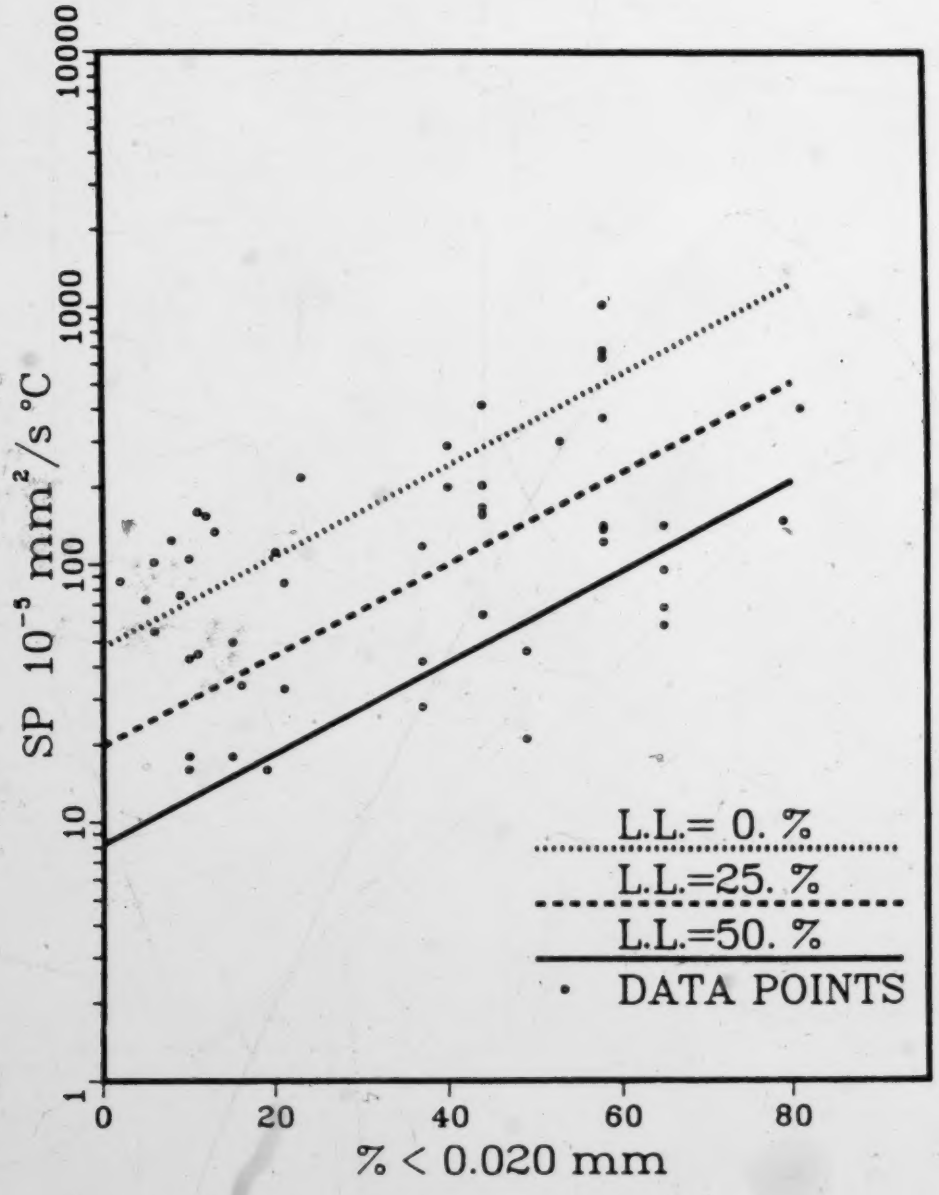

Figure E.11 Correlation between Index Properties and Segregation Potential.

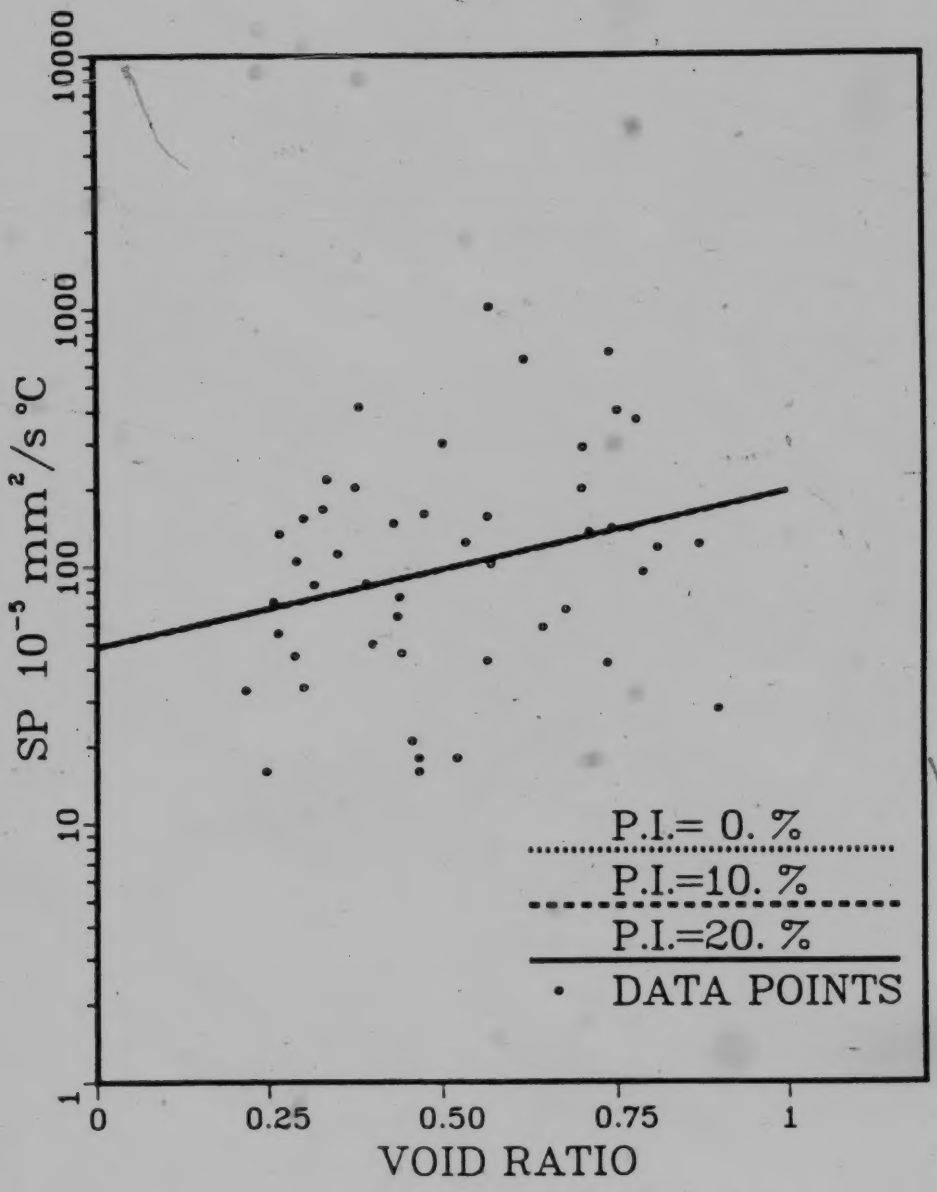

Figure E.12 Correlation between Index Properties and Segregation Potential.

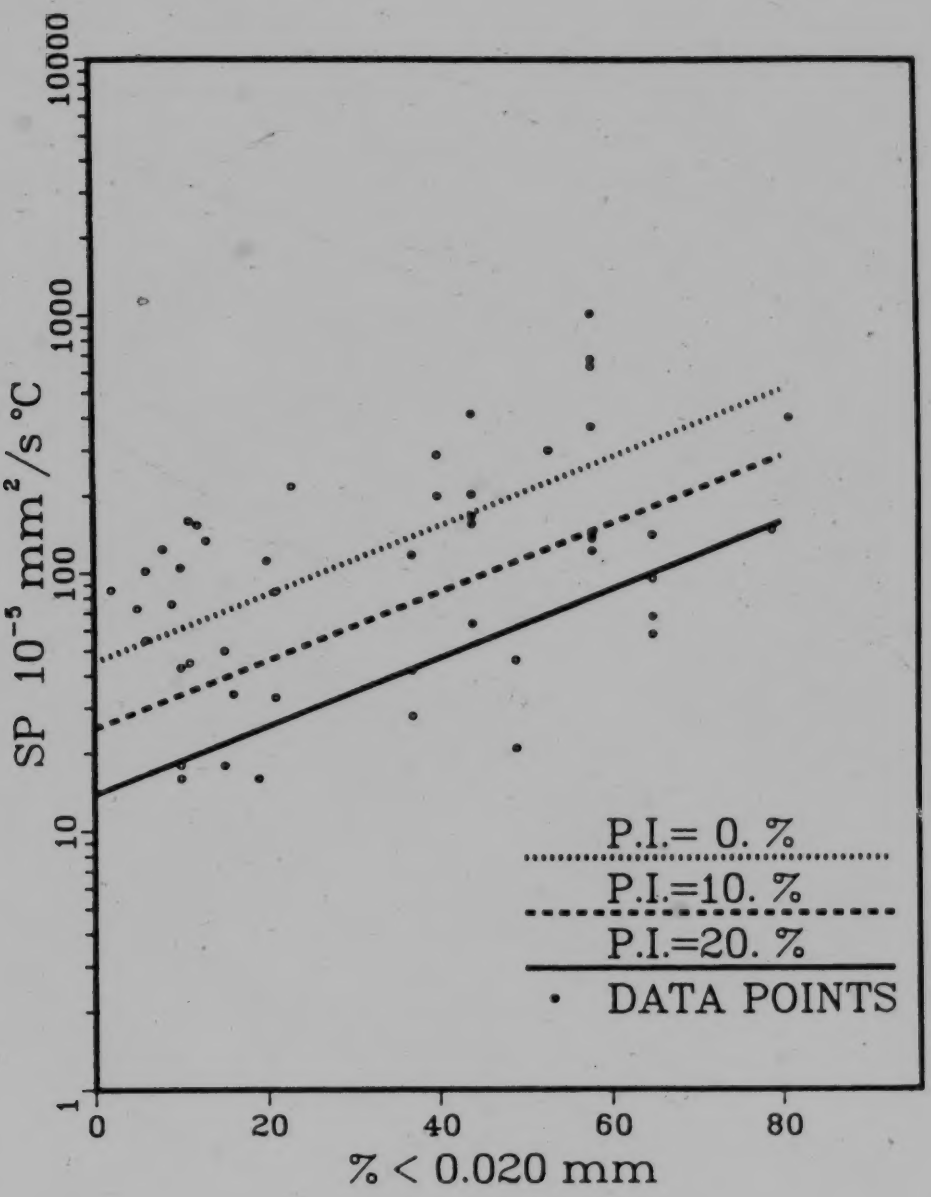

Figure E.13 Correlation between Index Properties and Segregation Potential.

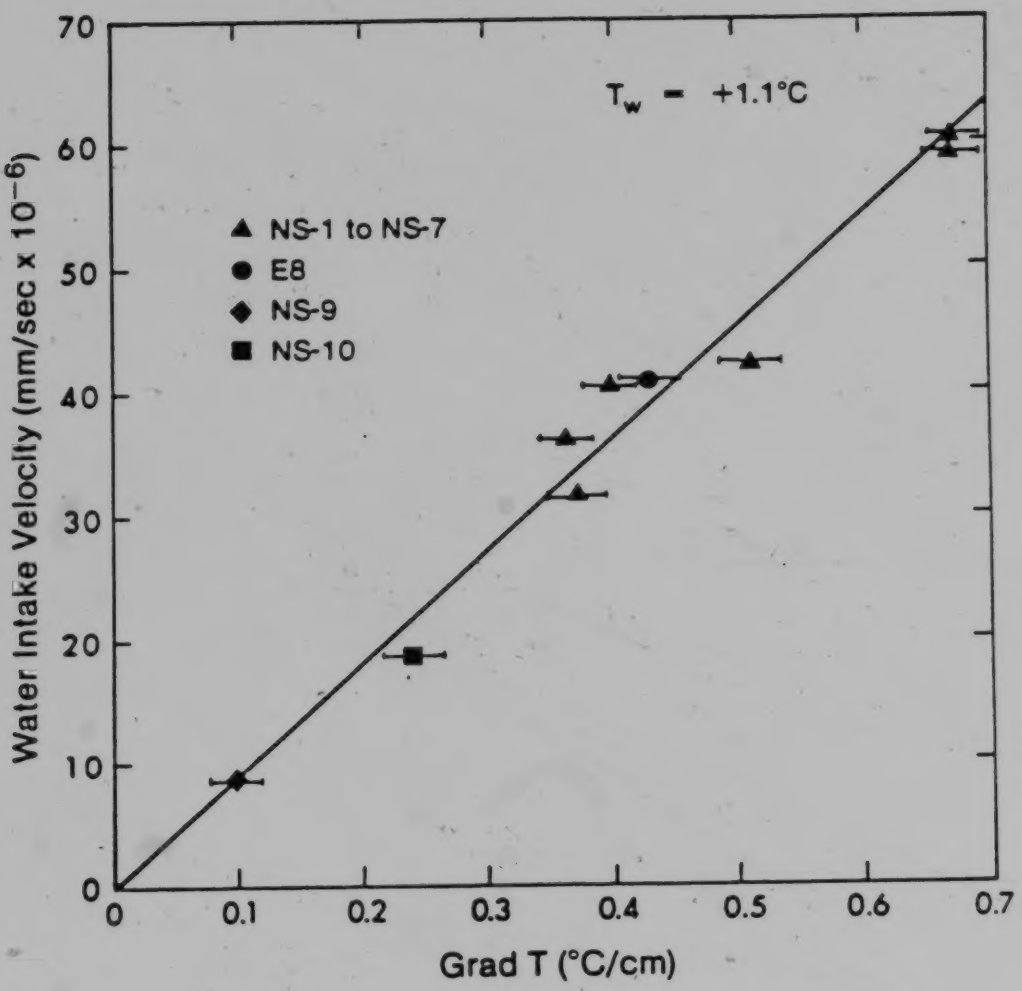

Figure E.14 Water Intake Velocity versus Temperature Gradient (modified from Konrad and Morgenstern, 1981)

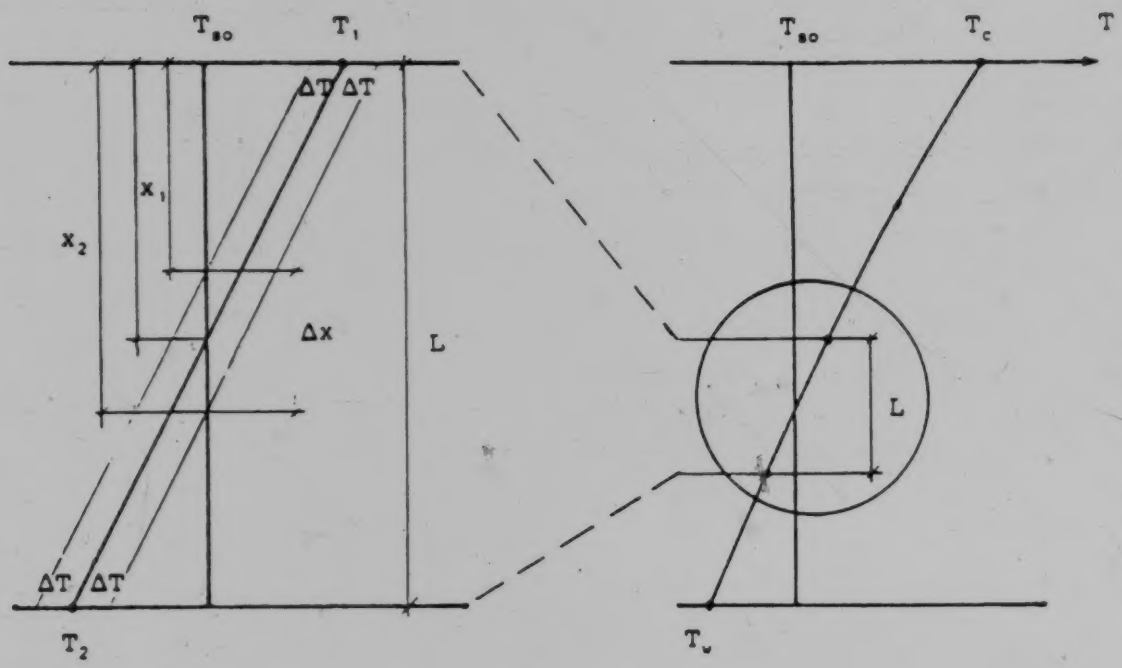

Figure E.15 Graphical representation of the consequences of an uncertainty ΔT of the temperature measuring system.

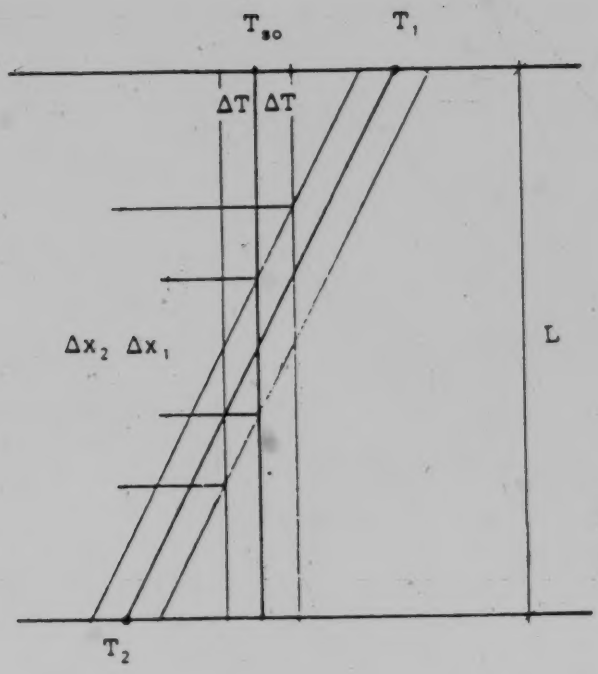

Figure E.16 Graphical representation of the consequences of an uncertainty ΔT of the estimate of the segregation temperature.

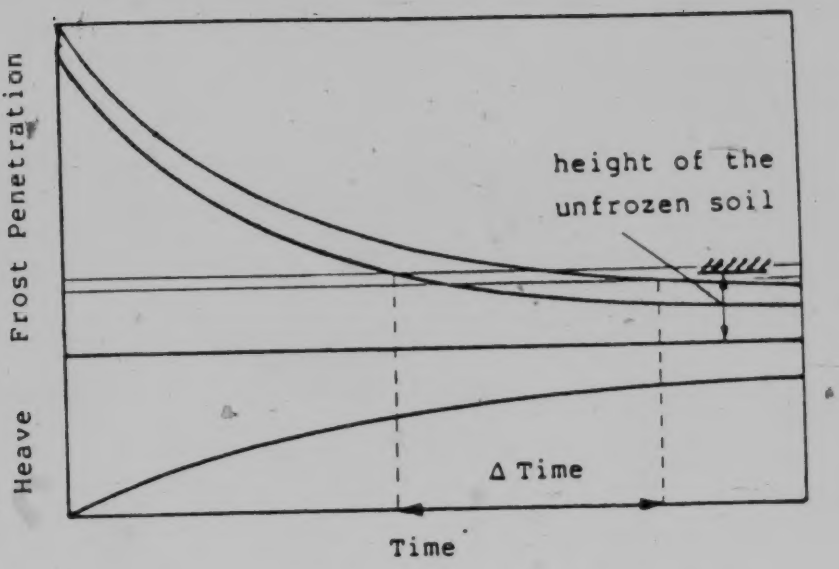

Figure E.17 Graphical representation of the accumulated influence of the three sources of error on the estimate of the moment of the initiation of the final ice lens.

SP.ACFEL

```
C ******************************************************************
C     This program allows the calculation of a number of
C     points in the SP-cooling rate-suction space. The
C     input data consist of the digitized form of
C        1. frost penetration versus time curve
C        2. frost heave versus time curve
C        3. cold side temperature versus time curve
C     and some data specific to the soil and test.
C     The program was written for evaluation of the ACFEL test
C     data.
C ******************************************************************
C     First a cubic spline is fitted through the
C     data points; some smoothing of the curves is allowed for.
C     The method is an IMSL subroutine: ICSSCU.
C ******************************************************************
      REAL X(24),F(24),DF(24),Y(24),C(23,3),WK(182),SM
      LOGICAL*1 TEST(15)
      INTEGER NX,IC,IER,I
      READ(5,281)(TEST(I),I=1,13)
      WRITE(6,281)(TEST(I),I=1,13)
      WRITE(8,281)(TEST(I),I=1,13)
      WRITE(7,281)(TEST(I),I=1,13)
281   FORMAT(13A1)
      READ(5,234)SM
234   FORMAT(F10.4)
      NX=24
      IC=NX-1
        DO 67 I=1,NX
        READ(5,101)X(I),F(I)
101     FORMAT(2F12.4)
67      CONTINUE
          DO 555 I=1,NX
          DF(I)=1.
555       CONTINUE
      CALL ICSSCU(X,F,DF,NX,SM,Y,C,IC,WK,IER)
      REAL P(24),G(24),DG(24),HY(24),HC(23,3),HWK(182),HSM
      INTEGER NXH,ICH,IERH,IH
      ICH=23
      NXH=24
       DO 68 I=1,NXH
       READ(5,20)P(I),G(I)
20     FORMAT(2F12.4)
68     CONTINUE
         DO 5555 I=1,NXH
         DG(I)=1.
5555     CONTINUE
      SMH=0.005
      CALL ICSSCU(P,G,DG,NXH,SMH,HY,HC,ICH,HWK,IERH)
      REAL XT(24),FT(24),DFT(24),YT(24),CT(23,3),WKT(182)
      INTEGER IERT
        DO 671 I=1,24
        READ(5,713)XT(I),FT(I)
713     FORMAT(2F12.4)
671     CONTINUE
          DO 333 I=1,24
          DFT(I)=1.
333       CONTINUE
      CALL ICSSCU(XT,FT,DFT,24,0.05,YT,CT,23,WKT,IERT)
```

SP.ACTEL

```
C ***********************************************************************
C   From here on the actual calculation starts.
C   XIN : time step size in Hrs.
C   HS  : height of soil in cm, before test started.
C   K   : permeability of soil sample * EXP(+4) in cm/s.
C   E   : (porosity of the soil sample)*(% water frozen).
C   As to be able to follow the calculation procedure, read Hanley
C   and Kaplar (1959).
C   H(I) : Total heave.
C   LS(I): Height of unfrozen soil (= drainage length).
C   Z(I) : HS - L(I), height of frozen soil, without heave.
C   L(I) : Height of frozen soil.
C ***********************************************************************
      REAL Z(200),DZ(200),H(200),V(200),L(200),DXDT(200),DTDX(200)
      REAL DTDT(200),VS(200),LS(200),PU(200),SP(200),VT(200)
      REAL K,HR(200),TC(200),TT(200)
      READ(5,1)XIN,HS,K,E,T
1     FORMAT(5F8.3)
      DO 5 I=1,200
      T=T+XIN
      TT(I)=T
C ***********************************************************************
C    The IF statement decides between which of the input values
C    of time the given value lies, thus giving the depth of frost
C    penetration using the appropriate part of the cubic spline.
C      Note also that the derivatives of Z(I) and H(I)
C      are calculated analytically.
C ***********************************************************************
        DO 45 J=1,24
          IF(T.LT.X(J)) GO TO 451
45        CONTINUE
451       J=J-1
      D=T-X(J)
      Z(I)=((C(J,3)*D+C(J,2))*D+C(J,1))*D+Y(J)
      DZ(I)=(3.*C(J,3)*D+2.*C(J,2))*D+C(J,1)
        DO 46 J=1,24
          IF(T.LT.P(J)) GO TO 461
46        CONTINUE
461       J=J-1
      D=T-P(J)
      H(I)=((HC(J,3)*D+HC(J,2))*D+HC(J,1))*D+HY(J)
      HR(I)=H(I)-Z(I)*0.09*E
C ***********************************************************************
C    V(I) : The water intake velocity, it is calculated from
C    VHEA : which is the total heave rate, corrected for in situ
C           freezing water.
C    VT(I): The total heave rate.
C ***********************************************************************
      VHEA=(3.*HC(J,3)*D+2.*HC(J,2))*D+HC(J,1)-DZ(I)*0.09*E
      V(I)=VHEA*0.92
      VT(I)=(3.*HC(J,3)*D+2.*HC(J,2))*D+HC(J,1)
        DO 47 J=1,24
          IF(T.LT.XT(J)) GO TO 471
47        CONTINUE
471       J=J-1
      D=T-XT(J)
      TC(I)=((CT(J,3)*D+CT(J,2))*D+CT(J,1))*D+YT(J)
      L(I)=Z(I)+H(I)
```

SP.ACTEL

```
C ***********************************************************************
C   DTDX(I) : Temperature gradient from the cold side.
C   DXDT(I) : Water intake velocity.
C   DTDT(I) : Cooling rate.
C   VS(I)   : V(I)/3600. Dimension of V(I) : cm/Hr
C                        Dimension of VS(I): cm/s
C ***********************************************************************
        DTDX(I)=TC(I)/L(I)
        DXDT(I)=DZ(I)*VT(I)
        DTDT(I)=DTDX(I)*DXDT(I)
        VS(I)=V(I)/3600.
        LS(I)=HS-Z(I)
C ***********************************************************************
C   Darcy's law. The factor 1000 : fit dimensions such that PU(I)
C   is in kPa.
C   Definition of SP. The factor 10000000 : fit dimensions such
C   that only the significant part of SP is printed out.
C   eg. : actual SP = 156.EXP(-5) mm*mm/s °C  will be printed
C   out as SP = 156.
C ***********************************************************************
        PU(I)=VS(I)*LS(I)/K*1000.
        SP(I)=VS(I)/DTDX(I)*10000000.
5       CONTINUE
          DO 141 I=1,200
          WRITE(7,891)TT(I),H(I),Z(I),TC(I)
891       FORMAT(4G12.5)
141       CONTINUE
            DO 157 I=1,200
            WRITE(8,912)DTDT(I),PU(I),SP(I)
912         FORMAT(3G15.5)
157         CONTINUE
C ***********************************************************************
C From here on the plotting program starts.
C   XMAX  : Total time scale
C   YMAX  : Total heave scale
C   XMAX2: Total frost heave penetration scale
C   XSTP  : Step size time scale (absolute values)
C   YSTP  :  "     "   heave scale
C   XSTP2 :  "     "   frost penetration scale
C   TMAX: ?
C   TSTP :?
C ***********************************************************************
        READ(5,110)XMAX,YMAX,XMAX2,XSTP,YSTP,XSTP2,TMAX,TSTP
        WRITE(6,110)XMAX,YMAX,XMAX2,XSTP,YSTP,XSTP2,TMAX,TSTP
110     FORMAT(8F8.3)
        NPTS=200
        CALL DSPDEV('PLOTTER ')
        CALL SCMPLX
        CALL BASALP('STAND')
        CALL PAGE(8.5,11.)
        CALL PHYSOR(2.,7.0)
        CALL AREA2D(5.,2.5)
        CALL XAXEND('NOFIRST')
        CALL RESET('YNAME')
        CALL YAXANG(0.)
        CALL XNAME('$',100)
        CALL YNAME('FROST HEAVE  (cm)$',100)
        CALL XINTAX
```

SP.ACTEL

```
175           CALL MARKER(16)
176           CALL SCLPIC(1.0)
177           CALL XMONUN
178           CALL XTICKS(0)
179           CALL GRAF(XORIG,XSTP,XMAX,YORIG,YSTP,YMAX)
180           CALL RESET('XMONUN')
181           CALL RESET('XTICKS')
182           CALL XGRAXS(0.,XSTP,XMAX,5.,'TIME (hrs)',-10,0.,2.5)
183           CALL CURVE(TT,H,NPTS,0)
184           CALL CURVE(P,G,24,-1)
185           CALL GRID(1,1)
186           CALL DASH
187           CALL CURVE(TT,HR,NPTS,0)
188           CALL RESET('DASH')
189           CALL RESET('XINTAX')
190           CALL HEIGHT(0.28)
191           CALL SETC(1,TEST(14),' ')
192           CALL SETC(1,TEST(15),'$')
193           CALL MESSAG(TEST,100,1.5,3.2)
194           CALL RESET('HEIGHT')
195           CALL ENDGR(-1)
196             DO 33 I=1,NPTS
197             TC(I)=-1.*TC(I)
198             FT(I)=-FT(I)
199    33       CONTINUE
200           TMAX=-1.*TMAX
201           CALL PHYSOR(2.,1.2)
202           CALL AREA2D(5.,2.5)
203           CALL RESET('XNAME')
204           CALL RESET('YNAME')
205           CALL XINTAX
206           CALL XNAME('TIME(hrs)$',100)
207           CALL KSNAP('#',96)
208           CALL YNAME('COLD SIDE TEMP.(#C)$',100)
209           CALL GRAF(0.,XSTP,XMAX,0.,TSTP,TMAX)
210           CALL CURVE(TT,TC,NPTS,0)
211           CALL CURVE(XT,FT,24,-1)
212           CALL GRID(1,1)
213           CALL RESET('XINTAX')
214           CALL ENDGR(-2)
215           CALL PHYSOR(2.,7.0)
216           CALL AREA2D(2.5,5.)
217           CALL XAXEND('NOFIRST')
218           CALL YAXEND('NOFIRST')
219           CALL BANGLE(-90.)
220           CALL RESET('XNAME')
221           CALL XAXANG(-90.)
222           CALL XNAME(' $',100)
223           CALL ANGLE(180.)
224           CALL MESSAG('FROST PEN. (cm)$',100,2.3,-0.75)
225           CALL RESET('YNAME')
226           CALL YMONUN
227           CALL YTICKS(0)
228           CALL GRAF(0.,XSTP2,XMAX2,0.,XSTP,XMAX)
229           CALL CURVE(Z,TT,NPTS,0)
230           CALL CURVE(F,X,24,-1)
231           CALL GRID(1,1)
232           CALL DONEPL
```

```
SP.ACFEL

233             STOP
234             END
```

Listing of LEAST at 13:43:11 on JUN 8, 1987 for CCid=GS56 on UALTAMTS

```
      C ***************************************************************
      C   This program fits a least squares surface through a number of
      C   points in a three dimensional space. The surface is of third
      C   order in one dimension and third order of the logarithm in
      C   a second. The problem is solved according to the spirit
      C   of a simple linear least squares model.
      C   It was necessary to use double precission for accuracy.
      C      XX    : x coordinate of points
      C      X     : logarithm of x coordinates of points
      C      Y     : y coordinate of points
      C      Z     : z coordinate of points
      C      B: contains the coefficients of the three dimensional
      C            surface.
      C      NPTS : number of points
      C      XSURMI : lowest value of x quoted in output.
      C      XSURMA : highest value of x quoted in output.
      C      PUMAX  : highest value of y quoted in output.
      C
      C    Output units:
      C    4. gives a matrix of values generated by the surface
      C    8. gives the coefficients B
     -C ***************************************************************
            REAL *8 H(7,7),XX(900),X(900),Y(900),Z(900),B(7,1),WK(1100)
            REAL *8 ZW(40,40),XSURMI,SULOMI,XSURMA,SULOMA,S(40),T(40),U(40)
            READ(5,12)NPTS,XSURMI,XSURMA,PUMAX
     12     FORMAT(I5,3F10.5)
              DO 7 I=1,NPTS
              READ(5,1000)XX(I),Y(I),Z(I)
              WRITE(6,1000)XX(I),Y(I),Z(I)
     1000     FORMAT(3G15.5)
              X(I)=DLOG10(XX(I))
     7        CONTINUE
            XXMIN=XX(1)
            XXMAX=XX(1)
            YMAX=Y(1)
            ZMAX=Z(1)
              DO 77 I=1,NPTS
              XTEM=XX(I)
              XXMIN=AMIN1(XXMIN,XTEM)
              XXMAX=AMAX1(XXMAX,XTEM)
              YTEM=Y(I)
              YMAX=AMAX1(YMAX,YTEM)
              ZTEM=Z(I)
              ZMAX=AMAX1(ZMAX,ZTEM)
     77       CONTINUE
           WRITE(8,111)XXMIN,XXMAX,YMAX,ZMAX
     111   FORMAT(4G15.5)
            DO 17 L=1,7
            DO 17 K=1,7
            H(L,K)=0.
     17     CONTINUE
               DO 47 I=1,7
               B(I,1)=0.
     47        CONTINUE
             DO 27 I=1,NPTS
             H(1,1)=H(1,1)+1.
             H(1,2)=H(1,2)+X(I)
             H(1,3)=H(1,3)+X(I)**2
```

Listing of LEAST at 13:43:11 on JUN 8, 1987 for CC1G-GS56 on UALTAMTS

```
      H(1,4)=H(1,4)+X(I)**3
      H(1,5)=H(1,5)+Y(I)
      H(1,6)=H(1,6)+Y(I)**2
      H(1,7)=H(1,7)+Y(I)**3
      H(2,1)=H(2,1)+X(I)
      H(2,2)=H(2,2)+X(I)**2
      H(2,3)=H(2,3)+X(I)**3
      H(2,4)=H(2,4)+X(I)**4
      H(2,5)=H(2,5)+Y(I)*X(I)
      H(2,6)=H(2,6)+Y(I)**2*X(I)
      H(2,7)=H(2,7)+Y(I)**3*X(I)
      H(3,1)=H(3,1)+X(I)**2
      H(3,2)=H(3,2)+X(I)**3
      H(3,3)=H(3,3)+X(I)**4
      H(3,4)=H(3,4)+X(I)**5
      H(3,5)=H(3,5)+X(I)**2*Y(I)
      H(3,6)=H(3,6)+X(I)**2*Y(I)**2
      H(3,7)=H(3,7)+X(I)**2*Y(I)**3
      H(4,1)=H(4,1)+X(I)**3
      H(4,2)=H(4,2)+X(I)**4
      H(4,3)=H(4,3)+X(I)**5
      H(4,4)=H(4,4)+X(I)**6
      H(4,5)=H(4,5)+Y(I)*X(I)**3
      H(4,6)=H(4,6)+Y(I)**2*X(I)**3
      H(4,7)=H(4,7)+Y(I)**3*X(I)**3
      H(5,1)=H(5,1)+Y(I)
      H(5,2)=H(5,2)+Y(I)*X(I)
      H(5,3)=H(5,3)+Y(I)*X(I)**2
      H(5,4)=H(5,4)+Y(I)*X(I)**3
      H(5,5)=H(5,5)+Y(I)**2
      H(5,6)=H(5,6)+Y(I)**3
      H(5,7)=H(5,7)+Y(I)**4
      H(6,1)=H(6,1)+Y(I)**2
      H(6,2)=H(6,2)+Y(I)**2*X(I)
      H(6,3)=H(6,3)+Y(I)**2*X(I)**2
      H(6,4)=H(6,4)+Y(I)**2*X(I)**3
      H(6,5)=H(6,5)+Y(I)**3
      H(6,6)=H(6,6)+Y(I)**4
      H(6,7)=H(6,7)+Y(I)**5
      H(7,1)=H(7,1)+Y(I)**3
      H(7,2)=H(7,2)+Y(I)**3*X(I)
      H(7,3)=H(7,3)+Y(I)**3*X(I)**2
      H(7,4)=H(7,4)+Y(I)**3*X(I)**3
      H(7,5)=H(7,5)+Y(I)**4
      H(7,6)=H(7,6)+Y(I)**5
      H(7,7)=H(7,7)+Y(I)**6
     B(1,1)=B(1,1)+Z(I)
     B(2,1)=B(2,1)+Z(I)*X(I)
     B(3,1)=B(3,1)+Z(I)*X(I)**2
     B(4,1)=B(4,1)+Z(I)*X(I)**3
     B(5,1)=B(5,1)+Z(I)*Y(I)
     B(6,1)=B(6,1)+Z(I)*Y(I)**2
     B(7,1)=B(7,1)+Z(I)*Y(I)**3
  27  CONTINUE
      CALL LEQT2F(H,1,7,7,B,3,WK,IER)
     WRITE(8,100)B
 100 FORMAT(D15.5)
      SULONI=DLOG10(XSURMI)
```

Listing of LEAST at 13:43:11 on JUN 8, 1987 for CCid=GS56 on UALTAMTS

```
117             SULOMA=DLOG10(XSURMA)
118            DO 37 I=1,11
119            S(I)=SULOMI+(SULOMA-SULOMI)*(I-1)/10.
120            U(I)=10**S(I)
121              DO 177 J=1,11
122              T(J)=(J-1)*PUMAX/10.
123              ZM(I,J)=((B(4,1)*S(I)+B(3,1))*S(I)+B(2,1))*S(I)+B(1,1)
124              ZM(I,J)=ZM(I,J)+((B(7,1)*T(J)+B(6,1))*T(J)+B(5,1))*T(J)
125     177      CONTINUE
126     37     CONTINUE
127            WRITE(4,232)(T(J),J=1,11)
128     232    FORMAT('***SUCTION* ',11F6.1)
129            WRITE(4,26)
130     26     FORMAT('*COOLING*************************************************
131          V**********************')
132            DO 46 I=1,11
133            WRITE(4,127)U(I),(ZM(I,J),J=1,11)
134     127    FORMAT('*',F6.3,'   * ',11F6.1)
135     46     CONTINUE
136             WRITE(4,1377)
137     1377    FORMAT('*************************************************************
138          V**********************')
139            REAL *8 A(900)
140            DIF=0.
141            DO 999 I=1,NPTS
142            A(I)=((B(4,1)*X(I)+B(3,1))*X(I)+B(2,1))*X(I)+B(1,1)
143            A(I)=A(I)+((B(7,1)*Y(I)+B(6,1))*Y(I)+B(5,1))*Y(I)
144            DIF=DIF+(Z(I)-A(I))**2
145     999    CONTINUE
146            STER=SQRT(DIF/(NPTS-7))
147            WRITE(8,159)STER
148     159    FORMAT(' STANDARD ERROR OF ESTIMATE : ',G15.5)
149           STOP
150           END
```

INPUT FILE FOR SP.ACFEL

LSG-16

.

1	LSG-16	
2	0.,	
3	-0.066,	0.188,
4	312.000,	6.358,
5	325.687,	7.498,
6	337.478,	8.346,
7	350.945,	9.040,
8	361.364,	9.573,
9	375.615,	9.651,
10	384.687,	9.742,
11	398.306,	10.109,
12	409.220,	10.339,
13	423.058,	10.760,
14	431.311,	10.987,
15	445.520,	11.331,
16	455.842,	11.577,
17	467.363,	11.833,
18	480.062,	12.036,
19	490.560,	12.219,
20	502.600,	12.438,
21	512.748,	12.567,
22	527.701,	12.754,
23	538.875,	13.353,
24	551.512,	14.149,
25	561.543,	14.710,
26	570.082,	15.187,
27	0.211,	-0.020,
28	289.335,	-0.069,
29	312.010,	0.182,
30	336.192,	0.478,
31	362.117,	1.012,
32	384.222,	1.476,
33	408.425,	1.864,
34	432.258,	2.327,
35	443.329,	2.654,
36	455.406,	2.832,
37	463.626,	3.009,
38	480.515,	3.403,
39	488.135,	3.583,
40	502.888,	3.993,
41	514.604,	4.360,
42	522.971,	4.646,
43	530.263,	4.821,
44	539.982,	5.057,
45	549.302,	5.166,
46	564.270,	5.543,
47	574.068,	5.888,
48	584.723,	6.253,
49	590.184,	6.498,
50	598.104,	6.745,
51	1.384,	2.299,
52	24.502,	2.342,
53	49.123,	2.539,
54	72.160,	2.766,
55	97.780,	2.737,
56	123.501,	2.594,
57	167.720,	2.833,
58	217.495,	3.226,

LSG-16

```
      265.106,      3.482,
      312.397,      4.253,
      336.495,      4.943,
      359.723,      5.376,
      384.341,      5.795,
      408.119,      6.295,
      433.101,      6.590,
      454.094,      6.872,
      478.635,      7.016,
      504.413,      7.308,
      526.045,      7.733,
      551.497,      8.516,
      565.350,      8.904,
      575.694,      9.091,
      592.762,      9.105,
      598.859,      9.065,
1.5,15.24,.12,.21,300.,
600.,8.,16.,100.,2.,4.,12.,3.,
 TEST LSG-16                          OUTPUT FILE FROM LEAST
0.001,10.,
.24,240.,
    0.89736E-02    0.63518E-01    0.26646        197.09
0.,0.,.12E-06,
    0.25299E+02
    0.31015E+03
    0.54272E+03
    0.17033E+03
   -0.20263E+04
    0.11985E+05
   -0.22148E+05
 STANDARD ERROR OF ESTIMATE :      27.134
```

OUTPUT FROM SP.ACFEL
INPUT FILE FOR LEAST

1	LSG-16		
2	0.63518E-01	0.19749	33.506
3	0.63184E-01	0.19575	34.143
4	0.62861E-01	0.19369	34.730
5	0.62550E-01	0.19133	35.265
6	0.62251E-01	0.18868	35.745
7	0.61963E-01	0.18575	36.169
8	0.61686E-01	0.18255	36.533
9	0.61419E-01	0.17908	36.836
10	0.61102E-01	0.17596	37.200
11	0.60681E-01	0.17376	37.756
12	0.60160E-01	0.17246	38.512
13	0.59546E-01	0.17202	39.473
14	0.58841E-01	0.17241	40.646
15	0.58050E-01	0.17360	42.037
16	0.57177E-01	0.17555	43.651
17	0.56225E-01	0.17823	45.495
18	0.55195E-01	0.18161	47.572
19	0.54061E-01	0.18568	49.892
20	0.52778E-01	0.19045	52.463
21	0.51352E-01	0.19590	55.289
22	0.49785E-01	0.20201	58.370
23	0.48081E-01	0.20877	61.708
24	0.46243E-01	0.21619	65.302
25	0.44271E-01	0.22426	69.150
26	0.42149E-01	0.23251	73.094
27	0.40188E-01	0.23999	76.822
28	0.38700E-01	0.24656	80.280
29	0.37671E-01	0.25222	83.469
30	0.37088E-01	0.25697	86.396
31	0.36940E-01	0.26079	89.067
175	0.35818E-01	0.31619E-01	156.09
176	0.36420E-01	0.28173E-01	163.58
177	0.36994E-01	0.24278E-01	171.22
178	0.37506E-01	0.19900E-01	178.72
179	0.37917E-01	0.15016E-01	185.55
180	0.38229E-01	0.97014E-02	191.67
181	0.38441E-01	0.40332E-02	197.09
182	0.38555E-01	-0.19103E-02	201.79
183	0.38574E-01	-0.80498E-02	205.77
184	0.38500E-01	-0.14308E-01	209.03
185	0.38368E-01	-0.20655E-01	212.07
186	0.38192E-01	-0.27078E-01	215.04
187	0.37973E-01	-0.33558E-01	217.93
188	0.37712E-01	-0.40075E-01	220.76
189	0.37411E-01	-0.46609E-01	223.51
190	0.37070E-01	-0.53140E-01	226.17
191	0.36690E-01	-0.59642E-01	228.73
192	0.36217E-01	-0.65849E-01	230.30
193	0.35625E-01	-0.71534E-01	230.44
194	0.34918E-01	-0.76577E-01	229.11
195	0.34117E-01	-0.80981E-01	226.61
196	0.33330E-01	-0.85296E-01	224.60
197	0.32571E-01	-0.89652E-01	223.33
198	0.31838E-01	-0.94100E-01	222.80
199	0.31133E-01	-0.98686E-01	223.02
200	0.30454E-01	-0.10346	224.00
201	0.29801E-01	-0.10845	225.75

APPENDIX F: Some comments on the results of the finite difference program

In this appendix the peculiar shape of the curves in Figs. 4.6 to 4.10 is discussed. Two features are of interest: a first peak of the "amount of water stored" near the top of the soil sample, and a second peak near the interface between the soil sample and the bentonite.

The peak near the top of the soil sample is similar to the peak obtained in homogeneous soil samples as analysed by Esrig (1968). It is explained by the following consideration: an electrical gradient is established across a soil sample when a power source is switched on inducing water flow instantaneously. When the electrodes form closed boundaries negative pore water pressures are generated near the positive electrode and positive pore water pressures near the negative electrode. Equilibrium is reached when the flow of water due to the hydraulic gradient equals the flow due to the electric gradient. However, in the interim, before equilibrium is established, there is a net flow towards the negative electrode, which explains the accumulation of water near this electrode.

The process at the interface between the soil sample and the bentonite is of similar nature. Say the voltage drop across the soil sample is half that across the bentonite, and the hydraulic conductivity of the frozen soil sample is half that of the frozen bentonite. Consider the configuration as presented in Fig. F.1, initially the power

source is switched on, and a linear ξ distribution is established. We will now look at the instant just after, using the finite difference technique. Say the initial electrical potentials are given by the numbers in the figure. An instant later ξ in the soil sample and in the bentonite is everywhere determined by:

$$\xi_{x,t+\Delta t} = \frac{1}{3}(\xi_{x,t} + \xi_{x+\Delta x,t} + \xi_{x-\Delta x,t}) ,$$

except near the boundaries at the top, bottom and in the middle. ξ near the top and bottom boundary is determined by no flow conditions, ξ in the middle is determined by continuity of flow.

Expressing continuity of flow the instant after application of the electrical gradient leads to the values shown in the second column in Fig. F.1. The amount of water stored in an element is then determined by the difference between the amount of water flowing across the top and bottom boundary of that element. The flow towards the division just above the interface is calculated quite easily and yields (when the hydraulic conductivity of the soil is 1, that of the bentonite 2, the area is assumed to be equal to unity, and the distance between the divisions is unity):

$$q_{in} = \frac{6 - 5}{0.5} = 2$$

The flow away from the same boundary is given by:

$$q_{out} = \frac{5 - 4}{1} = 1,$$

q_{in} is larger than q_{out} which shows that water is accumulated at this division. It can be seen that no water is accumulated at the division just above the one considered, resulting in a pronounced peak.

The abrupt sharp changes in the curves close to the boundaries are due to the discretization, and could be minimized by using smaller elements, they can not be avoided; they are inherent to the method and have to be lived with.

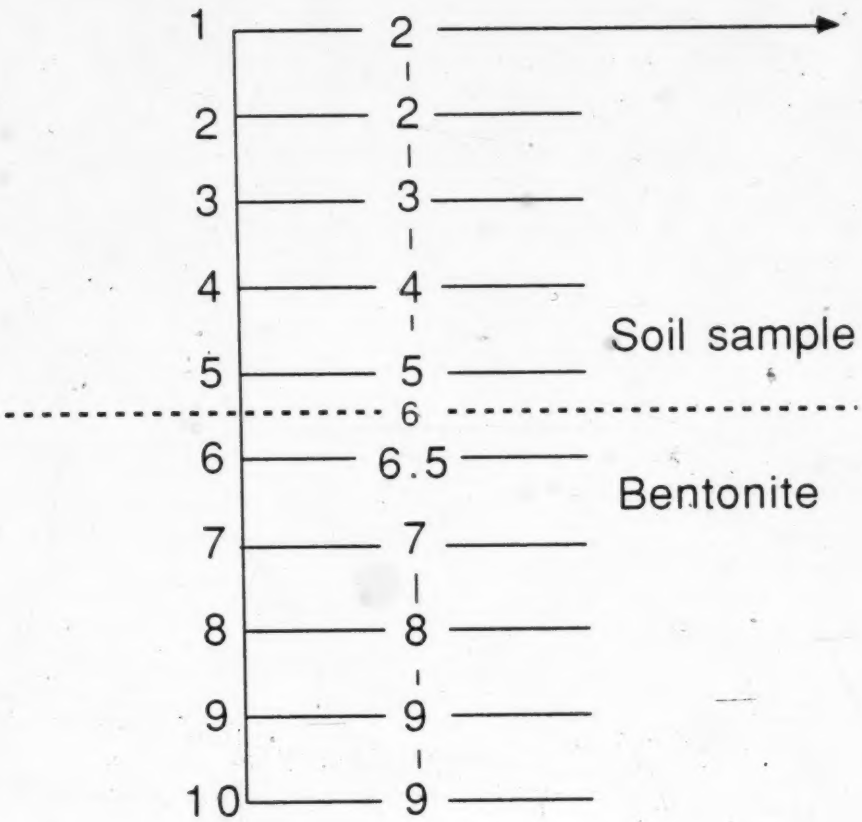

Figure F.1 ξ-distribution for a soil-bentonite sample under conditions as described in the text.